

1 **Spatial mapping of key plant functional traits in terrestrial**
2 **ecosystems across China**

3 Nannan An^{1,2,3}, Nan Lu^{2,3}, Weiliang Chen², Yongzhe Chen^{2,4}, Hao Shi^{2,3},

4 Fuzhong Wu¹, Bojie Fu^{2,3}

5
6
7 ¹Key Laboratory of Humid Subtropical Eco-geographical Process of Ministry of Education, School of
8 Geographical Sciences, Fujian Normal University, Fuzhou 350117, PR China

9 ²State Key Laboratory of Urban and Regional Ecology, Research Center for Eco-Environmental
10 Sciences, Chinese Academy of Sciences, Beijing 100085, PR China

11 ³University of Chinese Academy of Sciences, Beijing 101408, PR China

12 ⁴Department of Geography, The University of Hong Kong, Hongkong, 999077, PR China

13
14 *Correspondence to:* Nan Lu (nanlv@rcees.ac.cn)

15 **Abstract**

16 Trait-based approaches are of increasing concern in predicting vegetation changes and
17 linking ecosystem structures to functions at large scales. However, a critical challenge for such
18 approaches is acquiring spatially continuous plant functional trait maps. Here, six key plant
19 functional traits were selected as they can reflect plant resource acquisition strategies and
20 ecosystem functions, including specific leaf area (SLA), leaf dry matter content (LDMC), leaf N
21 concentration (LNC), leaf P concentration (LPC), leaf area (LA) and wood density (WD). A total
22 of 34589 in-situ trait measurements of 3447 seed plant species were collected from 1430 sampling
23 sites in China and were used to generate spatial plant functional trait maps (~1 km), together with
24 environmental variables and vegetation indices based on two machine learning models (random
25 forest and boosted regression trees). To obtain the optimal estimates, a weighted average algorithm
26 was further applied to merge the predictions of the two models to derive the final spatial plant
27 functional trait maps. The models showed a good accuracy in estimating WD, LPC and SLA, with
28 average R^2 values ranging from 0.48 to 0.68. In contrast, both the models had weak performance
29 in estimating LDMC, with average R^2 values less than 0.30. Meanwhile, LA showed considerable
30 differences between the two models in some regions. Climatic effects were more important than
31 those of edaphic factors in predicting the spatial distributions of plant functional traits. Estimates
32 of plant functional traits in the northeast China and the Qinghai-Tibet Plateau had relatively high
33 uncertainties due to sparse samplings, implying a need of more observations in these regions in the
34 future. Our spatial trait maps could provide critical support for trait-based vegetation models and
35 allow exploration into the relationships between vegetation characteristics and ecosystem
36 functions at large scales. The six plant functional trait maps for China with 1 km spatial resolution
37 are now available at <https://figshare.com/s/c527c12d310cb8156ed2> (An et al., 2023).

38 **1 Introduction**

39 Climate change has been affecting vegetation distributions and biogeochemical cycling globally
40 and altering their feedbacks to the climate system (Kirilenko et al., 2000; Finzi et al., 2011;
41 Jónsdóttir et al., 2022). Dynamic global vegetation models (DGVMs) are powerful tools for
42 predicting changes in vegetation and ecosystem-atmosphere exchanges (e.g., water, carbon and
43 nutrient cycling) in a changing climate (Foley et al., 1996; Peng, 2000). However, conventional
44 DGVMs are still insufficient realistic, largely due to their dependence on the plant functional types
45 (PFTs) assumption (Sitch et al., 2008; Yurova and Volodin, 2011; Scheiter et al., 2013). PFTs in
46 conventional DGVMs commonly have fixed attributes (mostly trait values) (van Bodegom et al.,
47 2012; Wullschleger et al., 2014) that do not reflect plant adaptation to environments, limiting the
48 quantification of carbon-water-nutrient feedbacks between terrestrial ecosystems and the
49 atmosphere (Zaehle and Friend, 2010; Liu and Yin, 2013). Trait-based approaches can provide a
50 robust theoretical basis for developing the next generation of DGVMs (van Bodegom et al., 2012;
51 Sakschewski et al., 2015; Matheny et al., 2017). Plant functional traits, which are closely
52 associated with ecosystem functions (Diaz et al., 2004; Yan et al., 2023), can effectively reflect
53 response and adaptation of plants to environmental conditions (Myers-Smith et al., 2019; Qiao et
54 al., 2023).

55 Attempts to predict spatially continuous trait maps have been conducted at regional to global
56 scales (e.g., Madani et al., 2018; Moreno-Martínez et al., 2018; Boonman et al., 2020; Loozen et
57 al., 2020; Dong et al., 2023). Webb et al. (2010) proposed that the environment creates a filtered
58 trait distribution along an environmental gradient, and such trait-environment relationships offer
59 fundamental support to predict the spatial distributions of plant functional traits through
60 extrapolating local trait measurements. Boonman et al. (2020) mapped the global patterns of
61 specific leaf area (SLA), leaf N concentration (LNC) and wood density (WD) based on a set of
62 climate and soil variables. As the number of available regional and global trait databases increases
63 (Wang et al., 2018; Kattge et al., 2020), trait-environment relationships are becoming increasingly
64 quantitative and accurate (Bruehlheide et al., 2018; Myers-Smith et al., 2019). Alternatively, remote
65 sensing approaches, such as empirical methods and physical radiative transfer models (e.g., partial
66 least squares regression and PROSPECT model), have been developed to estimate plant
67 physiological, morphological and chemical traits (e.g., leaf chlorophyll content, SLA, LNC and
68 leaf dry matter content (LDMC)) (Darvishzadeh et al., 2008; Romero et al., 2012; Ali et al., 2016).
69 Vegetation indices, such as normalized difference vegetation index and enhanced vegetation index
70 (EVI), have been successful in estimating plant functional traits of croplands, grasslands and
71 forests (Clevers and Gitelson, 2013; Li et al., 2018; Loozen et al., 2018). Loozen et al. (2020)
72 demonstrated that EVI was the most important predictor for mapping the spatial pattern of canopy
73 nitrogen in European forests. Admittedly, a recent study has suggested that combining
74 environmental variables and vegetation indices can improve the predictive accuracy of canopy

75 nitrogen compared to those based on vegetation indices alone (Loozen et al., 2020).

76 Although there have been reports on plant functional trait distributions in China in some
77 global or regional researches (e.g., Yang et al., 2016; Butler et al., 2017; Madani et al., 2018;
78 Moreno-Martínez et al., 2018; Boonman et al., 2020), there are still large uncertainties in
79 characterizing the spatial distributions of plant functional traits in China. First, global studies
80 generally have relatively few and unevenly distributed sampling sites across China (Butler et al.,
81 2017; Madani et al., 2018; Boonman et al., 2020), impeding our understanding of the true spatial
82 characteristics of trait variability. Second, the spatial patterns of traits among these studies are
83 usually inconsistent. For example, Moreno-Martínez et al. (2018) and Madani et al. (2018)
84 demonstrated that SLA values were low in the southeast areas but high in the southwest areas of
85 China, whereas Boonman et al. (2020) found the opposite. Third, most studies focused on leaf
86 traits (Yang et al., 2016; Loozen et al., 2018; Moreno-Martínez et al., 2018), whereas traits
87 associated with the whole-plant strategies, such as WD, were ignored. Therefore, mapping and
88 verifying the spatial patterns of key functional traits that reflect the whole plant economics
89 spectrum in China is a top priority.

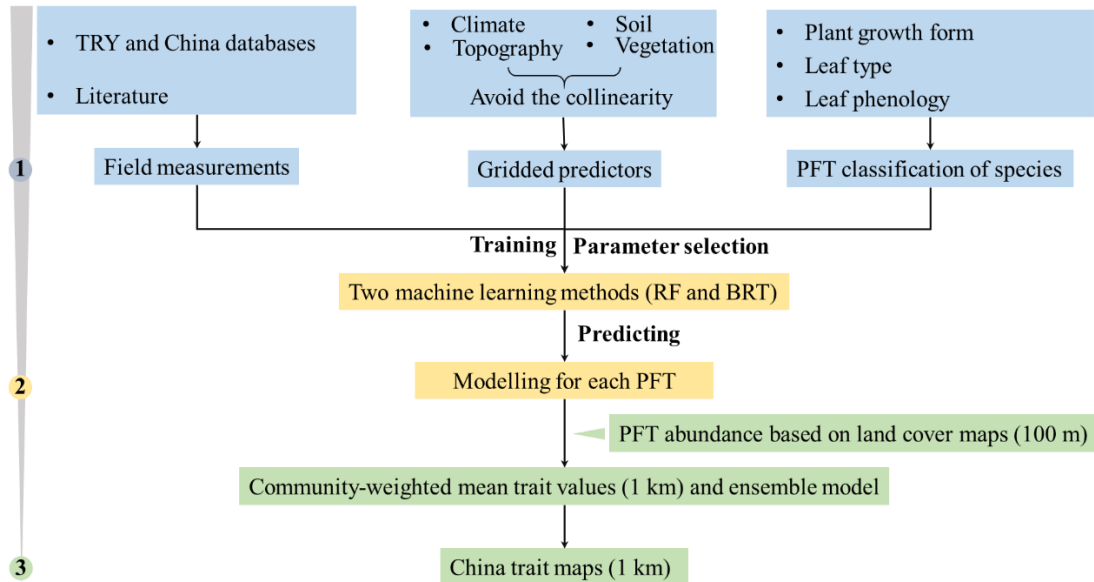
90 In this study, our main objective was to generate spatial maps for several key plant functional
91 traits, through combining field measurements, environmental variables and vegetation indices. We
92 selected six plant functional traits including SLA, LDMC, LNC, LPC, LA and WD. As key leaf
93 economics traits, SLA, LDMC, LNC and LPC were selected because they are closely linked to
94 plant growth rate, resource acquisition and ecosystem functions (Wright et al., 2004; Diaz et al.,
95 2016). LA is indicative of the trade-off between carbon assimilation and water-use efficiency
96 (Wright et al., 2017), and WD reflects the trade-off between plant growth rate and support cost,
97 with a higher WD linked to a lower growth rate, a higher survival rate and a higher biomass
98 support cost (King et al., 2006). For each plant functional trait, we predicted spatial pattern at a 1
99 km resolution using an ensemble modelling algorithm based on two machine learning methods
100 (i.e., random forest and boosted regression trees).

101 **2 Materials and Methods**

102 **2.1 Overview**

103 The spatial maps of plant functional traits in China were generated based on machine learning
104 methods trained by a large dataset of in-situ field measurements, environmental variables and
105 vegetation indices in three steps (Fig. 1). First, in-situ field measurements of six plant functional
106 traits were collected from TRY and China databases as well as published literature, and the PFTs
107 of plant species were classified based on plant growth form, leaf type and leaf phenology. Multiple
108 gridded predictors of climate, soil, topography and vegetation indices were used after avoiding the
109 collinearity among them. Second, random forest and boosted regression trees were used to train
110 the relationships between plant functional traits and predictors for each PFT individually. Third,

111 the spatial abundance of each PFT within 1 km grid cell was calculated using land cover map (100
 112 m). Community-weighted trait value within 1 km grid cell was calculated based on the abundance
 113 of each PFT and their predicted trait values in Step 2. To reduce the variability of different single-
 114 models, we derived the final spatial maps of plant functional traits using an ensemble model
 115 algorithm to merge the predictions of random forest and boosted regression trees according to
 116 their cross-validated R^2 values.



117
 118 **Figure 1.** Methodological workflow for spatial mapping of plant functional traits. Trait
 119 mapping is performed in three steps. Step 1: in-situ field measurements of plant functional traits,
 120 PFT classification of plant species and gridded predictors were collected. Step 2: two machine
 121 learning methods were used to predict trait values by training field measurements and predictors
 122 for each PFT. Step 3: spatialization of trait maps by calculating the abundance of each PFT using
 123 100 m land cover map and predicted trait values within 1 km grid cell. PFT, plant functional type;
 124 RF, random forest; BRT, boosted regression trees.

125 2.2 Plant functional trait collection and data processing

126 The information on the six plant functional traits and their ecological meanings are described in
 127 Table 1. Plant trait data was obtained and collected via two main sources. The first source was
 128 public trait databases, including the TRY database (Kattge et al., 2020) and the China Plant Trait
 129 Database (Wang et al., 2018). The second source was from literature (listed in Appendix A). To
 130 ensure data quality and comparability, we only included trait observations that met the following
 131 five criteria: 1) Measurements must be obtained from natural terrestrial fields in order to minimize
 132 the influence of management disturbance, and observations from croplands, aquatic habitats,
 133 control experiments and gardens were excluded; 2) According to the mass ratio hypothesis, the
 134 effect of plant species on ecosystem functioning is determined to an overwhelming extent by the
 135 traits and functional diversity of the dominant species and is relatively insensitive to the richness

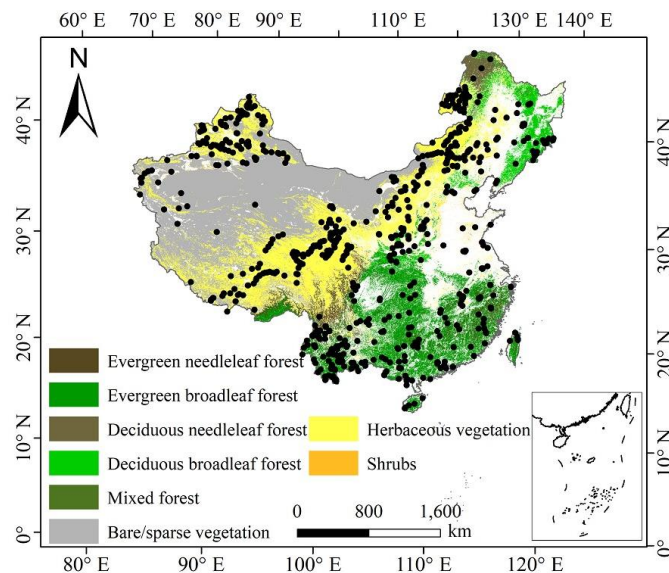
136 of subordinate species (Grime, 1998). Thus, we only included studies that measured plant trait
 137 observations from all species or dominant species within a community; 3) In order to consider the
 138 intraspecific trait variation, when the same species occurred at the same sampling site from
 139 different studies, we included all original observed data from different studies rather than
 140 averaging the values at the species level (Jung et al., 2010; Siefert et al., 2015); 4) Plant trait
 141 observations must be made on mature and healthy plant individuals, so some specific growth
 142 stages (e.g., seedling) and size classes (e.g., sapling) were excluded to reduce the confounding
 143 effect of ontogeny (Thomas, 2010); 5) We only included studies with clear geographical
 144 coordinates to match predictor variables. The sampling location and sampling time were also
 145 included in the dataset. The sampling time mostly focused on the growing season of a year (i.e.,
 146 May-October), which can ensure the relative consistency of sampling time to minimize the effects
 147 of seasonality. Plant functional traits must be sampled and measured according to standardized
 148 measurement procedures (Perez-Harguindeguy et al., 2013) to reduce the variation and uncertainty
 149 among different data sources. In this study, we included SLA measurements on sun-leaves, and
 150 WD measurements on main stem of woody species.

151 **Table 1** Description of plant functional traits selected in this study and their relevant
 152 ecosystem functions.

Trait	Abbreviation	Description	Relevant ecosystem functions
Specific leaf area	SLA	As a core leaf economics trait (Wright et al., 2004), it is related to trade-off between leaf lifespan and carbon acquisition as well as light competition (Reich et al., 1991)	Productivity, litter decomposition, competitive ability (Bakker et al., 2011; Smart et al., 2017)
Leaf dry matter content	LDMC	Strongly related to resource availability and potential growth rate (Hodgson et al., 2011)	Productivity, litter decomposition, herbivore resistance and drought tolerance (Bakker et al., 2011; Smart et al., 2017; Blumenthal et al., 2020)
Leaf N concentration	LNC	As a core leaf economics trait, it is strongly related to photosynthetic capacity (Wright et al., 2004)	Productivity, nutrient cycling, litter decomposition (LeBauer and Treseder, 2008; Bakker et al., 2011)
Leaf P concentration	LPC	As a core leaf economics trait, it is strongly related to photosynthetic capacity (Wright et al., 2004)	Productivity, nutrient cycling, litter decomposition (LeBauer and Treseder, 2008; Bakker et al., 2011)
Leaf area	LA	Trade-off between carbon assimilation and water use efficiency, it is related to energy balance (Wright et al., 2017)	Productivity (Li et al., 2020)
Wood density	WD	A measure of carbon investment, representing the trade-off between growth and mechanical support (Martínez-Vilalta et al., 2010)	Drought tolerance, productivity (Hoeber et al., 2014; Liang et al., 2021)

153 The plant trait data was checked for possible errors and corrected in three steps as follows.
 154 First, species name and taxonomic nomenclature were corrected and standardized according to the
 155 Plant List (<http://www.theplantlist.org/>) using the ‘plantlist’ package. Second, illogical values,

156 repeated values and outliers were removed, which were defined by observations exceeding 1.5
 157 standard deviations from the mean trait value for a given species (Kattge et al., 2011). Third, we
 158 appended information on plant growth form, leaf type and leaf phenology from the TRY
 159 categorical traits database (<https://www.try-db.org/TryWeb/Data.php#3>) and *Flora Reipublicae*
 160 *Popularis Sinicae* (<http://www.iplant.cn/frps>), which were used to match species names to PFTs.
 161 We associated each species with a corresponding PFT based on plant growth form (tree, shrub and
 162 grass), leaf type (broadleaf and needleleaf) and leaf phenology (evergreen and deciduous). For
 163 example, the information on *Salix matsudana* is: tree, deciduous and broadleaf, thus, we were able
 164 to associate the PFT of deciduous broadleaf forest (DBF) to this species. The species that did not
 165 correspond to any PFT were discarded. After these treatments, we collected a total of 34589 trait
 166 measurements from 1430 sampling sites for our database, representing 3447 species from 195
 167 families and 1066 genera (Fig. 2). Information on the statistics for the six plant functional traits
 168 collected in this study is shown in Table B1 in Appendix B.
 169



170
 171 **Figure 2.** The spatial distribution of sample sites across different ecosystems in China. The
 172 white areas represent artificial land cover types.

173 2.3 Preparing predictor variables

174 2.3.1 Climate data

175 Twenty-one climate variables were used in this study, including 19 bioclimate variables, solar
 176 radiation (RAD) and aridity index (AI) (Table B2 in Appendix B). The 19 bioclimate variables and
 177 RAD were obtained from WorldClim version 2.1 for the period from 1970 to 2000
 178 (<https://www.worldclim.org/data/worldclim21.html>). The AI data was extracted from the CGIAR
 179 Consortium of Spatial Information (CGIAR-CSI) for the period from 1970 to 2000
 180 (<http://www.csi.cgiar.org>) (Trabucco and Zomer, 2018). The spatial resolution of climate data is 1
 181 km.

182 2.3.2 Soil data

183 Twelve soil variables were included in this study, representing different aspects of soil properties,
184 i.e., soil texture, bulk density (BD), pH and soil nutrients (Table B2 in Appendix B). All soil
185 variables were extracted from the Soil Database of China for Land Surface Modeling
186 (<http://globalchange.bnu.edu.cn/research/soil2>) (Shangguan et al., 2013). Given the importance of
187 topsoil properties on community composition (Bohner, 2005), we averaged the first four layers to
188 represent the topsoil properties (~ 30 cm) in our study. The spatial resolution is 1 km.

189 **2.3.3 Topography**

190 The topographic variable was elevation. Elevation data was extracted from the STRM 90m dataset
191 in China based on the SRTM V4.1 database (<https://www.resdc.cn/data.aspx?DATAID=123>). The
192 spatial resolution is 1 km.

193 Given the collinearity among climate and soil variables, we reduced the dimensionality of
194 these predictors based on Pearson's correlation coefficient (r) (Figs. B1 and B2 in Appendix B).
195 Among a set of highly correlated variables ($r > 0.75$), only one variable was retained in subsequent
196 analysis to ensure a combination of different environmental variables. The final selection of
197 environment predictors included twenty variables: mean annual temperature (MAT), mean diurnal
198 range (MDR), min temperature of the coldest quarter (Tmin), max temperature of the warmest
199 quarter (Tmax), temperature seasonality (TS), mean annual precipitation (MAP), precipitation
200 seasonality (PS), precipitation of the wettest quarter (PEQ), precipitation of the driest quarter
201 (PDQ), AI, RAD, elevation, soil sand content (SAND), pH, BD, soil total N (STN), soil total P
202 (STP), soil available P (SAP), soil alkali-hydrolysable N (SAN) and cation exchange capacity
203 (CEC).

204 **2.3.4 Vegetation indices**

205 Three categories of vegetation indices were included in this study (Table B2 in Appendix B). First,
206 EVI was extracted from the MOD13A3 V006 product
207 (<https://lpdaac.usgs.gov/products/mod13a3v006/>). This product is available as a monthly average
208 with the spatial resolution of 1 km, ranging from January 2000 to December 2018. Second,
209 MODIS reflectance data was also extracted from the MOD13A3 V006 product, including MIR
210 reflectance, NIR reflectance, red reflectance and blue reflectance. Third, the MERIS terrestrial
211 chlorophyll index (MTCI) was extracted from the Natural Environment Research Council Earth
212 Observation Data Centre (NERC-NEODC, 2005) (<https://data.ceda.ac.uk/>). MTCI data is
213 available globally as a monthly average at 4.63 km spatial resolution, and ranges from June 2002
214 to December 2011. It is noted that valid MTCI values should be greater than 1, so our study
215 deleted any values less than 1.

216 To avoid collinearity, we also reduced the dimensionality of vegetation indices based on r
217 values (Fig. B3 in Appendix B). Most selected variables were related to growing season due that
218 plant functional traits were measured during the growing season. Furthermore, based on the results
219 of Pearson's correlation analysis, MTCI, MIR, NIR, red and blue in January showed low
220 correlations with those in growing season, thus they were included in subsequent analysis. The

221 final selection included 36 variables: annual EVI, monthly EVI (May, June, July, August and
222 September), monthly MTCI, MIR, NIR, red and blue (all for January, June, July, August and
223 September).

224 Both environmental variables and vegetation indices were resampled to a consistent spatial
225 resolution of 1 km using the nearest neighborhood method.

226 PFT is also an important factor in influencing the variation of plant functional traits
227 (Verheijen et al., 2016; Loozen et al., 2020), thus the trait predictions were performed for each
228 PFT individually. We used the 2015 land cover map at a 100 m spatial resolution to calculate the
229 relative abundance of each PFT within 1 km grid cell, which was extracted from the Copernicus
230 Global Land Service (CGLS-LC100, Version 3) (<https://land.copernicus.eu/global/products/lc>)
231 (Buchhorn et al., 2020). We focused on natural terrestrial vegetation, so all artificial land cover
232 types (e.g., croplands) were thus eliminated in our dataset. Seven categories were included:
233 evergreen needleleaf forest (ENF), evergreen broadleaf forest (EBF), deciduous needleleaf forest
234 (DNF), deciduous broadleaf forest (DBF), shrubland (SHL), grassland (GRL) and bare/sparse
235 vegetation.

236 **2.4 Model fitting and validation**

237 To predict spatial patterns of plant functional traits, we used two machine learning models, i.e.,
238 random forest and boosted regression trees.

239 Random forest is an ensemble machine learning method based on classification and
240 regression trees using collections of regression trees to classify observations according to a set of
241 predictive variables (Breiman, 2001). This method repeatedly constructs a set of trees from
242 random samples of training data, and the final prediction is produced by integrating the results of
243 all individual trees, which makes it a robust method. The model is controlled by two main
244 parameters: the number of sampled variables (mtry) and the number of trees (ntree). The mtry was
245 set to range from 1 to 57 (at an interval of 1), and the ntree was set as 500, 1000, 2000, 5000 and
246 10000 in subsequent runs. This analysis was performed using the ‘randomForest’ function in the
247 ‘randomForest’ package (Liaw and Wiener, 2002).

248 Boosted regression trees are machine learning methods based on generalized boosted
249 regression models and using a boosting algorithm to combine many sample tree models to
250 optimize predictive performance (Elith et al., 2006). There is no need for prior data transformation
251 or the elimination of outliers, and this method can fit complex non-linear relationships while
252 automatically handling interaction effects between predictors (Elith et al., 2008). The four
253 parameters to optimize in these models are the number of trees, interaction depth, learning rate
254 and bag fractions. We varied the parameter settings to find the optimal parameter combination that
255 achieves minimum predictive error. The number of trees was set to 3000, the interaction depth
256 varied from 1 to 7 (at an interval of 1), the learning rate was set to 0.001, 0.01, 0.05 and 0.1, and
257 the bag fraction was set to 0.5, 0.6, 0.7 and 0.75. PFT was used as a dummy variable in the

258 boosted regression trees models. This analysis was conducted using the ‘gbm’ function in the
259 ‘gbm’ package (Ridgeway, 2006).

260 We built separate predictive model for each plant functional trait. To select the optimal
261 parameter combination and to evaluate the final model performance for each trait, we calibrated
262 the models 10 times using randomly selected 80% of the data for training models and validating
263 against the remaining 20% based on cross-validation (Table B3 in Appendix B). The predictive
264 performance was evaluated by regressing the predicted and observed trait values from all
265 repetitions of the cross-validation. The fitting performance of the random forest and boosted
266 regression trees was evaluated using determinate coefficient (R^2), normalized root-mean-square
267 error (NRMSE) and mean absolute error (MAE). These scores are calculated following Eq. (1), Eq.
268 (2) and Eq. (3):

$$269 \quad R^2 = 1 - \frac{\sum_{i=1}^n (p_i - o_i)^2}{\sum_{i=1}^n (p_i - \hat{o}_i)^2} \quad (1)$$

$$270 \quad \text{NRMSE} = \frac{\sqrt{\frac{1}{n} \sum_{i=1}^n (p_i - o_i)^2}}{p_{\max} - p_{\min}} \quad (2)$$

$$271 \quad \text{MAE} = \frac{1}{n} \sum_{i=1}^n |o_i - p_i| \quad (3)$$

272 where p_i and o_i are the predictive values and observed values, respectively; \hat{o}_i is the mean of the
273 observed values.

274 To quantify the relative importance of each predictor across the two models consistently, we
275 used the method proposed by Thuiller et al. (2009). This method applies correlation between the
276 standard predictions fitted with the original data and predictions where the variable under
277 investigation has been randomly permuted. If the correlation is high, which indicates little
278 difference between the two predictions, the variable permuted is considered not important for the
279 model. This step was repeated multiple times for each predictor, and the mean correlation
280 coefficient over runs was recorded. Then the relative importance of each predictor was quantified
281 as one minus the Spearman rank correlation coefficient (see Boonman et al., 2020). In addition,
282 we used generalized additive models to fit the relationships between plant functional traits and the
283 most important variables using the ‘gam’ function in the ‘mgcv’ package.

284 **2.5 Generation of plant functional trait maps and model performance**

285 The generation of spatial maps of plant functional traits was performed in three steps. First, we
286 predicted trait values for each natural PFT (i.e., EBF, ENF, DBF, DNF, SHL and GRL) within 1
287 km grid cell separately. Second, the abundance of individual natural PFT within 1 km grid cell
288 was estimated using a land cover map with a spatial resolution of 100 m. Third, refer to the Eq. (4)
289 that has been widely applied in a community (Garnier et al., 2004), the final trait value in a given
290 1 km grid cell was calculated as the sum of the predicted trait values multiplying by corresponding
291 abundance of each natural PFT.

$$292 \quad \text{CWM} = \sum_{i=1}^n W_i X_i \quad (4)$$

293 where n is the total number of PFT in a given grid; W_i is the relative abundance of the i th natural
 294 PFT; and X_i is the predicted trait value of the i th natural PFT.

295 To reduce the variability of different single-models and to construct a more stable and
 296 accurate model, the ensemble model was further applied to merge the predictions of random forest
 297 and boosted regression trees according to their cross-validated R^2 values. The predicted value of
 298 ensemble model was calculated in a given grid cell as described by Eq. (5) (Marmion et al., 2009).
 299 The model accuracy was calculated by regressing the predicted values of ensemble model against
 300 the observed trait values.

$$301 \quad Pred_EM_t = \frac{\sum_{m=1}^2 (pred_{m,t} \times r_{m,t}^2)}{\sum_{m=1}^2 r_{m,t}^2} \quad (5)$$

302 where $Pred_EM_t$ is the predicted value of t trait in ensemble model; $pred_{m,t}$ is the predicted
 303 value of t trait in m model; $r_{m,t}^2$ is the cross-validated R^2 of t trait in m model.

304 To evaluate the model performance (i.e., the variability in the prediction across models), the
 305 coefficient of variation (CV) was calculated as the difference between the predictions of random
 306 forest and boosted regression trees methods and ensemble model. CV is calculated as following
 307 Eq. (6):

$$308 \quad CV_t = \frac{\sqrt{\sum_{m=1}^2 (pred_{m,t} - obs_t)^2 + r_{m,t}^2}}{\frac{\sum_{m=1}^2 r_{m,t}^2}{obs_t}} \quad (6)$$

309 where $pred_{m,t}$ is the predicted value of t trait in m model; obs_t is the value of t trait in ensemble
 310 model; $r_{m,t}^2$ is the cross-validated R^2 of t trait in m model.

311 2.6 Uncertainty assessments

312 Multivariate environmental similarity surface analysis (MESS) was used to identify the range of
 313 the extrapolated predictor values across locations in the plant trait dataset (Elith et al., 2010). This
 314 method is often used to evaluate the extent of extrapolation and the applicability domain. If the
 315 value is negative, this indicates that at a given grid cell, at least one predictor variable is outside
 316 the extent of the referenced predictor layer. This analysis was conducted using the ‘mess’ function
 317 in the ‘dismo’ package.

318 All analyses were performed in R 4.0.2 (R Core Team, 2020).

319 3 Results

320 3.1 Performance of prediction models

321 Cross-validation showed that the performance of the predictive models differed greatly among the
 322 plant functional traits (Table 2, Tables C1 and C2 in Appendix C). WD had the best performance
 323 in all three models, with R^2 values of 0.64, 0.68 and 0.67 for random forest, boosted regression
 324 trees and ensemble model, respectively. SLA and LPC had R^2 values greater than 0.45, while
 325 LDMC performed the worst, with R^2 values below 0.30.

326 **Table 2** Results of plant functional traits for cross-validated R^2 , NRMSE and MAE for
 327 random forest, boosted regression trees and ensemble model.

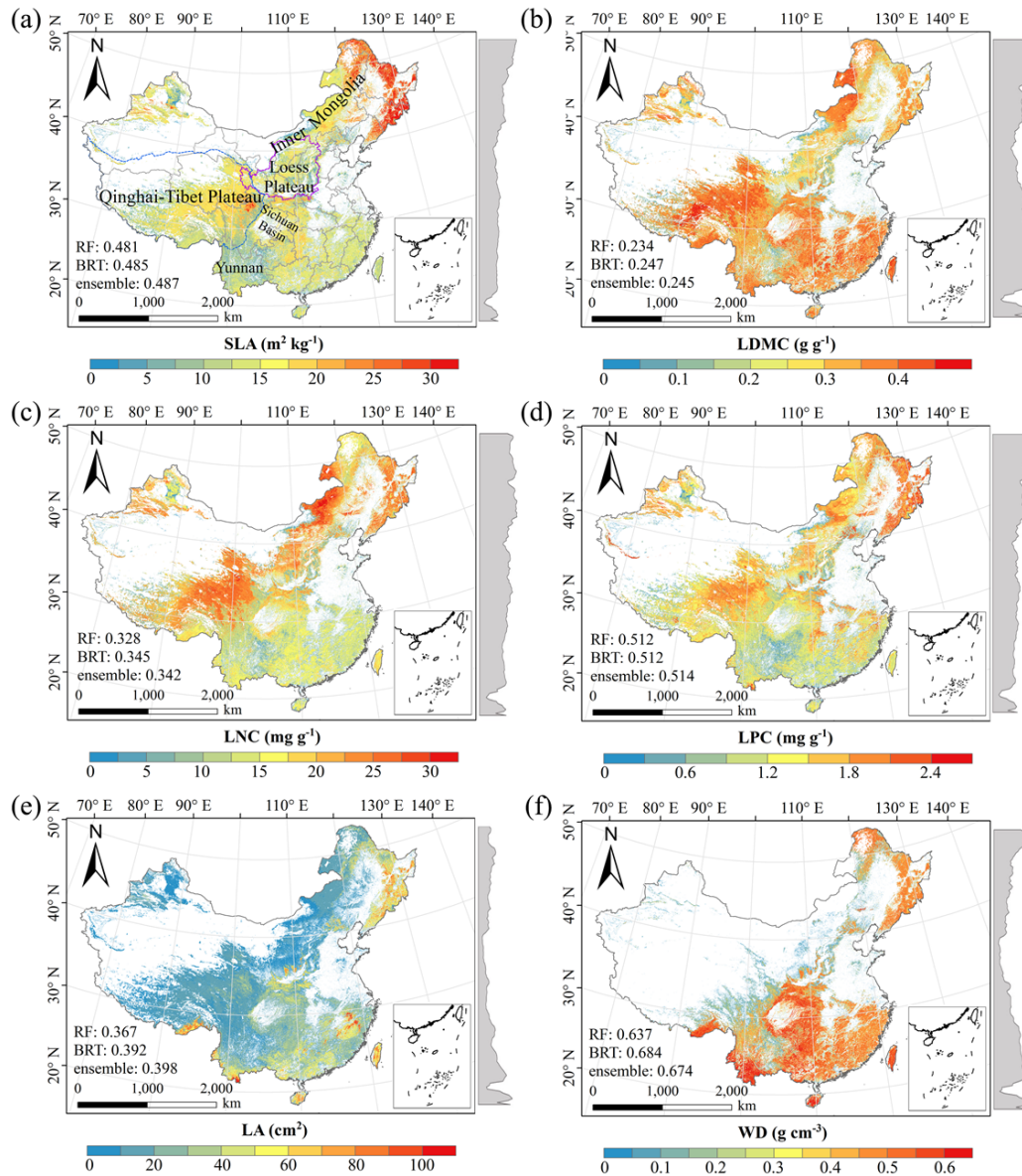
Traits	Random forest			Boosted regression trees			Ensemble model		
	R^2	NRMSE	MAE	R^2	NRMSE	MAE	R^2	NRMSE	MAE
SLA	0.48	0.22	5.10	0.48	0.20	5.08	0.49	0.21	5.07
LDMC	0.23	0.21	0.07	0.28	0.18	0.07	0.24	0.20	0.07
LNC	0.33	0.19	4.92	0.34	0.18	4.85	0.34	0.19	4.85
LPC	0.51	0.24	0.53	0.51	0.22	0.53	0.51	0.27	0.53
LA	0.37	0.45	26.76	0.39	0.51	27.47	0.40	0.58	26.59
WD	0.64	0.20	0.10	0.68	0.13	0.10	0.67	0.17	0.10

328 SLA, specific leaf area ($\text{m}^2 \text{kg}^{-1}$); LDMC, leaf dry matter content (g g^{-1}); LNC, leaf N concentration
 329 (mg g^{-1}); LPC, leaf P concentration (mg g^{-1}); LA, leaf area (cm^2); WD, wood density (g cm^{-3}); R^2 ,
 330 determinate coefficient; NRMSE, normalized root-mean-square error; MAE, mean absolute error.

331 **3.2 Spatial patterns of predicted plant functional traits**

332 There were relatively consistent spatial patterns for SLA, LNC and LPC, with high values in the
 333 northeastern and northwestern China and the southeastern Qinghai-Tibet Plateau, and low values
 334 in the southwestern China (Figs. 3a, 3c and 3d, Figs. D1, D2, D3, D5 and D6 in Appendix D).
 335 SLA and LPC increased with latitude, while LNC did not vary significantly along latitudinal
 336 gradient. For SLA, LNC and LPC, the variability was low among random forest, boosted
 337 regression trees and ensemble model, with an overall CV less than 0.30 (Figs. 4a, 4c and 4d).
 338 LDMC values were relatively high in most regions of China, and the low values were mainly
 339 located in the eastern Yunnan Province and the Loess Plateau (Fig. 3b, Figs. D1, D2 and D4 in
 340 Appendix D). LA showed high values in the northeastern and southern regions (except for the
 341 Sichuan Basin), and the southeastern Qinghai-Tibet Plateau (Fig. 3e, Figs. D1, D2 and D7 in
 342 Appendix D). The strong latitudinal gradient was observed in LA, where the values decreased
 343 with latitude.

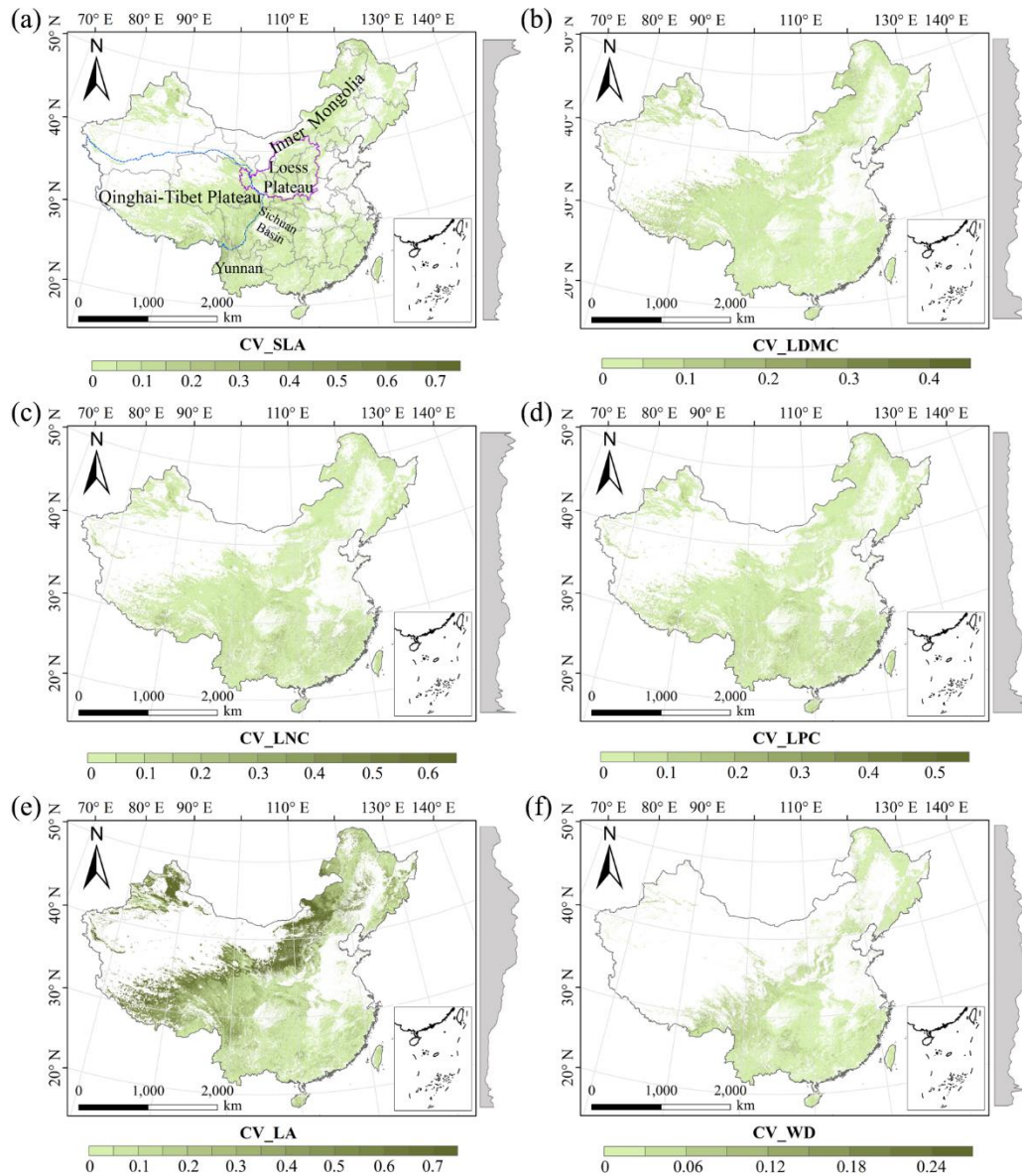
344 The CV values of LPC decreased with latitude, but other traits did not show latitudinal
 345 patterns (Fig. 4). The CV values of LA were relatively high, especially in the northwestern China
 346 and the Inner Mongolia-Loess Plateau region (Fig. 4e). WD had high values in the northeastern
 347 and southern regions (Fig. 2f, Figs. D1, D2 and D8 in Appendix D), while CV values for WD
 348 were low throughout China (Fig. 4f).



349

350

Figure 3. Spatial patterns of predicted plant functional traits in China based on the ensemble
 351 model. The grey curves to the right of the maps display trait distribution along with latitude. The
 352 white areas represent artificial land cover types and bare vegetation. The lines in grey, blue and
 353 purple represent the boundaries of province, the Qinghai-Tibet Plateau and the Loess Plateau,
 354 respectively. RF, random forest; BRT, boosted regression trees; ensemble, ensemble model; SLA,
 355 specific leaf area; LDMC, leaf dry matter content; LNC, leaf N concentration; LPC, leaf P
 356 concentration; LA, leaf area; WD, wood density.



357

358 **Figure 4.** The variability in plant functional trait predictions among random forest, boosted
 359 regression trees and ensemble model. The grey curves to the right of the maps display coefficient
 360 of variation along with latitude. The white areas represent artificial land cover types and bare
 361 vegetation. The lines in grey, blue and purple represent the boundaries of province, the Qinghai-
 362 Tibet Plateau and the Loess Plateau, respectively. SLA, specific leaf area; LDMC, leaf dry matter
 363 content; LNC, leaf N concentration; LPC, leaf P concentration; LA, leaf area; WD, wood density.

364 **3.3 Relative importance of predictive variables**

365 The dominant factors explaining spatial variation differed greatly among plant functional traits
 366 (Table 3). Overall, climate variables were more important for predicting plant functional traits
 367 than were soil variables. Temperature variables (i.e., MAT, MDR and TS) showed close
 368 relationships with SLA, LDMC, LPC and WD, while precipitation variables (i.e., PS, PEQ, MAP

369 and PDQ) were more important for predicting the spatial patterns of LNC, LPC and LA. RAD was
 370 the fourth most dominant factor in predicting the spatial patterns of SLA and WD. Elevation also
 371 played an important role in LDMC and LPC predictions. Within soil variables, soil nutrients (i.e.,
 372 pH and SAP) showed close associations with SLA and LNC. In addition to the environmental
 373 variables, MTCI emerged as an important predictor for explaining SLA, LDMC and LA. Finally,
 374 EVI was the most important predictor for LA, and MIR in January and May were the primary
 375 predictors of WD. The relationships between plant functional traits and the most important
 376 variables were shown in Figs. E1 and E2 in Appendix E.

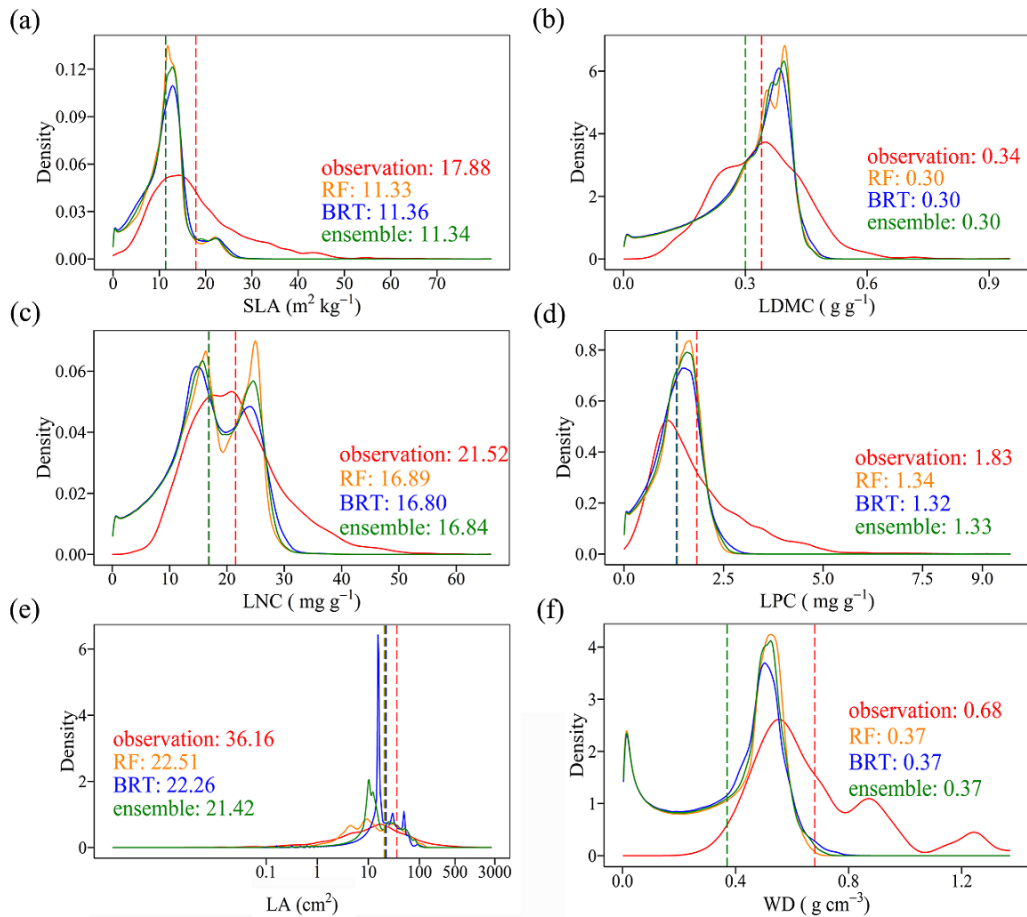
377 **Table 3** List of the eight most important variables for plant functional trait predictions.

Rank	SLA	LDMC	LNC	LPC	LA	WD
1	SAP	MAT	PS	MDR	EVI5	MIR1
2	TS	Elevation	SAP	PDQ	PEQ	TS
3	blue9	MTCI5	pH	Elevation	MTCI9	MIR5
4	RAD	blue8	MDR	MIR8	NIR9	RAD
5	MTCI4	MTCI4	MAP	Tmax	AI	MIR6
6	MTCI6	MTCI6	PEQ	MTCI6	MTCI6	pH
7	Elevation	NIR1	MIR1	MIR7	MAP	red5
8	MTCI7	CEC	Tmax	MIR9	red5	PS

378 SLA, specific leaf area ($\text{m}^2 \text{kg}^{-1}$); LDMC, leaf dry matter content (g g^{-1}); LNC, leaf N concentration
 379 (mg g^{-1}); LPC, leaf P concentration (mg g^{-1}); LA, leaf area (cm^2); WD, wood density (g cm^{-3}); SAP, soil
 380 available P; TS, temperature seasonality; blue, blue reflectance; RAD, solar radiation; MTCI, MERIS
 381 terrestrial chlorophyll index; MAT, mean annual temperature; NIR, near-infrared reflectance; CEC,
 382 cation exchange capacity; PS, precipitation seasonality; MDR, mean diurnal range; MAP, mean annual
 383 precipitation; PEQ, precipitation of the wettest quarter of a year; MIR, middle infrared reflectance;
 384 Tmax, max temperature of the warmest month of a year; PDQ, precipitation of the driest quarter of a
 385 year; EVI, enhanced vegetation index; AI, aridity index; red, red reflectance.

386 **3.4 Model performance**

387 The distributions of the predicted values based on random forest, boosted regression trees and
 388 ensemble model were consistent with the original observations, especially the peak values (Fig. 5).
 389 The mean values of trait observations were relatively higher than those of the predicted values.

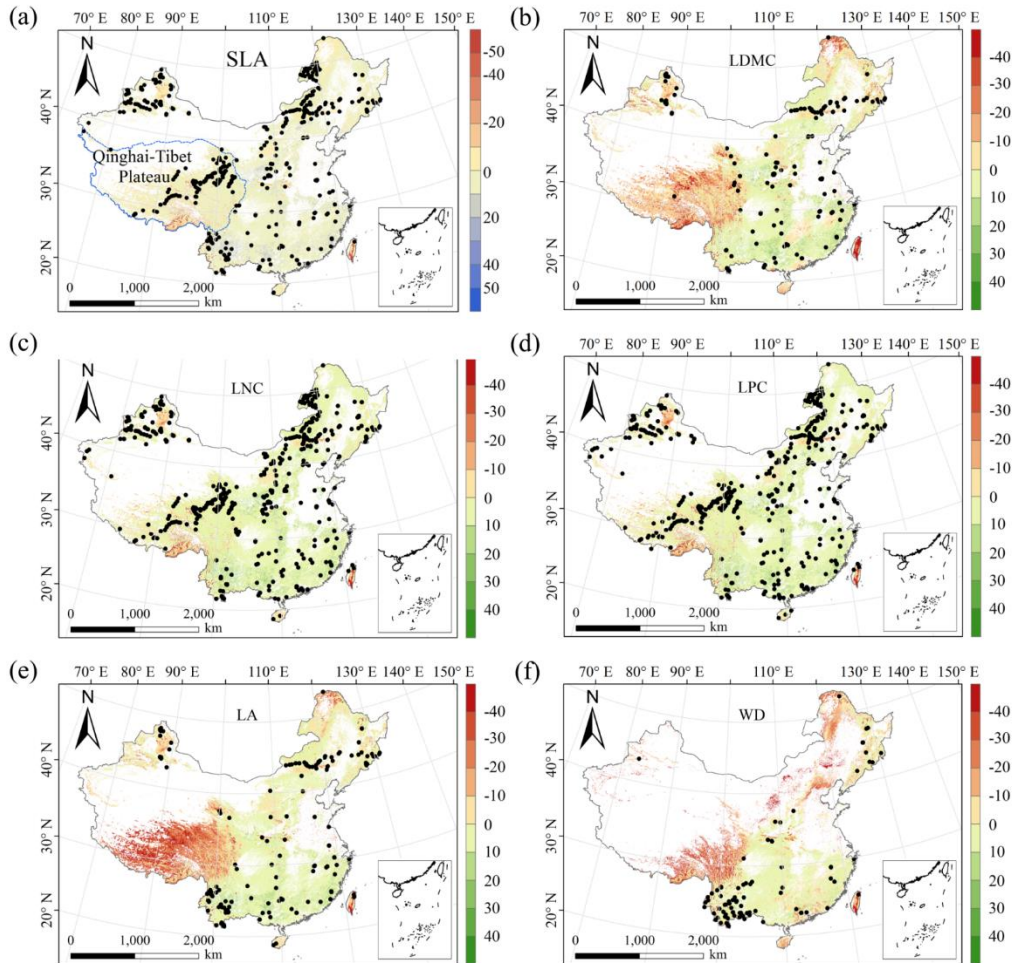


390

391 **Figure 5.** Comparison of trait distribution between observations and predictions in the three
 392 models. Each panel depicts the distribution of observations in solid red, of the random forest (RF)
 393 in yellow, of the boosted regression trees (BRT) in blue, and of the ensemble model in green. The
 394 dashed vertical lines indicate mean values. SLA, specific leaf area; LDMC, leaf dry matter content;
 395 LNC, leaf N concentration; LPC, leaf P concentration; LA, leaf area; WD, wood density.

396 3.5 Uncertainty assessments

397 The MESS values of all plant functional traits were positive in most regions, indicating a wide
 398 applicability domain of our models (Fig. 6). Nevertheless, trait predictions should be interpreted
 399 carefully for the northeastern China and the Qinghai-Tibet Plateau due to sparse samplings in
 400 these regions.



401

402

403

404

405

406

407

408

Figure 6. Multivariate environmental similarity surface (MESS) assessments for the six plant functional traits. The blue line represents the boundary of the Qinghai-Tibet Plateau. The black dots represent the locations of trait observations. More intense shades indicate greater similarity (blue) or difference (red) in environmental conditions of the location compared to the predictive factors covered by the training dataset. The white areas represent artificial land cover types and bare vegetation. SLA, specific leaf area; LDMC, leaf dry matter content; LNC, leaf N concentration; LPC, leaf P concentration; LA, leaf area; WD, wood density.

409

4 Discussion

410

4.1 Comparison with previous work

411

412

413

414

415

416

Our study predicted the spatial patterns of six key plant functional traits across China using machine learning methods and identified the applicability domain of the models. WD had the highest precision with an average of R^2 of 0.66, which was higher than the global WD prediction (Boonman et al., 2020). This improvement in precision may be attributed to the large number and dense occurrence of sample sites as well as the inclusion of vegetation indices in our study. In addition, SLA and LPC also showed good accuracy with R^2 values of 0.50, which was higher than

417 that of Boonman et al. (2020) and consistent with that of Moreno-Martínez et al. (2018). However,
418 LNC and LA showed relatively poor performance, which may be related to the reason that the two
419 traits were more influenced by phylogeny than environmental variables (Yang et al., 2017; An et
420 al., 2021). In addition, we found that mean values of trait predictions were lower than those of
421 observations, which may be attributable to the reason that the mean values of trait observations
422 were from the individual level, while the mean values of predicted values were based on the
423 relative abundance of PFTs and corresponding predicted values within 1 km grid cell.

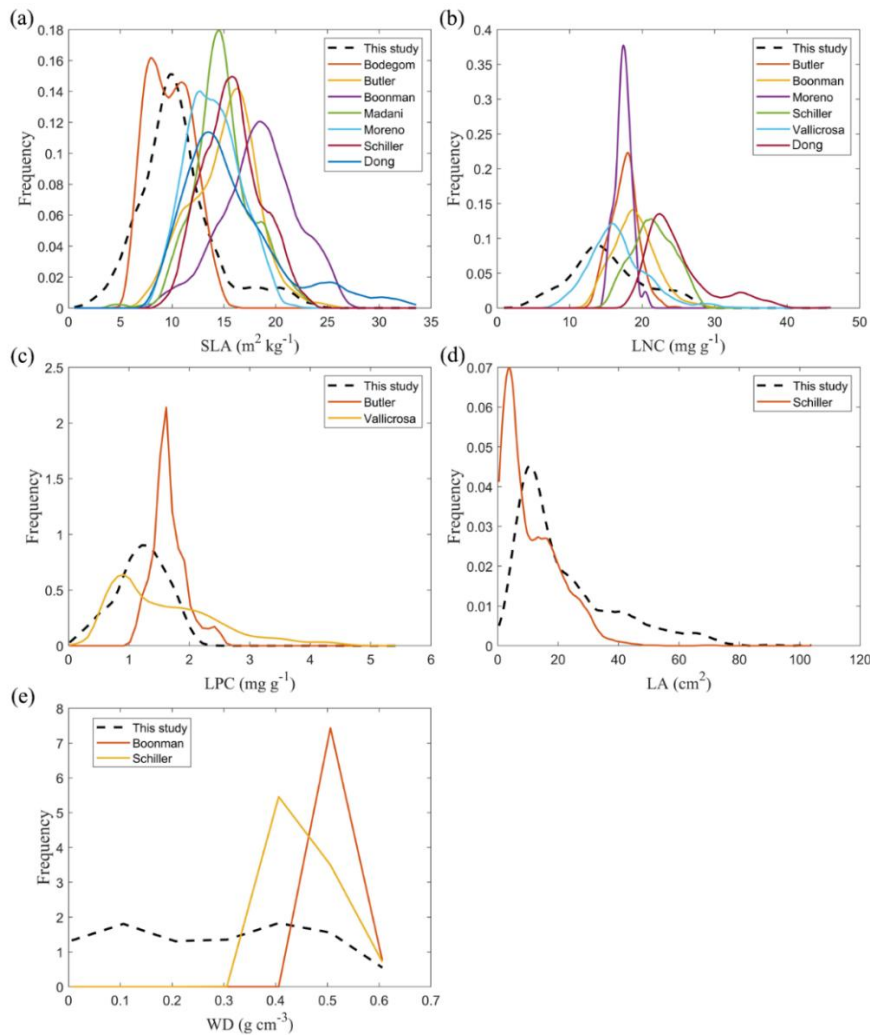
424 The frequency distributions of plant functional traits in China differed between our study and
425 previous studies (Fig. 7, Fig. F1, Table F1 in Appendix F). Given that the spatial resolution of trait
426 maps in most previous studies was 0.5° (except for Moreno-Martínez et al. (2018) and Vallicrosa
427 et al. (2022)), we resampled the data products of previous studies and our study to 0.5° spatial
428 resolution. The distributions in our study contained more predictions at lower values of SLA, LNC
429 and LPC and were broader than those for SLA and LNC in previous global studies. However, the
430 distribution of LNC in our study was consistent with that in the study of Vallicrosa et al. (2022)
431 with a 1 km spatial resolution (Fig. F1 in Appendix F). LA in our study contained more
432 predictions at higher values and was also broader than those in previous global studies. WD did
433 not show lower and higher predicted values in this study, however, the WD values in the studies of
434 Boonman et al. (2020) and Schiller et al. (2021) had more predictions at higher values and no
435 lower values ($< 0.30 \text{ g cm}^{-3}$). Our predicted values of SLA showed the highest spatial correlation
436 with those of Dong et al. (2023), and LNC showed the strongest spatial correlation with those of
437 Butler et al. (2017) (Table 4). LA and WD showed the best spatial correlation with those of
438 Schiller et al. (2021), but LPC showed relatively weak spatial correlation with those of published
439 studies.

440 In addition, we compared our results with the other studies focused on China. Yang et al.
441 (2016) predicted the spatial distributions of leaf mass per area (i.e., 1/SLA) and LNC based on
442 trait-environment relationships in China and had R^2 values of 0.13-0.16. The lower predictive
443 precision may be because Yang et al. (2016) only used MAT, MAP and RAD as predictors in
444 estimating the spatial patterns of leaf mass per area and LNC, which likely led to poor
445 performance and low heterogeneity. These results also demonstrated the advantage of our methods
446 in mapping the spatial patterns of plant functional traits at a regional scale.

447 **Table 4** Spatial correlations for SLA, LNC, LPC, LA and WD between this study and
 448 previous trait maps, labelled by the first author of the corresponding publication (see Table F1 in
 449 Appendix F for citations)

Spatial correlation	Dong	Vallicrosa	Schiller	Boonman	Moreno	Madani	Butler	Bodegom
SLA	0.40		-0.08	0.33	0.24	0.14	-0.04	0.32
LNC	0.16	0.36	0.23	0.25			0.39	
LPC		0.14					0.06	
LA			0.51					
WD			0.65	0.11				

450 The spatial correlation of leaf dry matter content (LDMC) between our study and previous studies was
 451 not included, as the LDMC maps were not available. SLA, specific leaf area ($\text{m}^2 \text{kg}^{-1}$); LNC, leaf N
 452 concentration (mg g^{-1}); LPC, leaf P concentration (mg g^{-1}); LA, leaf area (cm^2); WD, wood density (g cm^{-3}).
 453



454 **Figure 7.** Frequency distributions of plant functional traits in our study (“This study”, dashed
 455 black lines) and other trait maps identified by the first author of the corresponding publication (see
 456 Table F1 for citations). SLA, specific leaf area ($\text{m}^2 \text{kg}^{-1}$); LNC, leaf N concentration (mg g^{-1}); LPC,
 457 leaf P concentration (mg g^{-1}); LA, leaf area (cm^2); WD, wood density (g cm^{-3}).
 458

459 **4.2 Spatial patterns of plant functional traits in China**

460 Our study revealed the spatial patterns of different plant functional traits across China, and the
461 variability among the two machine learning methods was relatively low. We compared the spatial
462 differences of trait maps between our study and previous studies at the global scale (Figs. F2-F6 in
463 Appendix F). For example, our study showed high SLA values in the southeastern Qinghai-Tibet
464 Plateau, which concurred with the global study of Boonman et al. (2020). The spatial difference of
465 SLA between our study and van Bodegom et al. (2014) was relatively low, and the predicted
466 values in most regions were slightly lower in our study than those in van Bodegom et al. (2014).
467 The spatial pattern of difference in SLA between our study and Moreno et al. (2018), Bulter et al.
468 (2017) and van Bodegom et al. (2014) was consistent, and the values were higher in the
469 northeastern China and the southwestern Qinghai-Tibet Plateau in our study than those studies.
470 Our study showed higher LNC values in the northern Inner Mongolia-the Loess Plateau-the
471 eastern Qinghai-Tibet Plateau and the northwestern China than those global studies (Butler et al.,
472 2017; Moreno-Martínez et al., 2018; Boonman et al., 2020; Vallicrosa et al., 2022; Dong et al.,
473 2023), reflecting the consistent spatial pattern among these studies. However, Yang et al. (2016)
474 predicted high LNC values in the northeastern and the northwestern China, the northern Inner
475 Mongolia and the entire Qinghai-Tibet Plateau, and SLA and LNC had low heterogeneity overall.
476 The discrepancy with Yang et al. (2016) may be attributed to spatial extrapolation based on trait-
477 climate relationships with a low predictive precision. There was no consistent spatial pattern in
478 LPC between our study and previous studies. Consistent with the global pattern (Wright et al.,
479 2017), LA was larger in the southern regions than in the northern regions and showed a decreasing
480 trend with latitude. In addition, LA and WD values in our study were lower in most regions than
481 those ones at the global scale. These discrepancies between our study and previous studies at the
482 global scale may be related to three reasons. First, there is bias in the available in-situ field
483 measurement data from China in global studies, with a large gap in the western China for SLA and
484 no data in China for WD (Boonman et al., 2020). Second, some trait-environment relationships
485 may be scale-dependent (Bruehlheide et al., 2018), and these studies we compared are from the
486 global scale because the trait maps in China are not available. Third, the methods used for trait
487 mapping were different among studies, including eco-evolutionary optimality models (Dong et al.,
488 2023), Convolutional Neural Networks based on RGB photographs (Schiller et al., 2021), machine
489 learning algorithms (Vallicrosa et al., 2022; Boonman et al., 2020) and multiple regression
490 analysis (van Bodegom et al., 2014).

491 Moreover, our study also identified the applicability domain of our models for predicting the
492 spatial patterns of plant functional traits across China. Five leaf traits and WD appeared to have
493 poor applicability in the northeastern China and the Qinghai-Tibet Plateau, primarily due to sparse
494 samplings. Future studies predicting plant functional traits across a large scale through remote
495 sensing observations or other supplementary data will be needed to re-evaluate our results.

496 **4.3 The role of predictive variables**

497 Our study indicated that environmental variables were important for predicting the spatial patterns
498 of plant functional traits, especially climate variables. Temperature variables were primary
499 predictors for SLA, LDMC, LPC and WD. The relationships between leaf traits and temperature
500 have been widely discussed in global and regional studies (Reich and Oleksyn, 2004; Bruelheide
501 et al., 2018). The positive linkage between WD and temperature may be driven by changes in
502 water viscosity. Plants can adapt to low water viscosity at high temperatures by reducing the
503 diameter and density of their vessels and thickening cell walls (Roderick and Berry, 2002; Thomas
504 et al., 2004). Precipitation variables were important predictors for leaf nutrient traits and LA. For
505 example, precipitation of the wettest quarter of a year was the factor that most influenced LA
506 variation, which has been confirmed by a previous study (An et al., 2021). A smaller LA could be
507 an adaptive strategy to decrease water loss via reducing the surface area for transpiration under
508 dry environmental conditions (Du et al., 2019). Although the effects of soil on trait predictions
509 were relatively weak, we found that SAP and pH played key roles in SLA and LNC predictions.
510 These results were similar with the previous studies reporting that soil pH was an important driver
511 of trait variation at the global scale and in tundra regions (Maire et al., 2015; Kempainen et al.,
512 2021). Additionally, from the perspective of cost-efficient theory, the strong effects of SAP
513 reflected that high SLA may be an adaptation for facilitating soil exploration more efficiently in
514 fertile soils (Freschet et al., 2010).

515 Vegetation indices have recently been proposed as important predictors of spatial patterns of
516 plant functional traits (Loozen et al., 2018). Our results corroborated these findings and further
517 suggested that EVI, MTCI and MIR reflectance were important predictors in models. Here, the
518 underlying mechanisms between vegetation indices and plant functional traits were not further
519 discussed due to their complexity. However, our results indicated that vegetation indices and NIR
520 reflectance were not key predictors of LNC estimation, which contrasted the findings from global
521 and regional studies (Wang et al., 2016; Loozen et al., 2018; Moreno-Mart ínez et al., 2018). This
522 may be related to the multitude of factors that influence the relationships between LNC and
523 vegetation indices and NIR reflectance, such as forest type and canopy structure (Dahlin et al.,
524 2013).

525 **4.4 Uncertainties**

526 Although our study mapped the spatial patterns of key functional traits in terrestrial ecosystems
527 across China through large-scale field investigations and compared the predictions with previous
528 studies at global and regional scales, there persisted some uncertainties in the interpretation of
529 these results. First, the predictive ability of models was relatively worse for certain traits,
530 especially LDMC. Beyond the environmental effects, the variation in plant functional traits is also
531 regulated by phylogenetic structure among plant species (e.g., family, order and phylogenetic
532 clade) (Li et al., 2017). Consequently, incorporating phylogenetic information will be a promising

533 avenue for further improving the accuracy of spatial predictions of plant functional traits (Butler et
534 al., 2017). A second potential issue is sampling bias; there are major spatial gaps in field
535 investigations in the northeastern China and the Qinghai-Tibet Plateau. Due to the few
536 measurements for shrubs and herbs, WD data is mainly confined to eastern forests, and the overall
537 quantity of WD data is much lower than that of leaf traits, even in the TRY database. The
538 environmental information of sampling sites was not always obtained from original literature, thus
539 using the public environmental products is a common resolution in large-scale plant trait studies
540 (Boonman et al., 2020; Vallicrosa et al., 2022). Such mismatch between in-situ trait measurements
541 and predictors should be resolved in further work. Finally, an additional key challenge in data
542 availability must be resolved to scale up from the species to the community levels, in particular
543 with data surrounding species co-occurrence and their relative cover or abundance in ecological
544 communities (He et al., 2023). For example, Global biodiversity data (e.g., sPlot and Global
545 Biodiversity Information Agency databases) that contains information on species occurrence or
546 the proportion of species in a community has the potential for enabling the calculation of
547 community-weighted trait values and the re-evaluation of our results in future work (Telenius,
548 2011; Bruelheide et al., 2019). The lack of consistent time period and spatial resolution of
549 predictors due to limitation of data availability is a key challenge in the spatial mapping of plant
550 functional traits. In addition, although WorldClim version 2.1 product has high spatial resolution
551 and includes various aspects of climatic parameters, there exists certain limitation and uncertainty
552 in predicting trait maps. Therefore, integrating satellite remote sensing monitoring methods with
553 in-situ trait data can also provide an effective way to estimate and assess the species diversity at
554 large scales (Cavender-Bares et al., 2022).

555 **4.5 Potential applications**

556 Maps of these key functional traits in terrestrial ecosystems highlighted large-scale variability in
557 space, which will significantly advance ecological analyses and future interdisciplinary research.
558 First, using the spatially continuous trait maps, one can optimize and develop trait-flexible
559 vegetation models to reduce uncertainty of conventional vegetation models based on PFTs, which
560 allows for exploration of the community assembly rules based on how plants with different trait
561 combinations perform under a given set of environmental conditions (Berzaghi et al., 2020). When
562 trait-flexible vegetation models are available, incorporating trait maps into models will bridge the
563 gap for vegetation classifications and predictions of vegetation distribution under global change
564 (van Bodegom et al., 2012; Yang et al., 2019). Second, most studies focused on the effects of plant
565 functional traits on ecosystem carbon processes at individual, species and community scales, while
566 how such effects scale up to regional or larger scales remains challenging. In addition, the
567 assessments of China's terrestrial ecosystem carbon sink have large uncertainties (Piao et al.,
568 2022). The spatial continuous trait maps will provide an effective way to link ecosystem
569 characteristics to ecosystem carbon sink estimates in China (Madani et al., 2018; Šímová et al.,

570 2019). These analyses will help shed light on the mechanisms underlying plant functional traits
571 and terrestrial ecosystem carbon storage at a large scale.

572 **5 Data availability**

573 The original plant functional trait data collected in this study that was used for machine learning
574 models (named by Data file used for machine learning models.csv) and final maps of plant
575 functional traits in a GeoTIFF format (named by plant functional trait category) are now available
576 for the private link <https://figshare.com/s/c527c12d310cb8156ed2> (An et al., 2023). Once the
577 article is accepted, we will publicly publish the data at the figshare website.

578 **6 Conclusions**

579 We generated a set of spatial continuous trait maps at a 1-km spatial resolution using machine
580 learning methods in combination with field measurements, environmental variables and vegetation
581 indices. Models for leaf traits (except for LDMC) and WD showed good accuracy and robustness,
582 whereas models of LDMC had relatively poor precision and robustness. Temperature variables
583 were the most important predictors for leaf traits (except for LA) and WD, and precipitation
584 variables were the most important predictors for leaf nutrient traits and LA. We caution that plant
585 functional trait predictions should be interpreted carefully for the northeastern China and the
586 Qinghai-Tibet Plateau. The spatial continuous trait maps generated in our study are
587 complementary to current terrestrial in-situ observations and offer new avenues for predicting
588 large-scale changes in vegetation and ecosystem functions under climate scenarios in China.

589

590 **Appendix A Data collection from literature**

591 An H. and Shanguan Z. P. Photosynthetic characteristics of dominant plant species at different succession stages
592 of vegetation on Loess Plateau. Chinese Journal of Applied Ecology, 2007, 18, 1175-1180.

593 Bai K. D., Jiang D. B., Wan C. X. Photosynthesis-nitrogen relationship in evergreen and deciduous tree species at
594 different altitudes on Mao'er Mountain, Guangxi. Acta Ecologica Sinica, 2013, 33, 4930-4938.

595 Bai W. J., Zheng F. L., Dong L. L., et al. Leaf traits of species in different habits in the water-wind erosion region
596 of the Loess Plateau. Acta Ecologica Sinica, 2010, 30, 2529-2540.

597 Chai Y F., Shang H. L., Zhang X. F., et al. Ecological variations of woody species along an altitudinal gradient in
598 the Qinling Mountains of Central China: area-based versus mass-based expression of leaf traits. Journal of
599 Forestry Research, 2021, 32, 599-608.

600 Chang Y. N., Zhong Q. L., Cheng D. L., et al. Stoichiometric characteristics of C, N, P and their distribution
601 pattern in plants of *Castanopsis carlesii* natural forest in Youxi. Journal of Plant Resources and Environment,
602 2013, 22, 1-10.

603 Chen F. Y., Luo T. X., Zhang L., et al. Comparison of leaf construction cost in dominant tree species of the
604 evergreen broadleaved forest in Jiulian Mountain, Jiangxi Province. Acta Ecologica Sinica, 2006, 26, 2485-
605 2493.

606 Chen H. Y., Huang Y. M., He K. J., et al. Temporal intraspecific trait variability drives responses of functional

607 diversity to interannual aridity variation in grasslands. *Ecology and Evolution*, 2018, 9, 5731-5742.

608 Chen L. X., Xiang W. H., Wu H. L., et al. Tree growth traits and social status affect the wood density of pioneer
609 species in secondary subtropical forest. *Ecology and Evolution*, 2017, 7, 5366-5377.

610 Chen L., Yang X. G., Song N. P., et al. Leaf water uptake strategy of plants in the arid-semiarid region of Ningxia.
611 *Journal of Zhejiang University*, 2013, 39, 565-574.

612 Chen Y. H., Han W. X., Tang L. Y., et al. Leaf nitrogen and phosphorus concentrations of woody plants differ in
613 responses to climate, soil and plant growth form. *Ecography*, 2011, 36, 178-184.

614 Cheng J. H., Chu P. F., Chen D. M., et al. Functional correlations between specific leaf area and specific root length
615 along a regional environmental gradient in Inner Mongolia grasslands. *Functional Ecology*, 2016, 30, 985-997.

616 Cheng W., Yu C. H., Xiong K. N., et al. Leaf functional traits of dominant species in karst plateau-canyon areas.
617 *Guihaia*, 2019, 39, 1039-1049.

618 Dong H. and Shekhar R. B. Negative relationship between interspecies spatial association and trait dissimilarity.
619 *Oikos*, 2019, 128, 659-667.

620 Dong T. F., Feng Y. L., Lei Y. B., et al. Comparison on leaf functional traits of main dominant woody species in
621 wet and dry habitats. *Chinese Journal of Ecology*, 2012, 31, 1043-1049.

622 Du H. D. Ecological responses of foliar anatomical structural & physiological characteristics of dominant plants at
623 different site conditions in north Shaanxi Loss Plateau. 2010, Graduation Thesis.

624 Fan Z. X., Zhang S. B., Hao G. Y., et al. Hydraulic conductivity traits predict growth rates and adult stature of 40
625 Asian tropical tree species better than wood density. *Journal of Ecology*, 2012, 100, 732-741.

626 Feng J. B., Fan S. X., Hou Y. F., et al. Interspecific and intraspecific variation of leaf function traits of herbaceous
627 plants in a forest-steppe zone, Hebei Province, China. *Journal of Northeast Forestry University*, 2021, 49, 23-
628 28.

629 Feng Q. H. The study on the response of foliar $\delta^{13}C$ of different life form plants to altitude in subalpine area of
630 Western Sichuan, China. 2011, Graduation Thesis.

631 Fu P. L., Zhu S. D., Zhang J. L., et al. The contrasting leaf functional traits between a karst forest and a nearby
632 non-karst forest in south-west China. *Functional Plant Biology*, 2019, 46, 907-915.

633 Gao S. P., Li J. X., Xu M. C., et al. Leaf N and P stoichiometry of common species in successional stages of the
634 evergreen broad-leaved forest in Tiantong National Forest Park, Zhejiang Province, China. *Acta Ecologica
635 Sinica*, 2007, 27, 947-952.

636 Geekiyana N., Goodale, U. M., Cao, K. F., et al. Leaf trait variations associated with habitat affinity of tropical
637 karst tree species. *Ecology and Evolution*, 2017, 8, 286-295.

638 Geng Y., Ma W. H., Wang L., et al. Linking above- and belowground traits to soil and climate variables: an
639 integrated database on China's grassland species. *Ecology*, 2017, 98, 1471.

640 Guo F. C. The photosynthetic characteristics of precious broad-leaved tree species in south subtropics and their
641 relationship with leaf functional traits. 2015, Graduation Thesis.

642 Guo W. J. Exploring the relationship between arbuscular mycorrhizal fungi and plant based on phylogeny and
643 plant traits. 2015, Graduation Thesis.

644 Hau C. H. Tree seed predation on degraded hillsides in Hong Kong. *Forest Ecology & Management*. 1997, 99,
645 215-221.

646 He J. S., Wang Z. H., Wang X. P., et al. A test of the generality of leaf trait relationships on the Tibetan Plateau.
647 *New Phytologist*, 2006, 170, 835-848.

648 He P. C., Wright I. J., Zhu S. D., et al. Leaf mechanical strength and photosynthetic capacity vary independently
649 across 57 subtropical forest species with contrasting light requirements. *New Phytologist*, 2019, 223, 607-618.

650 He Y. T. Studies on physioecological traits of 30 plant species in the Subalpine Meadow of the Qinling Mountains.

651 2007, Graduation Thesis.

652 Hou M. M. Adaptive evolution of some species from sedges (*Carex Cyperaceae*) based on phylogeny and leaf
653 functional traits to habitat in the Poyang Lake Area. 2017, Graduation Thesis.

654 Hou Y., Liu M. X., Sun H. R., et al. Response of plant leaf traits to microhabitat change in a subalpine meadow on
655 the eastern edge of Qinghai-Tibetan Plateau, China. *Chinese Journal of Applied Ecology*, 2017, 28, 71-79.

656 Hu Z. Z., Michaletz S. T., Johnson D. J., et al. Traits drive global wood decomposition rates more than climate.
657 *Global Change Biology*, 2018, 24, 5259-5269.

658 Hua L., He P., Goldstein G., et al. Linking vein properties to leaf biomechanics across 58 woody species from a
659 subtropical forest. *Plant Biology*, 2019, 22, 212-220.

660 Huang J. J. and Wang X. H. Leaf nutrient and structural characteristics of 32 evergreen broad-leaved species.
661 *Journal of East China Normal University (Natural Science)*, 2003, 1, 92-97.

662 Huang Y. L. The research about the turnover patterns and moisture adaptation mechanism of major species on the
663 South-North-facing slope. 2012, Graduation Thesis.

664 Iida Y., Kohyama T. S., Swenson N. G., et al. Linking functional traits and demographic rates in a subtropical tree
665 community: the importance of size dependency. *Journal of Ecology*, 2014, 102, 641-650.

666 Jia Q. Q. Functional traits of fine roots and their relationship with leaf traits of 50 major species in a subtropical
667 forest in Gutianshan. 2011, Graduation Thesis.

668 Jiang Y., Chen X., Ma J., et al., Interspecific and intraspecific variation in functional traits of subtropical evergreen
669 and deciduous broadleaved mixed forests in karst topography, Guilin, Southwest China. *Tropical*
670 *Conservation Science*, 2016, 9.

671 Jin Y., Wang C. K., Zhou Z. H., et al. Co-ordinated performance of leaf hydraulics and economics in 10 Chinese
672 temperate tree species. *Functional Plant Biology*, 2016, 43, 1082-1090.

673 Jing G. H. Responses of grassland community structure and functions to management practices on the semi-arid
674 area of Loess Plateau. 2017, Graduation Thesis.

675 Kang M. Spatial distribution pattern and its causes of woody plant functional traits in Tiantong region, Zhejiang
676 Province. 2012, Graduation Thesis.

677 Krober W., Li Y., Hardtle W., et al. Early subtropical forest growth is driven by community mean trait values and
678 functional diversity rather than the abiotic environment. *Ecology and Evolution*, 2015, 5, 3541-3556.

679 Krober W., Bohnke M., Welk E., et al. Leaf trait-environment relationships in a subtropical broadleaved forest in
680 south-east China. *PloS One*, 2012, 7, e35742.

681 Krober W., Zhang, S. R. Ehmgig, M., et al. Linking xylem hydraulic conductivity and vulnerability to the leaf
682 economics spectrum-a cross-species study. *PloS One*, 2014, e109211.

683 Li F. Comparison of functional traits in semi-humid evergreen broad-leaved in Western Hill of Kunming. 2011,
684 Graduation Thesis.

685 Li K. and Xiang W. H. Comparison of specific leaf area, SPAD value and seed mass among subtropical tree
686 species in hilly area of Central Hunan, China. *Journal of Central South University of Forestry & Technology*,
687 2011, 31, 213-218.

688 Li L., McCormack M. L., Ma C.G., et al. Leaf economics and hydraulic traits are decoupled in five species-rich
689 tropical-subtropical forests. *Ecology Letters*, 2015, 18, 899-906.

690 Li Q. Leaf functional traits and their relationships with environmental factors in Beishan Mountain of Jinhua,
691 Zhejiang Province. 2020, Graduation Thesis.

692 Li S. J., Su P. X., Zhang H. N., et al. Characteristics and relationships of foliar water and leaf functional traits of
693 desert plants. *Plant Physiology Journal*, 2013, 49, 153-160.

694 Li W. H., Xu F. W., Zheng S. X., et al. Patterns and thresholds of grazing-induced changes in community structure

695 and ecosystem functioning: species-level responses and the critical role of species traits. *Journal of Applied*
696 *Ecology*, 2017, 54, 963-975.

697 Li W. Q., Xu Q., Li J., et al. Quantification of ecotone width of returned forest land from farmland based on
698 specific leaf area. *Journal of West China Forestry Science*, 2017, 46, 117-121.

699 Li X. F., Pei K. Q., Kery M., et al. Decomposing functional trait associations in a Chinese subtropical forest. *PloS*
700 *One*, 2017, 12, e0175727.

701 Li X. F., Schmid B., Wang F., et al. Net assimilation rate determines the growth rates of 14 species of subtropical
702 forest trees. *PloS One*, 2016, 11, e0150644.

703 Li X. L., Li X. H., Jiang D. M., et al. Leaf morphological characters of 22 compositae herbaceous species in
704 Horqin sandy land. *Chinese Journal of Ecology*, 2005, 24, 1397-1401.

705 Li Y. H., Luo T. X., Lu Q., et al. Comparisons of leaf traits among 17 major plant species in Shazhuyu Sand
706 Control Experimental Station of Qinghai Province. *Acta Ecologica Sinica*, 2005, 25, 994-999.

707 Li Y. L., Meng Q. T., Zhao X. Y., et al. Relationships of fresh leaf traits and leaf litter decomposition in Kerqin
708 Sandy Land. *Acta Ecologica Sinica*, 2008, 28, 2486-2494.

709 Li Y., Yao J., Yang S., et al. Trait differences research on leaf function of Liaodong oak forest main species in
710 Dongling mountain. *Guangdong Agricultural Sciences*, 2012, 23, 159-162, 171.

711 Liang X. Y., Ye Q., Liu H., et al. Wood density predicts mortality threshold for diverse trees. *New Phytologist*,
712 2021, 229, 3053-3057.

713 Li, R., Zhu, S., Chen, H. Y. H., et al. Are functional traits a good predictor of global change impacts on tree species
714 abundance dynamics in a subtropical forest? *Ecology Letters*, 2015, 18, 1181-1189.

715 Li Y. Y., Shi H., Shao M. A. Cavitation resistance of dominant trees and shrubs in Loess hilly region and their
716 relationship with xylem structure. *Journal of Beijing Forestry University*, 2010, 32, 8-13.

717 Lin G. G., Guo, D. L., Li, L., et al. Contrasting effects of ectomycorrhizal and arbuscular mycorrhizal tropical tree
718 species on soil nitrogen cycling: the potential mechanisms and corresponding adaptive strategies. *Oikos*, 2018,
719 127, 518-530.

720 Liu C. H. and Li Y. Y. Relationship between leaf traits and PV curve parameters in the typical deciduous woody
721 plants occurring in Southern Huanglong Mountain. *Journal of Northwest Forestry University*, 2013, 28, 1-5.

722 Liu G. F., Freschet G. T., Pan X., et al. Coordinated variation in leaf and root traits across multiple spatial scales in
723 Chinese semi-arid and arid ecosystems. *New Phytologist*, 2010, 188, 543-553.

724 Liu G. F., Wang L., Jiang L., et al. Specific leaf area predicts dryland litter decomposition via two mechanisms.
725 *Journal of Ecology*, 2017, 106, 218-229.

726 Liu J. H., Zeng D. H. and Don K. L. Leaf traits and their interrelationships of main plant species in southeast
727 Horqin sandy land. *Chinese Journal of Ecology*, 2006, 25, 921-925.

728 Liu J. X., Chen J., Jiang M. X., et al. Leaf traits and persistence of relict and endangered tree species in a rare plant
729 community. *Functional Plant Biology*, 2012, 39, 512-518.

730 Liu L. H. The traits and adaptive strategies of main herbaceous plants and lianas on micro-topographical units in
731 Huangcangyu reserves of Anhui Province. 2012, Graduation Thesis.

732 Liu M. C., Kong D. L., Lu X. R., et al. Higher photosynthesis, nutrient- and energy-use efficiencies contribute to
733 invasiveness of exotic plants in a nutrient poor habitat in northeast China. *Physiologia Plantarum*, 2017, 160,
734 373-382.

735 Liu R. H., Bai J. L., Bao H., et al. Variation and correlation in functional traits of main woody plants in the
736 *Cyclobalanopsis glauca* community in the karst hills of Guilin, southwest China. *Chinese Journal of Plant*
737 *Ecology*, 2020, 44, 828-841.

738 Liu W. D., Su J. R., Li S. F., et al. Stoichiometry study of C, N and P in plant and soil at different successional

739 stages of monsoon evergreen broad-leaved forest in Pu'er, Yunnan Province. *Acta Ecologica Sinica*, 2010, 30,
740 6581-6590.

741 Liu X. C., Jia H. B., Wang Q. Y. Genetic variation and correlation in wood properties of *Betula platyphlla* in
742 natural Stands. *Journal of Northeast Forestry University*, 2018, 36, 8-10.

743 Liu Y. Y. Spatial distribution and habitat associations of trees in a typical mixed broad-leaved Korean pine (*Pinus*
744 *koraiensis*) forest. 2014, Graduation Thesis.

745 Luo Y. H., Cadotte M. W., Burgess K. S., et al. Greater than the sum of the parts: how the species composition in
746 different forest strata influence ecosystem function. *Ecology Letters*, 2019, 22, 1449-1461.

747 Lv J. Z., Miao Y. M., Zhang H. F., et al. Comparisons of leaf traits among different functional types of plant from
748 Huoshan Mountain in the Shanxi Province. *Plant Science Journal*, 2010, 28, 460-465.

749 Ma J., Wu L. F., Wei X., et al. Habitat adaptation of two dominant tree species in a subtropical monsoon forest:
750 leaf functional traits and hydraulic properties. *Guihaia*, 2015, 35, 261-268.

751 Mo J. M., Zhang D. Q., Huang Z. L., et al. Distribution pattern of nutrient elements in plants of Dinghushan Lower
752 Subtropical Evergreen Broad-Leaved Forest. *Journal of Tropical and Subtropical Botany*, 2000, 8, 198-206.

753 Niu C. Y., Meinzer F. C. and Hao G. Y. Divergence in strategies for coping with winter embolism among co-
754 occurring temperate tree species: the role of positive xylem pressure, wood type and tree stature. *Functional*
755 *Ecology*, 2017, 31, 1550-1560.

756 Niu D. C., Li Q., Jiang S. G., et al. Seasonal variations of leaf C:N:P stoichiometry of six shrubs in desert of
757 China's Alxa Plateau. *Chinese Journal of Plant Ecology*, 2013, 37, 317-325.

758 Niu K. C., He J. S. and Lechowicz M. J. Grazing-induced shifts in community functional composition and soil
759 nutrient availability in Tibetan alpine meadows. *Journal of Applied Ecology*, 2016, 53, 1554-1564.

760 Niu K. C., Zhang S. and Lechowicz M. Harsh environmental regimes increase the functional significance of
761 intraspecific variation in plant communities. *Functional Ecology*, 2020, 34, 1666-1677.

762 Niu S. L. Photosynthesis research on the predominant legume species in Hunshandak Sandland. 2004, Graduation
763 Thesis.

764 Qi L. X. Response of leaf traits of *Pinus mongoliensis* and *Pinus massoniana* to elevation gradient in Daiyun
765 Mountain. 2015, Graduation Thesis.

766 Ren Q. J., Li Q. J., Bu H. Y., et al. Comparison of physiological and leaf morphological traits for photosynthesis of
767 the 51 plant species in the Maqu alpine swamp meadow. *Chinese Journal of Plant Ecology*, 2015, 39, 593-603.

768 Ren Y. T. The study of leaf functional traits of typical plants across the Alashan Desert. 2017, Graduation Thesis.

769 Ren Y., Wei C. G. and Guo X. Y. Comparison on leaf function traits of six kinds of plant in Ordos. *Journal of Inner*
770 *Mongolia Forestry Science & Technology*, 2019, 45, 43-46, 55.

771 Rios R. S., Salgado-Luarte C. and Gianoli E. Species divergence and phylogenetic variation of ecophysiological
772 traits in lianas and trees. *PloS One*, 2007, 9, e99871.

773 Shang K. K. Differentiation and maintenance of relict deciduous broad-leaved forest patterns along micro-
774 topographic gradient in subtropical area, East China. 2011, Graduation Thesis.

775 Song Y T. Study on functional plant ecology in Songnen Grassland Northeast China. 2012, Graduation Thesis.

776 Song Y T., Zhou D. W., Li Q., et al. Leaf nitrogen and phosphorus stoichiometry in 80 herbaceous plant species of
777 Songnen grassland in Northeast China. *Chinese Journal of Plant Ecology*, 2012, 36, 222-230.

778 Tan X. Y. Research on leaf functional diversity of forest communities in rainy area of south-west China. 2014,
779 Graduation Thesis.

780 Tang Q. Q. Variation in functional traits of plants in the Subtropical Evergreen and Deciduous Broad-leaved Mixed
781 Forest. 2016, Graduation Thesis.

782 Tang Y. Inter-specific variations and relationship in leaf traits of major temperate species in northern China. 2011,

783 Graduation Thesis.

784 Tao J. P., Zuo J., He Z., et al. Traits including leaf dry matter content and leaf pH dominate over forest soil pH as
785 drivers of litter decomposition among 60 species. *Functional Ecology*, 2019, 33, 1798-1810.

786 Tian M., Yu G. R., He N. P., et al. Leaf morphological and anatomical traits from tropical to temperate coniferous
787 forests: Mechanisms and influencing factors. *Scientific Reports*, 2016, 6, 19703.

788 Wang B. Analysis of leaf functional traits of 13 species trees in northwestern Fujian Province. 2019, Graduation
789 Thesis.

790 Wang B. B. A study on ecological stoichiometry of six kinds of dominant shrubs in Huangcangyu Nature Reserve.
791 2015, Graduation Thesis.

792 Wang G. H. Leaf trait co-variation, response and effect in a chronosequence. *Journal of Vegetation Science*, 2007,
793 18, 563-570.

794 Wang G. H., Liu J. L. and Meng T. T. Leaf trait variation captures climate differences but differs with species
795 irrespective of functional group. *Journal of Plant Ecology*, 2015, 8, 61-69.

796 Wang J. Y., Wang S. Q., Li R. L., et al. C:N:P stoichiometric characteristics of four forest types' dominant tree
797 species in China. *Chinese Journal of Plant Ecology*, 2011, 35, 587-595.

798 Wang K. B. Vegetation ecological features and net primary productivity simulation in Yanggou watershed in the
799 Loess hill-gully areas of China. 2011, Graduation Thesis.

800 Wang S. S. The traits and adaptive strategies of main herbaceous plants and lianas on micro-topographical units in
801 Longjishan reserves of Anhui Province. 2016, Graduation Thesis.

802 Wei L. P. Variations in functional traits of main tree species along tree-crown in broadleaved Korean Pine Forest in
803 Jiaohe, Jilin Province. 2014, Graduation Thesis.

804 Wei L. P., Hou J. H. and Jiang S. S. Changes of leaf functional traits of two main species along tree height in
805 broad-leaved Korean pine forest. *Guangdong Agricultural Sciences*, 2014, 12, 55-58, 71.

806 Wei L. Y. and Shangguan Z. P. Relation between specific leaf areas and leaf nutrient contents of plants growing on
807 slopelands with different farming-abandoned periods in the Loess Plateau. *Acta Ecologica Sinica*, 2008, 28,
808 2526-2535.

809 Wei L. Y., Zhou J. W., Xiao H. G., et al. Variations in leaf functional traits among plant species grouped by growth
810 and leaf types in Zhenjiang, China. *Journal of Forestry Research*, 2011, 28, 241-248.

811 Wu D. H., Pietsch K. A., Staab M., et al. Wood species identity alters dominant factors driving fine wood
812 decomposition along a subtropical plantation forests tree diversity gradient in subtropical plantation forests.
813 *Biotropica*, 2021, 53, 643-657.

814 Wu T. G., Chen B. F., Xiao Y. H., et al. Leaf stoichiometry of trees in three forest types in Pearl River Delta, South
815 China. *Chinese Journal of Plant Ecology*, 2009, 34, 58-63.

816 Xie Y. J. The characteristics of 20 dominant plant functional traits in evergreen broad-leaf forest in Daming
817 Mountain Nature Reserve, Guangxi. 2013, Graduation Thesis.

818 Xu M. F., Ke X. H., Zhang Y., et al. Wood densities of six hardwood tree species in Eastern Guangdong and
819 influencing factors. *Journal of South China Agricultural University*, 2016, 37, 100-106.

820 Xu M. S., Zhao Y. T., Yang X. D., et al. Geostatistical analysis of spatial variations in leaf traits of woody plants in
821 Tiantong, Zhejiang Province. *Chinese Journal of Plant Ecology*, 2016, 40, 48-59.

822 Xu Y. Z. Biomass estimate and storage mechanisms in northern subtropical forest ecosystems, central China. 2016,
823 Graduation Thesis.

824 Xun Y. H., Di X. Y. and Jin G. Z. Vertical variation and economic strategy of leaf trait of major tree species in a
825 typical mixed broadleaved-Korean pine forest. *Chinese Journal of Plant Ecology*, 2020, 44, 730-741.

826 Yan E. R., Wang X. H., Guo M., et al. C:N:P stoichiometry across evergreen broad-leaved forests, evergreen

827 coniferous forests and deciduous broad-leaved forests in the Tiantong region, Zhejiang Province, eastern
828 China. *Chinese Journal of Plant Ecology*, 2010, 34, 48-57.

829 Yang S. The adaptive strategies of main herbaceous plants traits to different micro-topographical units in
830 Dashushan Mountain, Hefei. 2017, Graduation Thesis.

831 Yang Y., Xu X., Xu M., et al. Adaptation strategies of three dominant plants in the trough-valley karst region of
832 northern Guizhou Province, Southwestern China, evidence from associated plant functional traits and
833 ecostochiometry. *Earth and Environment*, 2020, 48, 413-423.

834 Yang Z., Fan S. X., Zhou B. C., et al. Leaf function and soil nutrient differences of dominant tree species on
835 different slope aspects at the south foothills of Taihang Mountains. *Journal of Henan Agricultural University*,
836 2020, 54, 408-414.

837 Yin Q. L., Wang L., Lei, M. L., et al. The relationships between leaf economics and hydraulic traits of woody
838 plants depend on water availability. *Science of the Total Environment*, 2018, 621, 245-252.

839 Yu Y. H., Zhong X. P. and Chen W. Analysis of relationship among leaf functional traits and economics spectrum
840 of dominant species in northwestern Guizhou Province. *Journal of Forest and Environment*, 2018, 38, 196-
841 201.

842 Yuan S. Preliminary research on plant functional traits and the capability of carbon sequestration of major tree
843 species in Changbai Mountain Area. 2011, Graduation Thesis.

844 Zhang H., Chen H. Y. H., Lian J. Y., et al. Using functional trait diversity patterns to disentangle the scale-
845 dependent ecological processes in a subtropical forest. *Functional Ecology*, 2018, 32, 1379-1389.

846 Zhang J. G., Fu S. L., Wen Z. D., et al. Relationship of key leaf traits of 16 woody plant species in Low
847 Subtropical China. *Journal of Tropical and Subtropical Botany*, 2009, 17, 395-400.

848 Zhang J. L., Poorter L., Cao K. F. Productive leaf functional traits of Chinese savanna species. *Plant Ecology*, 2012,
849 213, 1449-1460.

850 Zhang J. Y. Comparative study on the different plant functional groups leaf traits at the Maoershan Region. 2008,
851 Graduation Thesis.

852 Zhang Q. W., Zhu S. D., Jansen S., et al. Topography strongly affects drought stress and xylem embolism
853 resistance in woody plants from a karst forest in Southwest China. *Functional Ecology*, 2020, 35, 566-577.

854 Zhang S. B. and Cao K. F. Stem hydraulics mediates leaf water status, carbon gain, nutrient use efficiencies and
855 plant growth rates across dipterocarp species. *Functional Ecology*, 2009, 23, 658-667.

856 Zhang S. B., Cao K. F., Fan Z. X., et al. Potential hydraulic efficiency in angiosperm trees increases with growth-
857 site temperature but has no trade-off with mechanical strength. *Global Ecology and Biogeography*, 2013, 22,
858 971-981.

859 Zhang Y., Ren Y. X., Yao J., et al. Leaf nitrogen and phosphorous stoichiometry of trees in *Pinus tabulaeformis*
860 Carr stands, North China. *Journal of Anhui Agricultural University*, 2012, 39, 247-251.

861 Zhao Y. T., Ali, A. and Yan, E. R. The plant economics spectrum is structured by leaf habits and growth forms
862 across subtropical species. *Tree Physiology*, 2016, 37, 173-185.

863 Zheng X. J., Li S. and Li Y. Leaf water uptake strategy of desert plants in the Junggar Basin, China. *Chinese*
864 *Journal of Plant Ecology*, 2011, 35, 893-905.

865 Zheng Y. M. Carbon, nitrogen and phosphorus stoichiometry of plant and soil in the sandy hills of Poyang Lake.
866 2014, Graduation Thesis.

867 Zheng Z. X. Comparison of plant leaf, height and seed functional traits in dry-hot valleys. 2010, Graduation Thesis.

868 Zhou J. Y., He J. J., Guo Z. Y., et al. A study on specific leaf area and leaf dry matter content of five dominant
869 species in Xiangshan Mountain, Huaibei City, Anhui Province. *Journal of Huaibei Normal University*
870 (Natural Sciences), 2013, 34, 51-54.

- 871 Zhou X., Zuo X. A., Zhao X. Y., et al. Plant functional traits and interrelationship of 34 plant species in south
872 central Horqin Sandy Land, China. *Journal of Desert Research*, 2015, 35, 1489-1495.
- 873 Zhu B. R., Xu B. and Zhang D. Y. Extent and sources of variation in plant functional traits in grassland. *Journal of*
874 *Beijing Normal University (Natural Science)*, 2011, 47, 485-489.
- 875 Zhu S. D., Song J. J., Li R. H., et al. Plant hydraulics and photosynthesis of 34 woody species from different
876 successional stages of subtropical forests. *Plant Cell and Environment*, 2013, 36, 879-891.
- 877 Zhu X. B., Liu Y. M. and Sun S. C. Leaf expansion of the dominant woody species of three deciduous oak forests
878 in Nanjing, East China. *Chinese Journal of Plant Ecology*, 2005, 29, 125-136.

879 **Appendix B**

880 **Table B1** Summary of statistics in plant functional traits, environmental variables and
 881 geographical distribution in China.

Trait	Unit	Range	Mean	CV (%)	No. of species	Entries	Sites
SLA	m ² kg ⁻¹	0.06–81.68	17.88	54.96	2463	9195	1032
LDMC	g g ⁻¹	0.06–0.95	0.34	100.00	1582	3957	193
LNC	mg g ⁻¹	3.41–66.02	21.52	37.44	2335	7407	567
LPC	mg g ⁻¹	0.09–9.70	1.83	62.19	2074	6266	515
LA	cm ²	0.0033–2553.33	36.16	259.64	1838	5976	691
WD	g cm ⁻³	0.25–1.37	0.68	33.16	768	1788	639
Altitude	m	-144–5454					1430
MAT	°C	-12.07–24.32					1430
MAP	mm	15–2982					1430
Soil total N	g kg ⁻¹	0.11–10.25					1430
Bulk density	g cm ⁻³	0.83–1.45					1430

882 SLA, specific leaf area; LDMC, leaf dry matter content; LNC, leaf N concentration; LPC, leaf P concentration; LA,
 883 leaf area; WD, wood density; MAT, mean annual temperature; MAP, mean annual precipitation.

884 **Table B2** List of all predictors including environment and remote sensing variables used in
 885 this study.

Type of variables	Variable name	Abbreviations	Units	Time periods	Spatial resolution	Source	
Climate	Mean annual temperature	MAT	°C	1970-2000	1 km	WorldClim version 2.1	
	Mean diurnal range	MDR	°C	1970-2000	1 km	WorldClim version 2.1	
	Temperature seasonality	TS	°C	1970-2000	1 km	WorldClim version 2.1	
	Max temperature of the warmest month	Tmin	°C	1970-2000	1 km	WorldClim version 2.1	
	Min temperature of the coldest month	Tmax	°C	1970-2000	1 km	WorldClim version 2.1	
	Temperature annual range	TAR	°C	1970-2000	1 km	WorldClim version 2.1	
	Isothermality	IS	%	1970-2000	1 km	WorldClim version 2.1	
	Mean temperature of the wettest quarter	MTEQ	°C	1970-2000	1 km	WorldClim version 2.1	
	Mean temperature of the driest quarter	MTDQ	°C	1970-2000	1 km	WorldClim version 2.1	
	Mean temperature of the warmest quarter	MTWQ	°C	1970-2000	1 km	WorldClim version 2.1	
	Mean temperature of the coldest quarter	MTCQ	°C	1970-2000	1 km	WorldClim version 2.1	
	Mean annual precipitation	MAP	mm	1970-2000	1 km	WorldClim version 2.1	
	Precipitation of the wettest month	PEM	mm	1970-2000	1 km	WorldClim version 2.1	
	Precipitation of the driest month	PDM	mm	1970-2000	1 km	WorldClim version 2.1	
	Precipitation seasonality	PS	%	1970-2000	1 km	WorldClim version 2.1	
	Precipitation of the wettest quarter	PEQ	mm	1970-2000	1 km	WorldClim version 2.1	
	Precipitation of the driest quarter	PDQ	mm	1970-2000	1 km	WorldClim version 2.1	
	Precipitation of the warmest quarter	PWQ	mm	1970-2000	1 km	WorldClim version 2.1	
	Precipitation of the coldest quarter	PCQ	mm	1970-2000	1 km	WorldClim version 2.1	
	Aridity index	AI	/	1970-2000	1 km	Global CGIAR-CSI	
	Solar radiation	RAD	$\text{kJ m}^{-2} \text{day}^{-1}$	1970-2000	1 km	WorldClim version 2.1	
	Topography	Elevation	/	m		1 km	SRTM 90m V4.1
	Soil	Soil sand content	SAND	%	/	1 km	Shangguan et al. (2013)
Soil silt content		SILT	%	/	1 km	Shangguan et al. (2013)	
Soil clay content		CLAY	%	/	1 km	Shangguan et al. (2013)	
Bulk density		BD	g cm^{-3}	/	1 km	Shangguan et al. (2013)	
Soil pH		pH	/	/	1 km	Shangguan et al. (2013)	
Soil organic matter		SOC	g kg^{-1}	/	1 km	Shangguan et al. (2013)	
Soil total N		STN	g kg^{-1}	/	1 km	Shangguan et al. (2013)	
Soil total P		STP	g kg^{-1}	/	1 km	Shangguan et al. (2013)	
Soil alkali-hydrolysable N		SAN	mg kg^{-1}	/	1 km	Shangguan et al. (2013)	
Soil available P		SAP	mg kg^{-1}	/	1 km	Shangguan et al. (2013)	
Soil available K		SAK	mg kg^{-1}	/	1 km	Shangguan et al. (2013)	
Cation exchange capacity		CEC	me kg^{-1}	/	1 km	Shangguan et al. (2013)	

Continued

Type of variables	Variable name	Abbreviations	Units	Time periods	Spatial resolution	Source
EVI	MODIS EVI long-term monthly averages		/	2001-2018	1 km	MOD13A3 V006
NIR	MODIS NIR long-term monthly averages		/	2001-2018	1 km	MOD13A3 V006
MIR	MODIS MIR long-term monthly averages		/	2001-2018	1 km	MOD13A3 V006
Red	MODIS red long-term monthly averages		/	2001-2018	1 km	MOD13A3 V006
Blue	MODIS blue long-term monthly averages		/	2001-2018	1 km	MOD13A3 V006
MTCI	MTCI long-term monthly averages		/	2003-2011	4.63 km	MTCI level 3 product
Land cover	Land cover map		/	2015	100 m	Copernicus Global Land Service Collection 3

886 The vegetation indices are calculated as long-term monthly averages from 2001 to 2018, thus 12 variables of each
 887 vegetation index category are obtained.

888

889

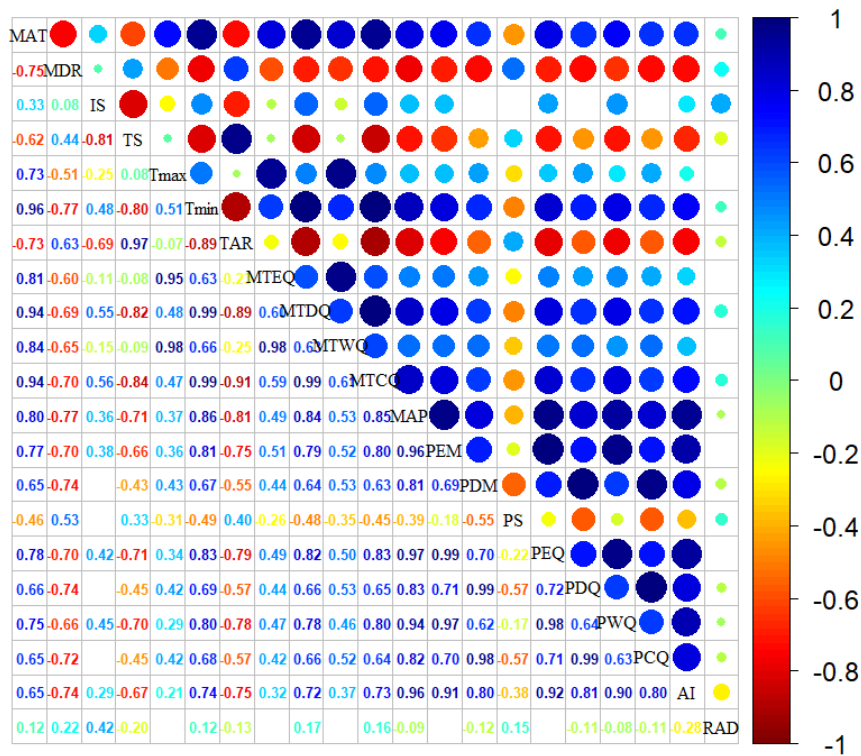
890

891

892 **Table B3** The number of samples of six plant functional traits used for model training (80%)
 893 and validation (20%).

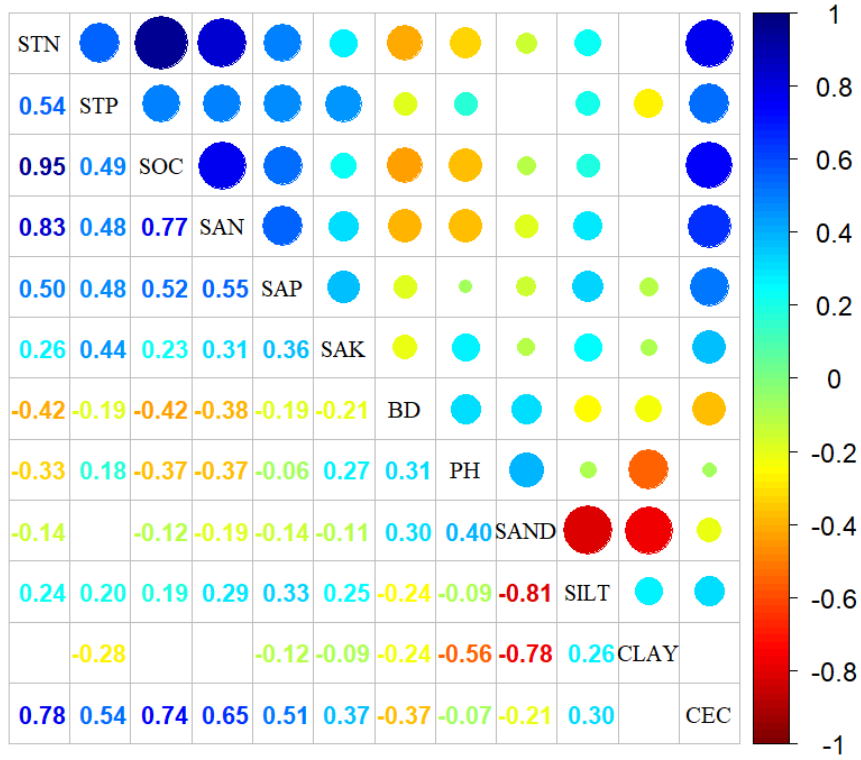
Traits	No. of samples	No. of samples used for model training	No. of samples used for model validation
SLA	9195	7356	1839
LDMC	3957	3166	791
LNC	7407	5926	1481
LPC	6266	5013	1253
LA	5976	4781	1195
WD	1787	1430	357

894 SLA, specific leaf area ($\text{m}^2 \text{kg}^{-1}$); LDMC, leaf dry matter content (g g^{-1}); LNC, leaf N concentration (mg g^{-1}); LPC,
 895 leaf P concentration (mg g^{-1}); LA, leaf area (cm^2); WD, wood density (g cm^{-3}).



896

897 **Figure B1.** Correlations among climate variables. The blank indicates that the correlations are not
 898 significant ($P > 0.05$). The size of the circles is proportional to the correlation coefficient. The
 899 abbreviations of climate variables are seen in Table B2.

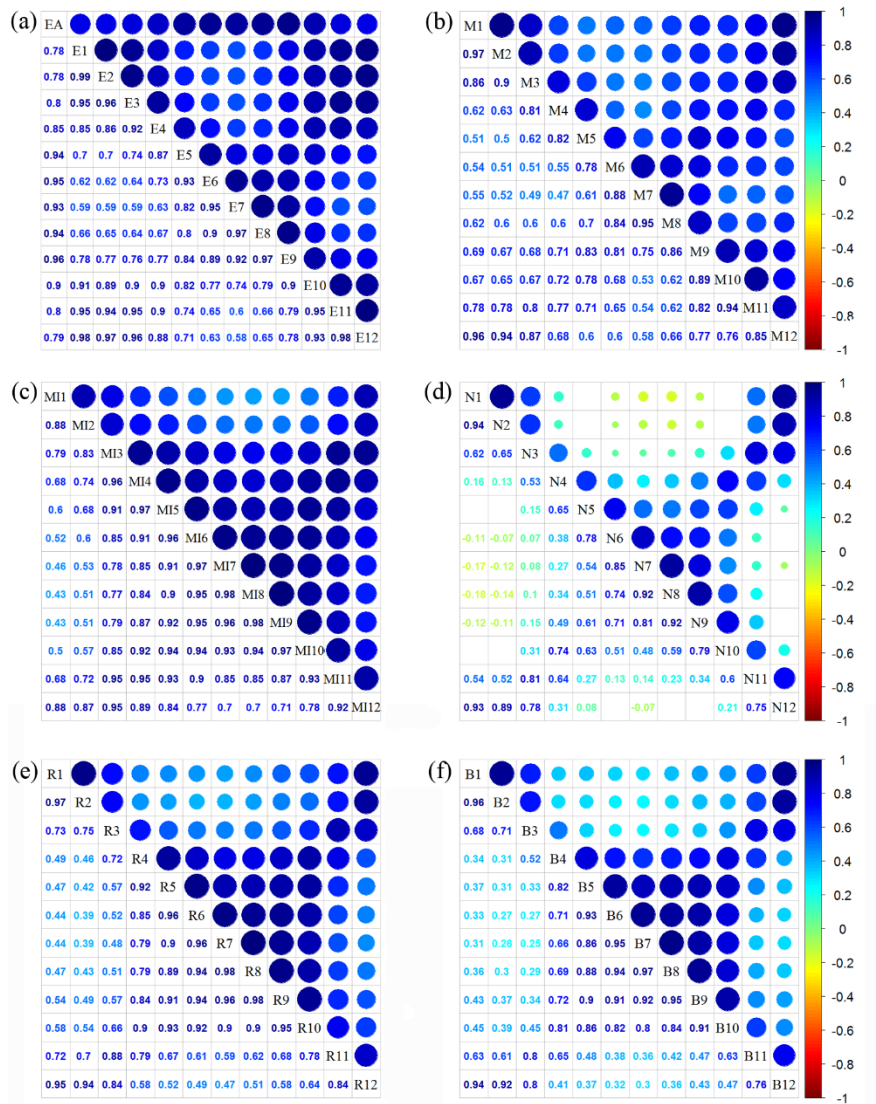


900

901 **Figure B2.** Correlations among soil variables. The blank indicates that the correlations are not

902 significant ($P > 0.05$). The size of the circles is proportional to the correlation coefficient. The

903 abbreviations of soil variables are seen in Table B2.



904

905 **Figure B3.** Correlations among monthly vegetation index variables. The blank indicates that the
 906 correlations are not significant ($P > 0.05$). The size of the circles is proportional to the correlation
 907 coefficient. (a) enhanced vegetation index (EVI); (b) MERIS terrestrial chlorophyll index (MTCI);
 908 (c) MIR reflectance; (d) NIR reflectance; (e) red reflectance; (f) blue reflectance.

909 **Appendix C**

910 **Table C1** Optimal parameter combination and model performance of random forest for plant
 911 functional traits.

Traits	ntree	mtry	R ²	NRMSE	MAE
SLA	1000	24	0.48	0.22	5.13
LDMC	1000	11	0.23	0.20	0.07
LNC	1000	57	0.39	0.00	0.10
LPC	1000	20	0.59	0.05	0.13
LA	1000	18	0.28	0.48	26.62
WD	1000	9	0.53	0.02	0.07

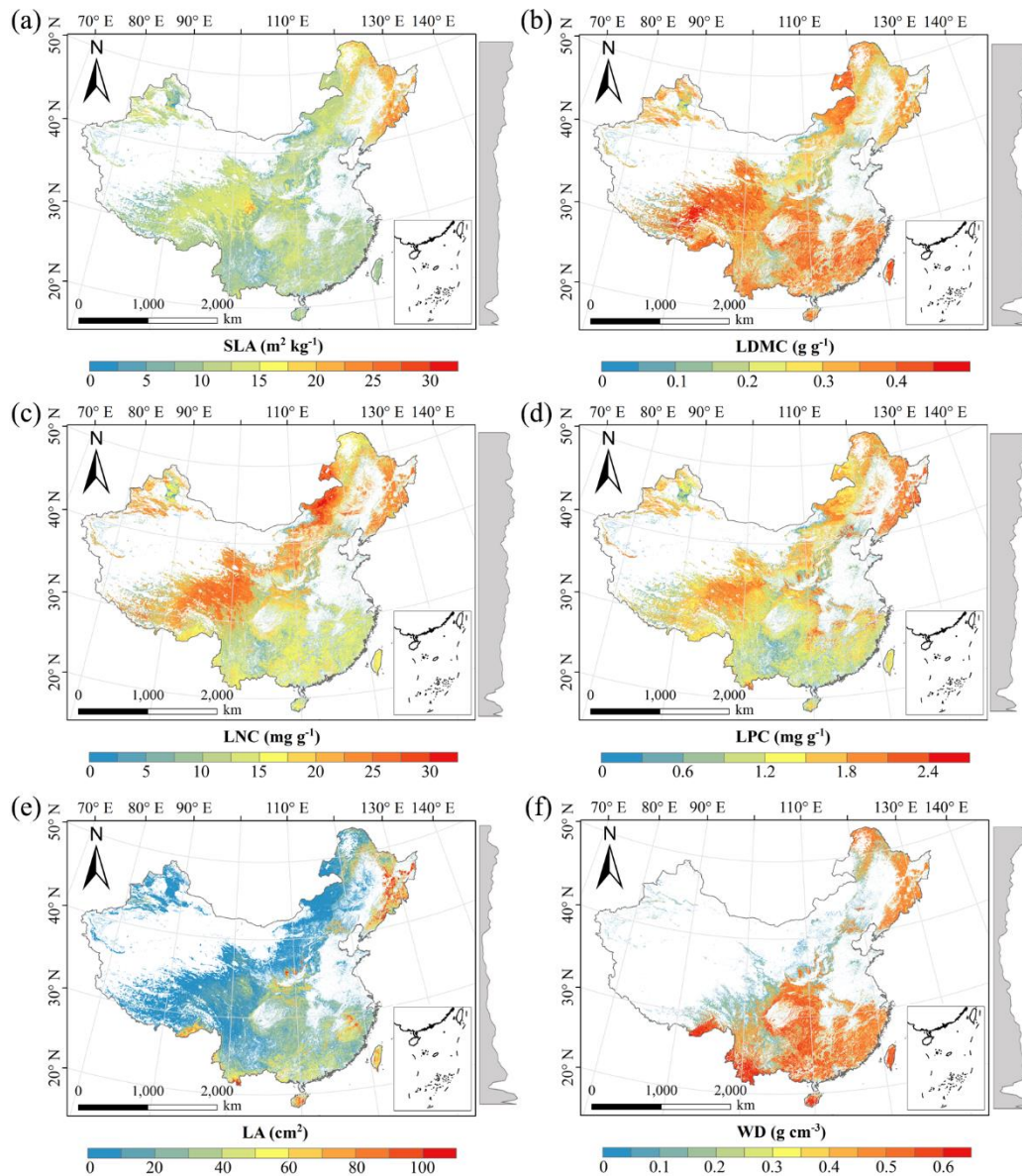
912 SLA, specific leaf area; LDMC, leaf dry matter content; LNC, leaf N concentration; LPC, leaf P concentration; LA,
 913 leaf area; WD, wood density; R², determinate coefficient; NRMSE, normalized root-mean-square error; MAE,
 914 mean absolute error.

915

916 **Table C2** Optimal parameter combination and model performance of boosted regression trees
 917 for plant functional traits.

Traits	n.tree	interaction depth	shrinkage	learning rate	bag fractions	R ²	NRMSE	MAE
SLA	3000	6	0.01	10	0.75	0.49	0.20	5.08
LDMC	3000	2	0.01	10	0.75	0.28	0.19	0.07
LNC	3000	6	0.01	10	0.70	0.41	0.00	0.10
LPC	3000	7	0.01	10	0.75	0.59	0.05	0.13
LA	3000	3	0.001	10	0.75	0.28	0.55	27.56
WD	3000	4	0.01	10	0.70	0.63	0.01	0.07

918 SLA, specific leaf area; LDMC, leaf dry matter content; LNC, leaf N concentration; LPC, leaf P concentration; LA,
 919 leaf area; WD, wood density; R², determinate coefficient; NRMSE, normalized root-mean-square error; MAE,
 920 mean absolute error.



922

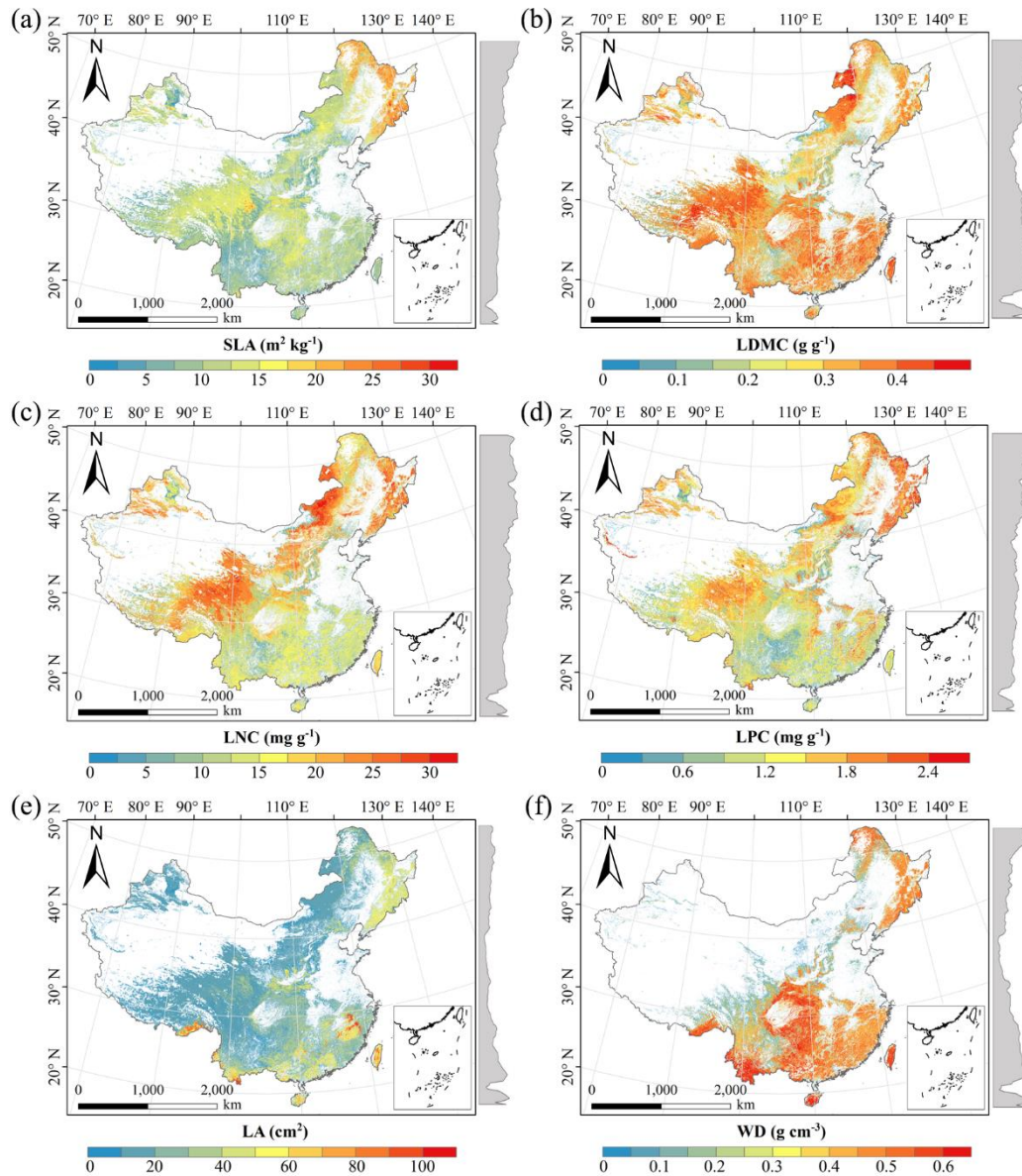
923

924

925

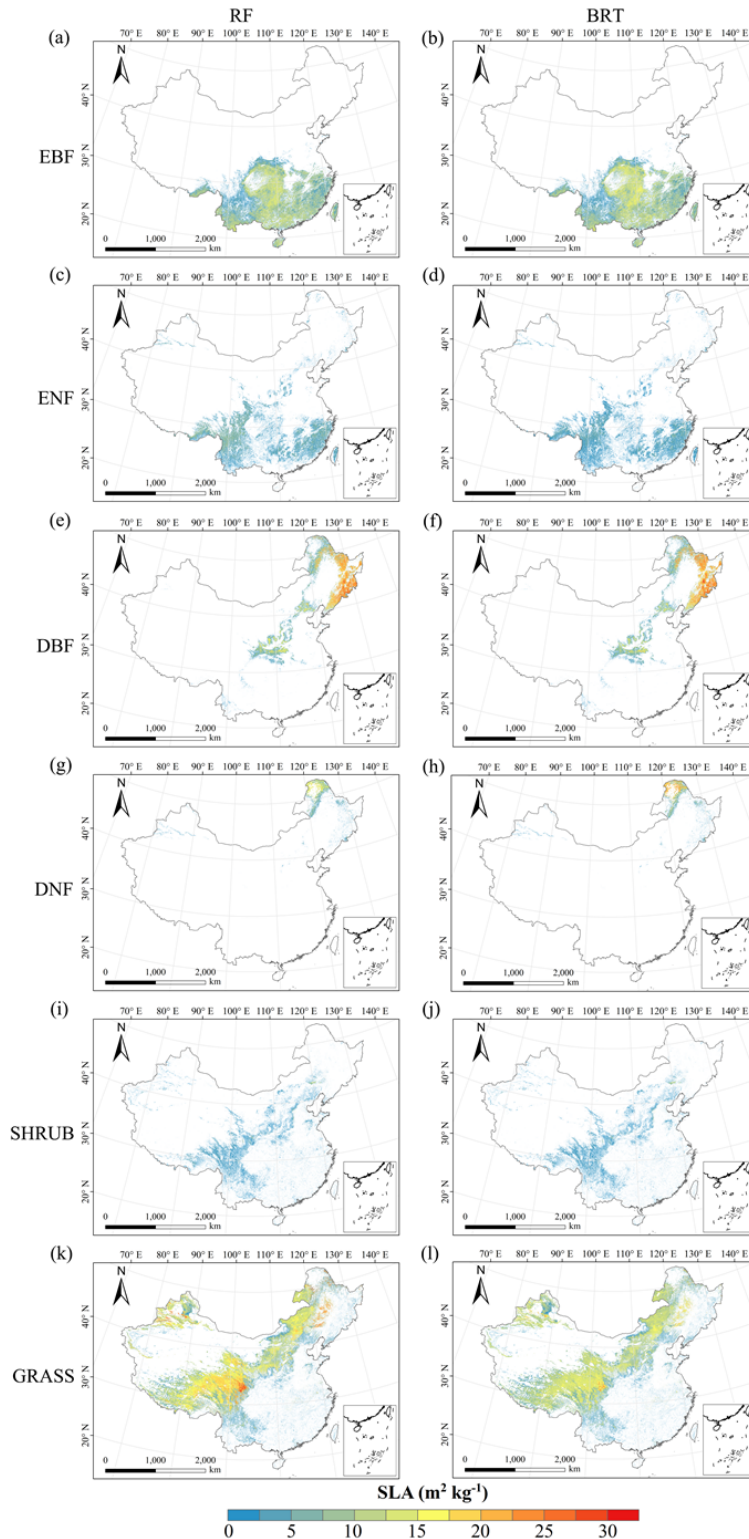
926

Figure D1. Spatial distributions of plant functional traits based on random forest. The grey curves on the right of maps are trait distribution along with latitude. The white areas represent artificial land cover types and bare vegetation. SLA, specific leaf area; LDMC, leaf dry matter content; LNC, leaf N concentration; LPC, leaf P concentration; LA, leaf area; WD, wood density.



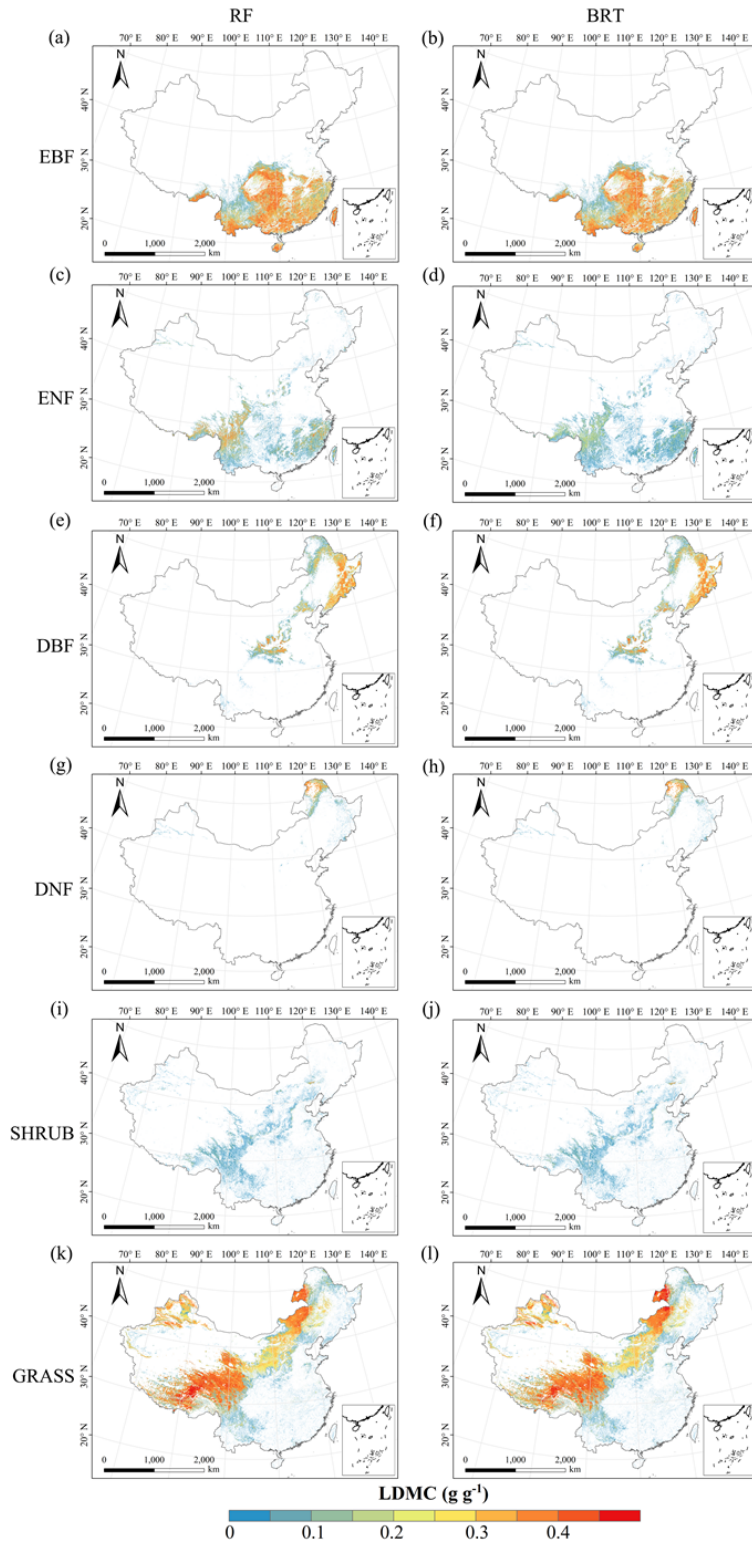
927

928 **Figure D2.** Spatial distributions of plant functional traits based on boosted regression trees. The
 929 grey curves on the right of maps are trait distribution along with latitude. The white areas
 930 represent artificial land cover types and bare vegetation. SLA, specific leaf area; LDMC, leaf dry
 931 matter content; LNC, leaf N concentration; LPC, leaf P concentration; LA, leaf area; WD, wood
 932 density.



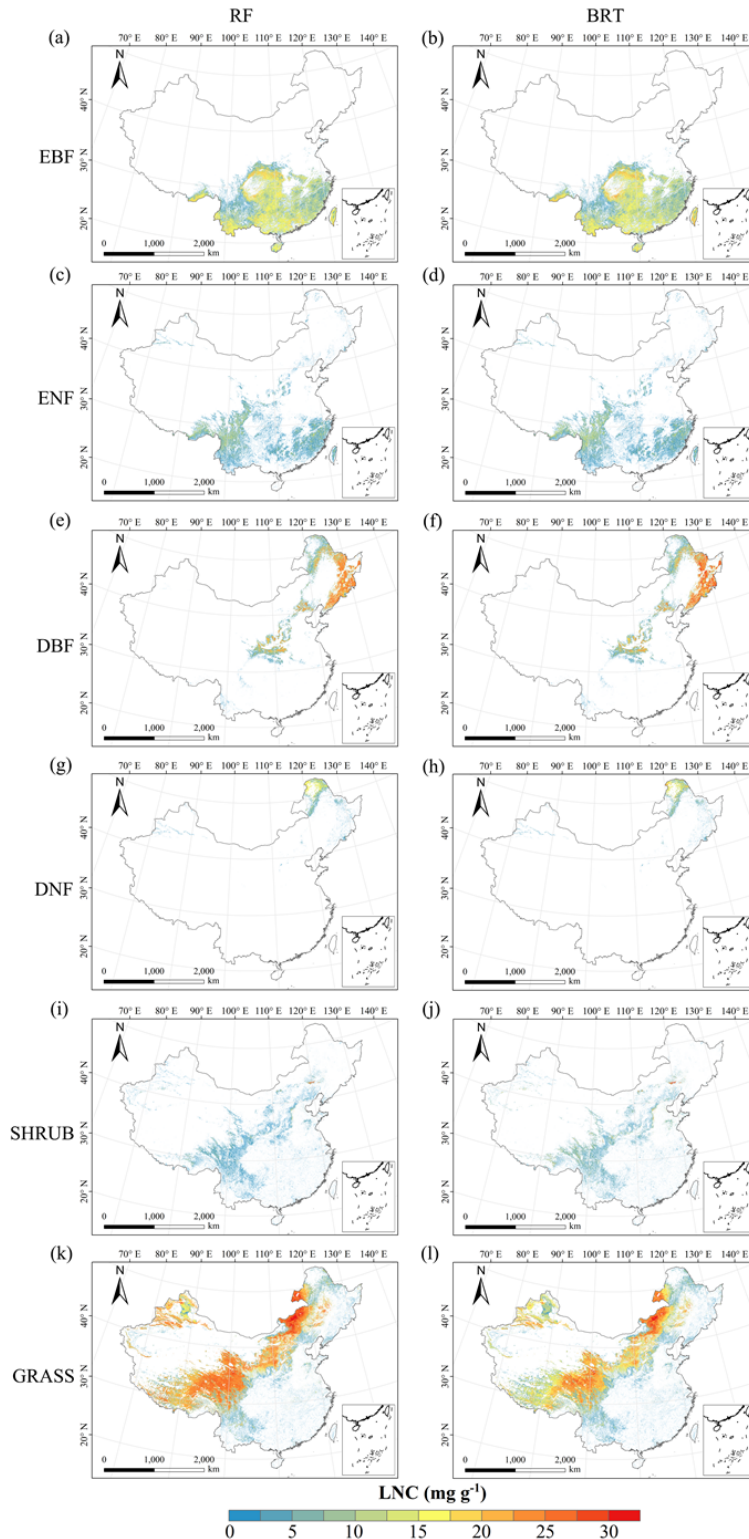
933

934 **Figure D3.** Spatial distribution of specific leaf area (SLA) for each plant functional type. The left
 935 penal is obtained from RF (random forest) method, the right penal is obtained from BRT (boosted
 936 regression trees) method. The white areas represent other natural vegetation types and artificial
 937 land cover types. EBF, evergreen broadleaf forest; ENF, evergreen needleleaf forest; DBF,
 938 deciduous broadleaf forest; DNF, deciduous needleleaf forest; SHRUB, shrubland; GRASS,
 939 grassland.



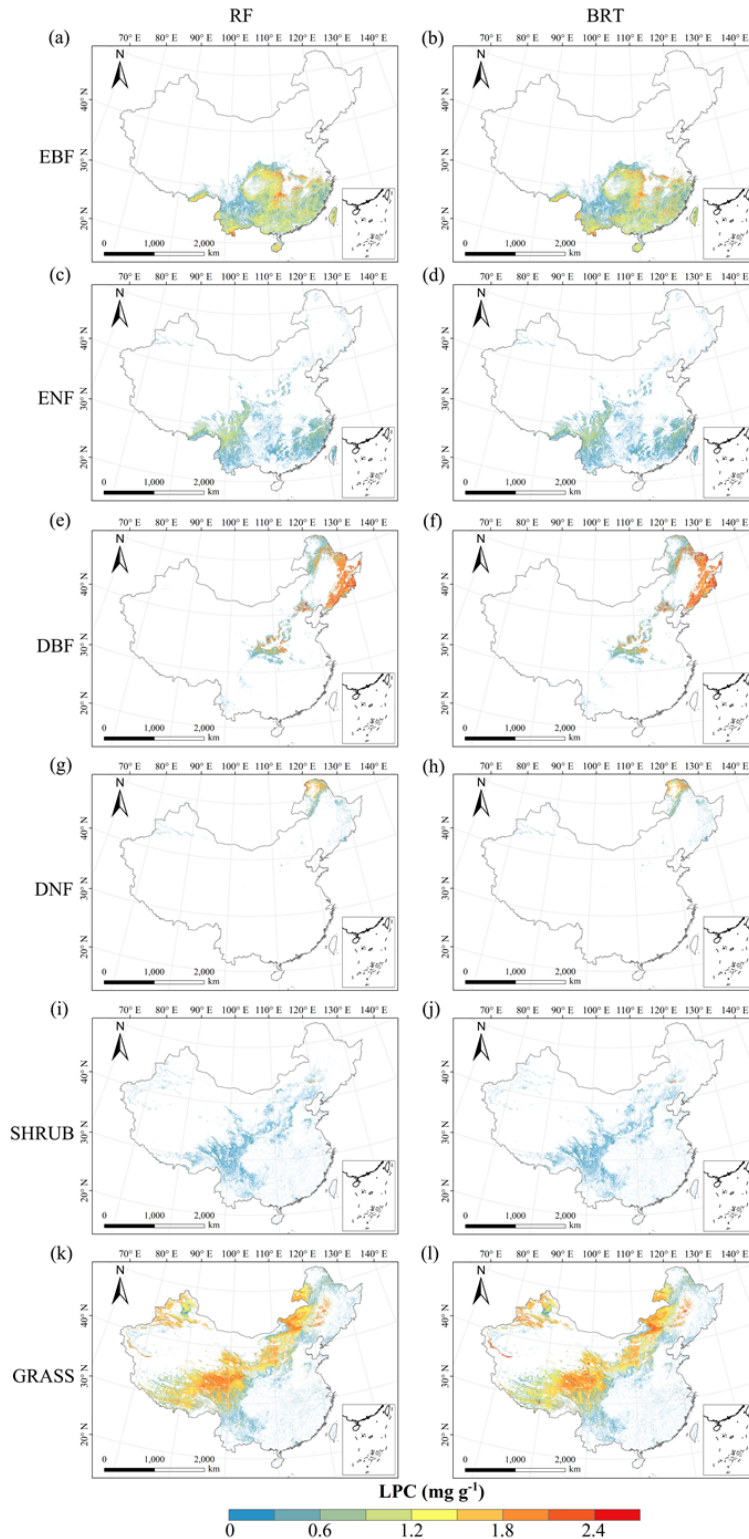
940

941 **Figure D4.** Spatial distribution of leaf dry matter content (LDMC) for each plant functional type.
 942 The left panel is obtained from RF (random forest) method, the right panel is obtained from BRT
 943 (boosted regression trees) method. The white areas represent other natural vegetation types and
 944 artificial land cover types. EBF, evergreen broadleaf forest; ENF, evergreen needleleaf forest; DBF,
 945 deciduous broadleaf forest; DNF, deciduous needleleaf forest; SHRUB, shrubland; GRASS,
 946 grassland.



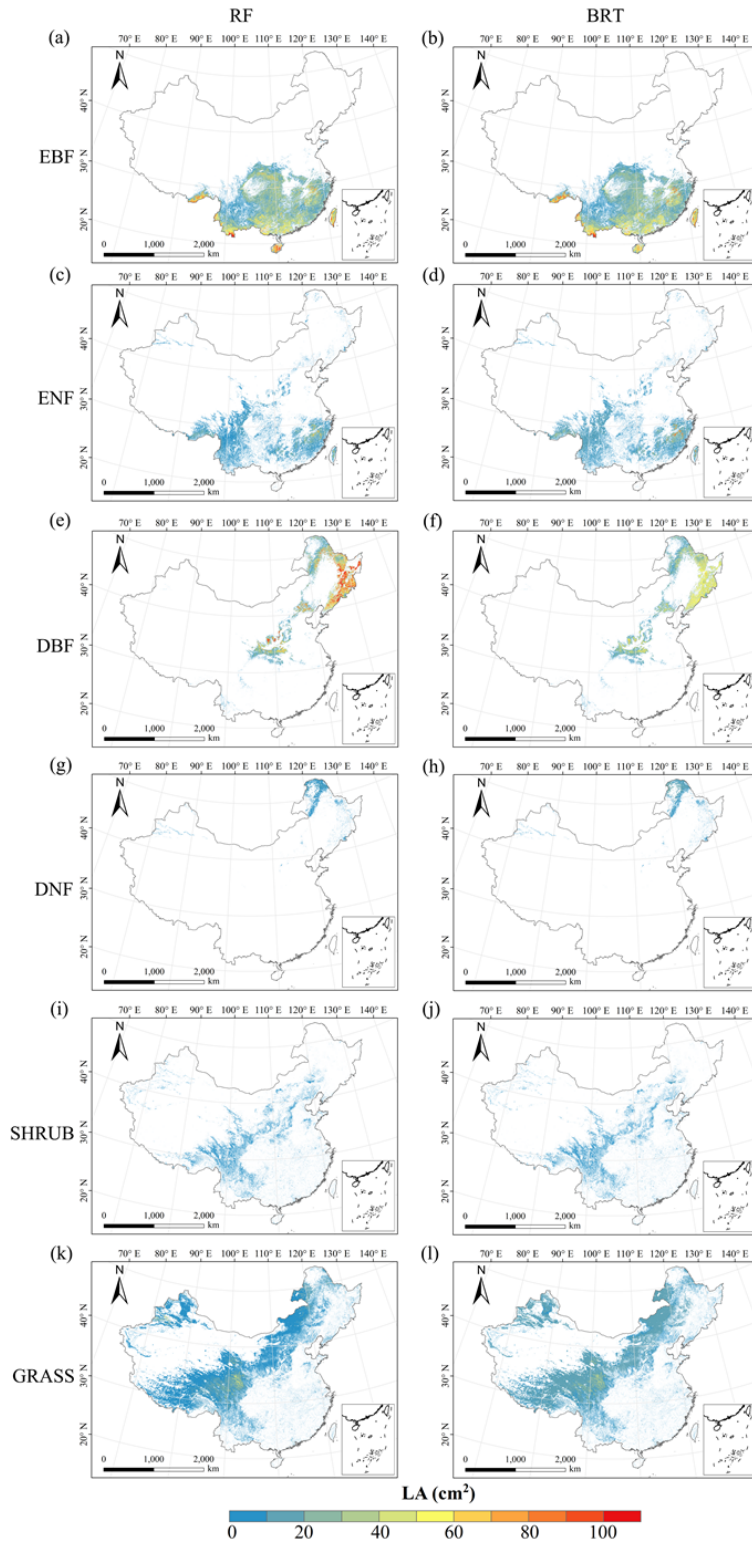
947

948 **Figure D5.** Spatial distribution of leaf N concentration (LNC) for each plant functional type. The
 949 left panel is obtained from RF (random forest) method, the right panel is obtained from BRT
 950 (boosted regression trees) method. The white areas represent other natural vegetation types and
 951 artificial land cover types. EBF, evergreen broadleaf forest; ENF, evergreen needleleaf forest; DBF,
 952 deciduous broadleaf forest; DNF, deciduous needleleaf forest; SHRUB, shrubland; GRASS,
 953 grassland.



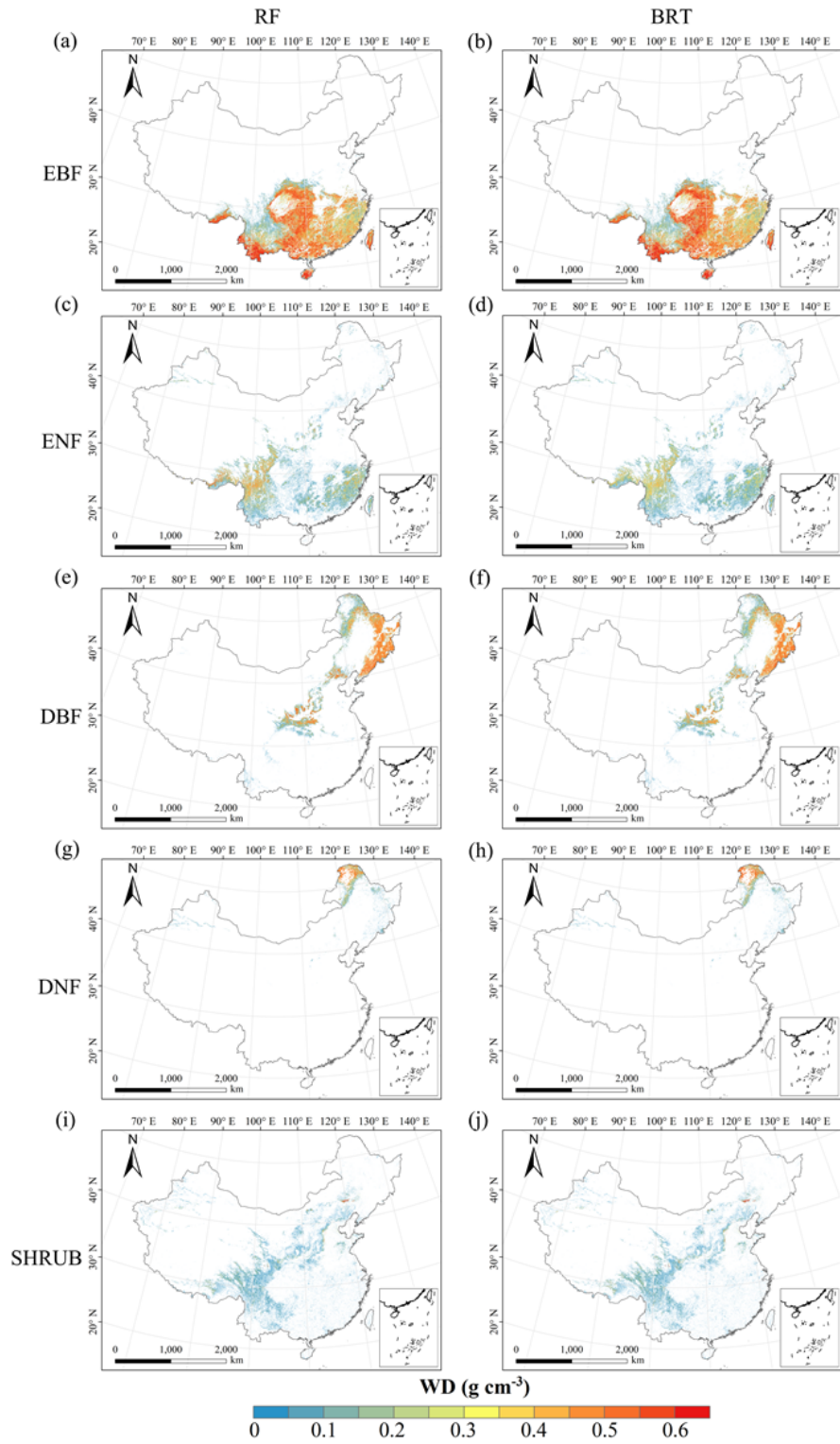
954

955 **Figure D6.** Spatial distribution of leaf P concentration (LPC) for each plant functional type. The
 956 left panel is obtained from RF (random forest) method, the right panel is obtained from BRT
 957 (boosted regression trees) method. The white areas represent other natural vegetation types and
 958 artificial land cover types. EBF, evergreen broadleaf forest; ENF, evergreen needleleaf forest; DBF,
 959 deciduous broadleaf forest; DNF, deciduous needleleaf forest; SHRUB, shrubland; GRASS,
 960 grassland.



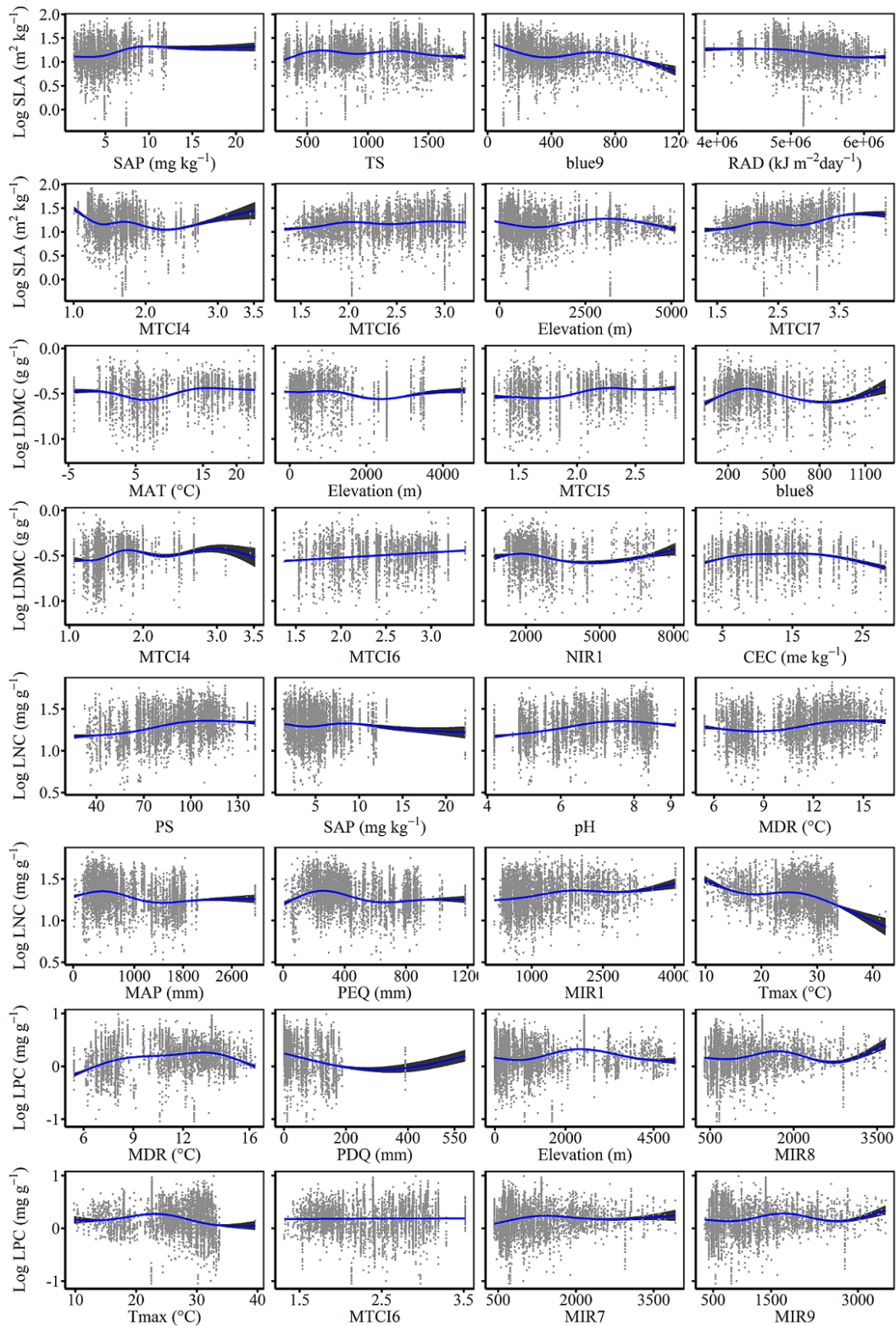
961

962 **Figure D7.** Spatial distribution of leaf area (LA) for each plant functional type. The left panel is
 963 obtained from RF (random forest) method, the right panel is obtained from BRT (boosted
 964 regression trees) method. The white areas represent other natural vegetation types and artificial
 965 land cover types. EBF, evergreen broadleaf forest; ENF, evergreen needleleaf forest; DBF,
 966 deciduous broadleaf forest; DNF, deciduous needleleaf forest; SHRUB, shrubland; GRASS,
 967 grassland.

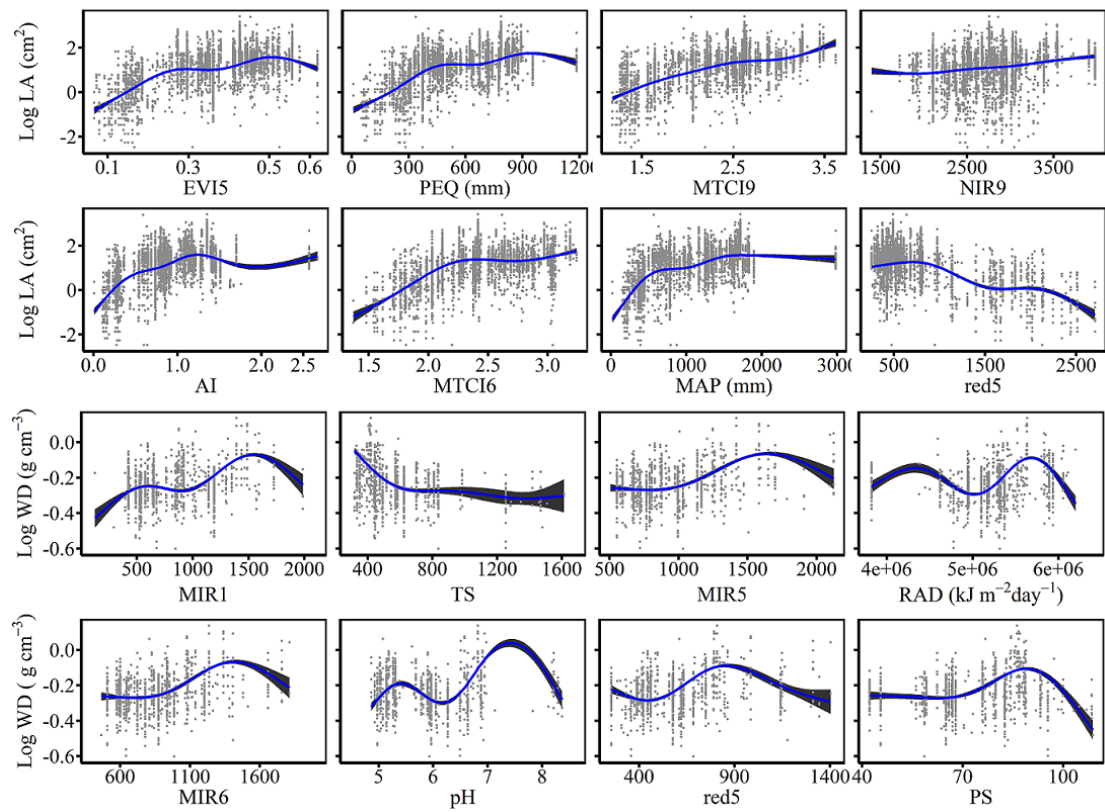


968

969 **Figure D8.** Spatial distribution of wood density (WD) for each plant functional type. The left
 970 panel is obtained from RF (random forest) method, the right panel is obtained from BRT (boosted
 971 regression trees) method. The white areas represent other natural vegetation types and artificial
 972 land cover types. EBF, evergreen broadleaf forest; ENF, evergreen needleleaf forest; DBF,
 973 deciduous broadleaf forest; DNF, deciduous needleleaf forest; SHRUB, shrubland.



975
 976 **Figure E1.** The relationships between SLA (specific leaf area), LDMC (leaf dry matter content),
 977 LNC (leaf N concentration), LPC (leaf P concentration) and their eight most important predictors.



978

979

980

Figure E2. The relationships between LA (leaf area), WD (wood density) and their eight most important predictors.

981 **Appendix F Comparisons between our study with trait maps from previous**
 982 **studies**

983 Given that the trait maps predicted for China were not available from the literature and their
 984 authors, we compared our study with those studies performed at the global scale (Table F1). Thus,
 985 we extracted the data in China from global trait maps. Before the quantitative comparisons with
 986 previous studies, we performed two steps to make the data products as comparable as possible and
 987 improve the consistency between different studies. First, due to different spatial resolution of
 988 global trait maps (mainly 0.5 °) and our study, we resampled the data products of previous studies
 989 and our maps to 0.5 ° spatial resolution. In addition, Vallicrosa et al. (2022) generated the global
 990 maps of LNC and LPC with a 1 km spatial resolution, we also compared the frequency
 991 distribution of Vallicrosa et al. (2022) with that of our study at a 1 km spatial resolution. Second,
 992 our study focused on natural vegetation, so the global trait maps were used to filter out non-natural
 993 vegetation (e.g., croplands). For example, Madani et al. (2018) predicted the spatial distribution of
 994 SLA that included croplands. We quantitatively compared our maps with previous studies from
 995 two perspectives. The comparisons among trait maps were made using frequency plots and spatial
 996 correlation (Fig. 7, Table 4 and Fig. F1 in Appendix F). And the maps of spatial differences
 997 between our study and previous studies were displayed as Figs. F2-F6 in Appendix F.

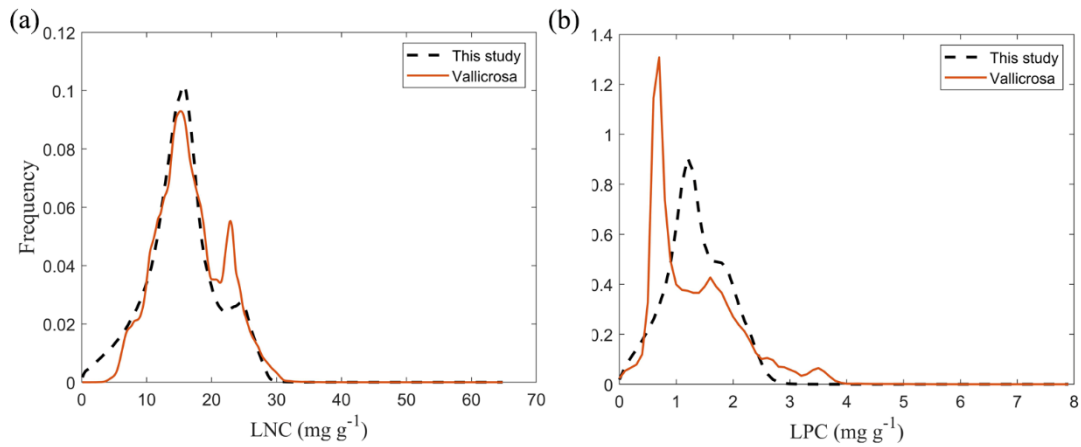
998

999 **Table F1** Summary of related trait maps of previous studies used in this study.

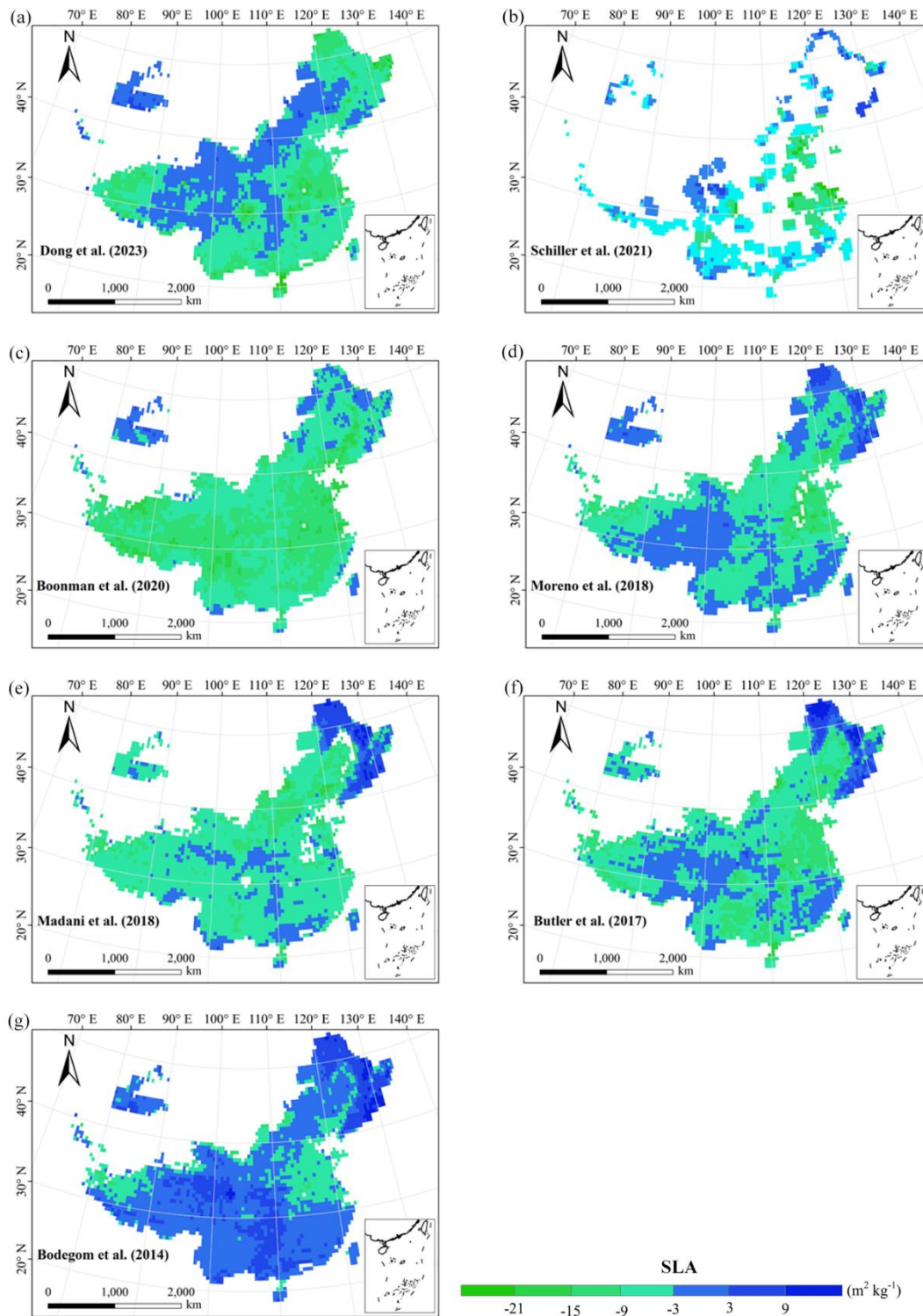
References	Related traits	Methods	Predictors	Consideration of PFT	Spatial resolution
Dong et al. (2023)	SLA LNC	Optimality models	Climate	Yes	0.5 °
Vallicrosa et al. (2022)	LNC LPC	Neural networks	Climate Soil N and P deposition	Yes	0.0083 °
Schiller et al. (2021)	SLA LNC LA WD	Convolutional Neural Networks	Climate In-situ RGB images	No	0.5 °
Boonman et al. (2020)	SLA LNC WD	Generalized linear model, Generalized additive model, Random forest, Boosted regression trees, Ensemble model	Climate Soil	No	0.5 °
Moreno et al. (2018)	SLA LNC LPC	Regularized linear regression, Random forest, Neural	Climate Elevation Reflectance	Yes	0.0045 °

	LDMC	networks,	Kernel			
Madani et al. (2018)	SLA	Generalized additive model	Climate	No	0.5 °	
Butler et al. (2017)	SLA LNC LPC	Bayesian model	Climate Soil	Yes	0.5 °	
Bodegom et al. (2014)	SLA WD	Multiple regression analysis	Climate Soil	No	0.5 °	

1000 The resolutions 0.5 °, 0.0083 ° and 0.0045 ° correspond to square grid cell sizes of about 50 km, 1 km and 500 m at
 1001 the equator. PFT, plant functional type; SLA, specific leaf area; LDMC, leaf dry matter content; LNC, leaf N
 1002 concentration; LPC, leaf P concentration; LA, leaf area; WD, wood density.

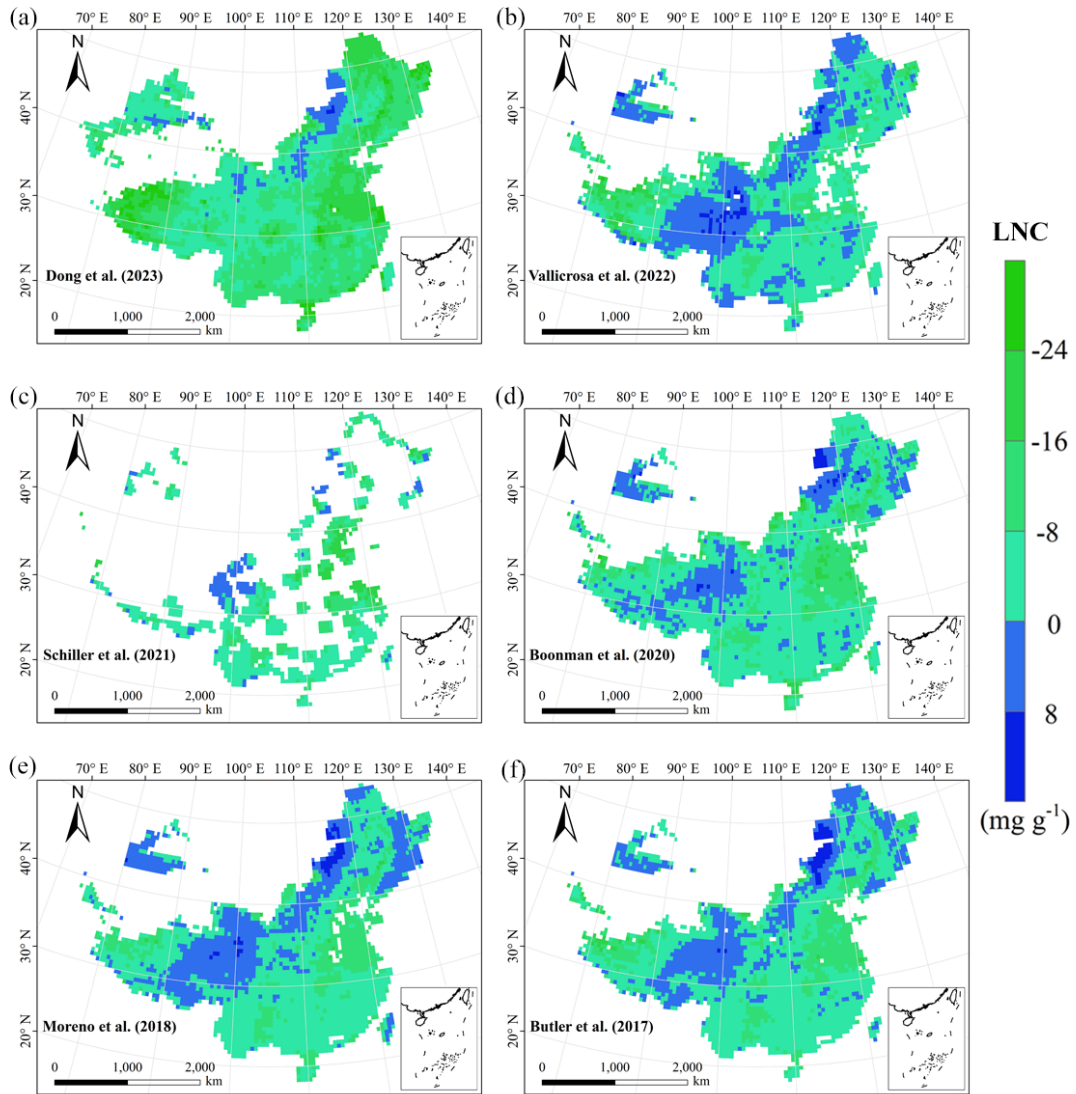


1003
 1004 **Figure F1.** Frequency distributions of plant functional traits in our study (“This study”, dashed
 1005 black lines) and Vallicrosa et al. (2022) at 1 km spatial resolution. (a) LNC, leaf N concentration
 1006 (mg g⁻¹); (b) LPC, leaf P concentration (mg g⁻¹).



1007
1008
1009

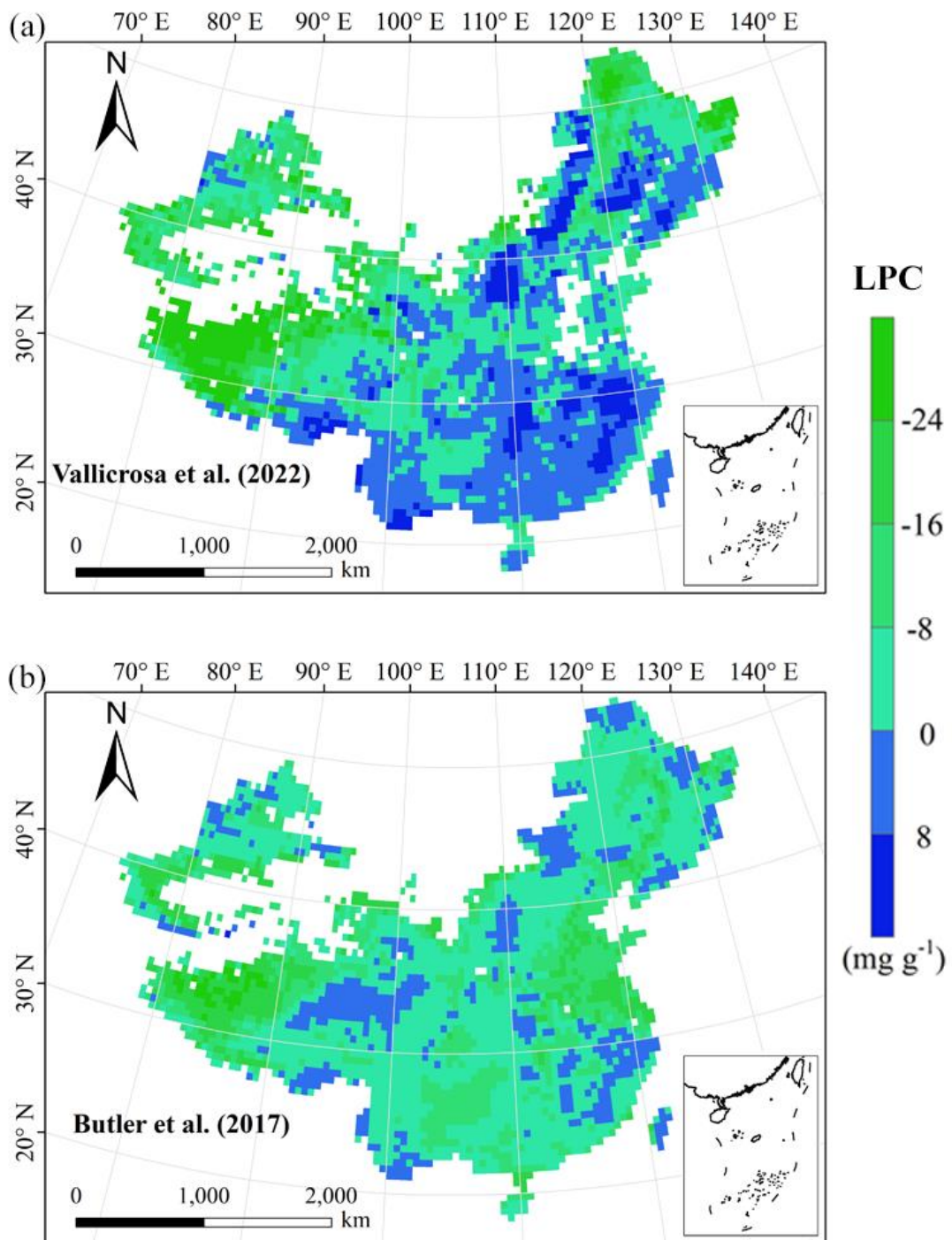
Figure F2. Spatial differences in SLA (specific leaf area, $\text{m}^2 \text{kg}^{-1}$) between our study and trait maps from previous studies (see Table F1 for citations).



1010

1011 **Figure F3.** Spatial differences in LNC (leaf N concentration, mg g^{-1}) between our study and trait

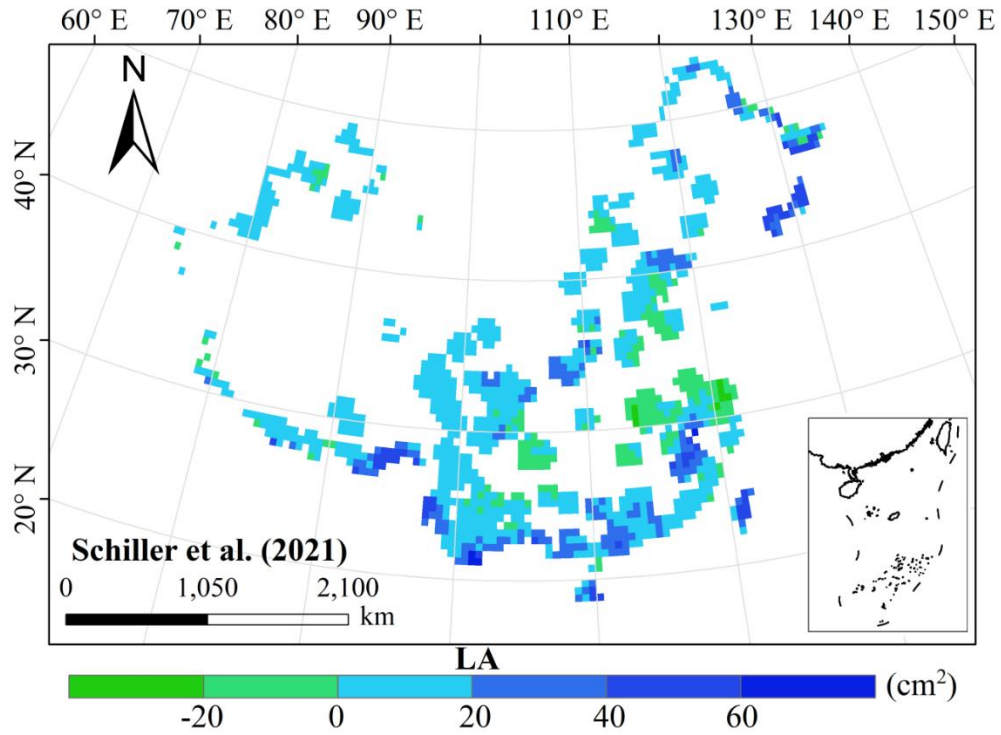
1012 maps from previous studies (see Table F1 for citations).



1013

1014 **Figure F4.** Spatial differences in LPC (leaf P concentration, mg g⁻¹) between our study and trait

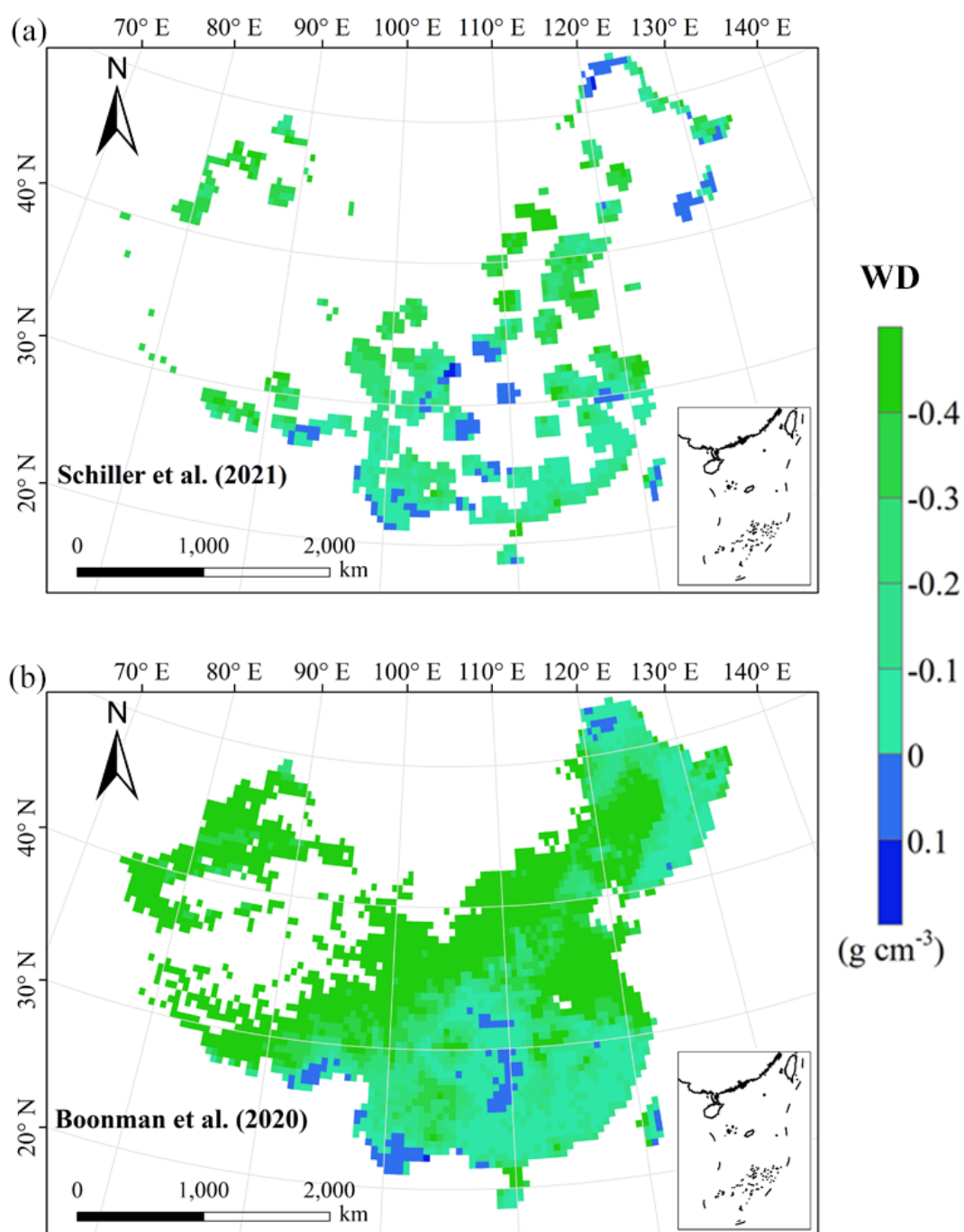
1015 maps from previous studies (see Table F1 for citations).



1016

1017 **Figure F5.** Spatial differences in LA (leaf area, cm²) between our study and trait maps from

1018 previous studies (see Table F1 for citations).



1019

1020 **Figure F6.** Spatial differences in WD (wood density, g cm^{-3}) between our study and trait maps

1021 from previous studies (see Table F1 for citations).

1022 **Author contributions.** NA and NL designed the research. NA did the analysis, processed the data
1023 and wrote the draft of the paper. All co-authors commented on the manuscript and agreed upon the
1024 final version of the paper.

1025
1026 **Competing interests.** The contact author has declared that none of the authors has any competing
1027 interests.

1028
1029 **Disclaimer.** Publisher's note: Copernicus Publications remains neutral with regard to
1030 jurisdictional claims in published maps and institutional affiliations.

1031
1032 **Acknowledgement.** We acknowledge financial supports from the National Natural Science
1033 Foundation of China (41991234) and the Joint CAS-MPG Research Project (HZXM20225001MI).

1034
1035 **Financial support.** This work has been supported by the National Natural Science Foundation of
1036 China (grant no. 41991234) and the Joint CAS-MPG Research Project (grant no.
1037 HZXM20225001MI).

1038

1039 **References**

1040 Ali, A. M., Darvishzadeh, R., Skidmore, A. K., van Duren, I., Heiden, U., and Heurich, M.:
1041 Estimating leaf functional traits by inversion of PROSPECT: Assessing leaf dry matter
1042 content and specific leaf area in mixed mountainous forest. *Int. J. Appl. Earth Obs. Geoinf.*,
1043 45, 66–76, <https://doi.org/10.1016/j.jag.2015.11.004>, 2016.

1044 An, N. N., Lu, N., Fu, B. J., Wang, M. Y., and He, N. P.: Distinct responses of leaf traits to
1045 environment and phylogeny between herbaceous and woody angiosperm species in China.
1046 *Front. Plant Sci.*, 12, 799401, <https://doi.org/10.3389/fpls.2021.799401>, 2021.

1047 Bakker, M. A., Carreño-Rocabado, G., and Poorter, L.: Leaf economics traits predict litter
1048 decomposition of tropical plants and differ among land use types. *Funct. Ecol.*, 25, 473–483,
1049 <https://doi.org/10.1111/j.1365-2435.2010.01802.x>, 2011.

1050 Berzaghi, F., Wright, I. J., Kramer, K., Oddou-Muratorio, S., Bohn, F. J., Reyer, C. P. O., Sabate,
1051 S., Sanders, T. G. M., and Hartig, F.: Towards a new generation of trait-flexible vegetation
1052 models. *Trends Ecol. Evol.*, 35, 191–205, <https://doi.org/10.1016/j.tree.2019.11.006>, 2020.

1053 Blumenthal, D. M., Mueller, K. E., Kray, J. A., Ocheltree, T. W., Augustine, D. J., Wilcox, K. R.,
1054 and Cornelissen, H.: Traits link drought resistance with herbivore defence and plant
1055 economics in semi-arid grasslands: The central roles of phenology and leaf dry matter
1056 content. *J. Ecol.*, 108, 2336–2351, <https://doi.org/10.1111/1365-2745.13454>, 2020.

1057 Bohner, A. Soil chemical properties as indicators of plant species richness in grassland
1058 communities. Integrating efficient grassland farming and biodiversity, Proceedings of the
1059 13th International Occasional Symposium of the European Grassland Federation, Tartu,

1060 Estonia, 29–31 August, 48–51, 2005.

1061 Boonman, C. C. F., Benitez-Lopez, A., Schipper, A. M., Thuiller, W., Anand, M., Cerabolini, B. E.
1062 L., Cornelissen, J. H. C., Gonzalez-Melo, A., Hattingh, W. N., Higuchi, P., Laughlin, D. C.,
1063 Onipchenko, V. G., Penuelas, J., Poorter, L., Soudzilovskaia, N. A., Huijbregts, M. A. J., and
1064 Santini, L.: Assessing the reliability of predicted plant trait distributions at the global scale.
1065 *Global Ecol. Biogeogr.*, 29, 1034–1051, <https://doi.org/10.1111/geb.13086>, 2020.

1066 Breiman, L.: Random forests. *Mach. Learn.*, 45, 5–32, <https://doi.org/10.1023/a:1010933404324>,
1067 2001.

1068 Bruelheide, H., Dengler, J., Purschke, O., Lenoir, J., Jimenez-Alfaro, B., Hennekens, S. M., Botta-
1069 Dukat, Z., Chytrý, M., Field, R., Jansen, F., Kattge, J., Pillar, V. D., Schrodte, F., Mahecha, M.
1070 D., Peet, R. K., Sandel, B., van Bodegom, P., Altman, J., Alvarez-Davila, E., Arfin Khan, M.
1071 A. S., et al.: Global trait-environment relationships of plant communities. *Nat. Ecol. Evol.*, 2,
1072 1906–1917, <https://doi.org/10.1038/s41559-018-0699-8>, 2018.

1073 Bruelheide, H., Dengler, J., Jiménez-Alfaro, B., Purschke, O., Hennekens, S. M., Chytrý, M.,
1074 Pillar, V. D., Jansen, F., Kattge, J., Sandel, B., Aubin, I., Biurrun, I., Field, R., Haider, S.,
1075 Jandt, U., Lenoir, J., Peet, R. K., Peyre, G., Sabatini, F. M., Schmidt, M., et al.: sPlot – A new
1076 tool for global vegetation analyses. *J. Veg. Sci.*, 30, 161–186,
1077 <https://doi.org/10.1111/jvs.12710>, 2019.

1078 Buchhorn, M., Bertels, L., Smets, B., De Roo, B., Lesiv, M., Tsendbazar, N. E., Masiliunas, D.,
1079 and Linlin, L.: Copernicus Global Land Service: Land Cover 100m: Version 3 Globe 2015-
1080 2019: Algorithm Theoretical Basis Document. <https://doi.org/10.5281/zenodo.3938968>, 2020.

1081 Butler, E. E., Datta, A., Flores-Moreno, H., Chen, M., Wythers, K. R., Fazayeli, F., Banerjee, A.,
1082 Atkin, O. K., Kattge, J., Amiaud, B., Blonder, B., Boenisch, G., Bond-Lamberty, B., Brown,
1083 K. A., Byun, C., Campetella, G., Cerabolini, B. E. L., Cornelissen, J. H. C., Craine, J. M.,
1084 Craven, D., de Vries, F. T., Diaz, S., Domingues, T. F., Forey, E., Gonzalez-Melo, A., Gross,
1085 N., Han, W., Hattingh, W. N., Hickler, T., Jansen, S., Kramer, K., Kraft, N. J. B., Kurokawa,
1086 H., Laughlin, D. C., Meir, P., Minden, V., Niinemets, U., Onoda, Y., Penuelas, J., Read, Q.,
1087 Sack, L., Schamp, B., Soudzilovskaia, N. A., Spasojevic, M. J., Sosinski, E., Thornton, P. E.,
1088 Valladares, F., van Bodegom, P. M., Williams, M., Wirth, C., and Reich, P. B.: Mapping local
1089 and global variability in plant trait distributions. *P. Natl. Acad. Sci. USA*, 114, 10937–10946,
1090 <https://doi.org/10.1073/pnas.1708984114>, 2017.

1091 Cavender-Bares, J., Schneider, F. D., Santos, M. J., Armstrong, A., Carnaval, A., Dahlin, K. M.,
1092 Fatoyinbo, L., Hurr, G. C., Schimel, D., Townsend, P. A., Ustin, S. L., Wang, Z. H., and
1093 Wilson, A. M.: Integrating remote sensing with ecology and evolution to advance
1094 biodiversity conservation. *Nat. Ecol. Evol.*, 6, 506–519, <https://doi.org/10.1038/s41559-022-01702-5>, 2022.

1096 Clevers, J. G. P. W., and Gitelson, A. A.: Remote estimation of crop and grass chlorophyll and
1097 nitrogen content using red-edge bands on Sentinel-2 and -3. *Int. J. Appl. Earth Obs. Geoinf.*,

1098 23, 344–351, <https://doi.org/10.1016/j.jag.2012.10.008>, 2013.

1099 Dahlin, K. M., Asner, G. P., and Field, C. B.: Environmental and community controls on plant
1100 canopy chemistry in a Mediterranean-type ecosystem. *P. Natl. Acad. Sci. USA*, 110, 6895–
1101 6900, <https://doi.org/10.1073/pnas.1215513110>, 2013.

1102 Darvishzadeh, R., Skidmore, A., Schlerf, M., and Atzberger, C.: Inversion of a radiative transfer
1103 model for estimating vegetation LAI and chlorophyll in a heterogeneous grassland. *Remote
1104 Sens. Environ.*, 112, 2592–2604, <https://doi.org/10.1016/j.rse.2007.12.003>, 2008.

1105 Diaz, S., Kattge, J., Cornelissen, J. H., Wright, I. J., Lavorel, S., Dray, S., Reu, B., Kleyer, M.,
1106 Wirth, C., Prentice, I. C., Garnier, E., Bonisch, G., Westoby, M., Poorter, H., Reich, P. B.,
1107 Moles, A. T., Dickie, J., Gillison, A. N., Zanne, A. E., Chave, J., Wright, S. J., Sheremet'ev, S.
1108 N., Jactel, H., Baraloto, C., Cerabolini, B., Pierce, S., Shipley, B., Kirkup, D., Casanoves, F.,
1109 Joswig, J. S., Gunther, A., Falczuk, V., Ruger, N., Mahecha, M. D., and Gorne, L. D.: The
1110 global spectrum of plant form and function. *Nature*, 529, 167–171,
1111 <https://doi.org/10.1038/nature16489>, 2016.

1112 Diaz, S., Hodgson, J. G., Thompson, K., Cabido, M., Cornelissen, J. H. C., Jalili, A., Montserrat-
1113 Marti, G., Grime, J. P., Zarrinkamar, F., Asri, Y., Band, S. R., Basconcelo, S., Castro-Diez, P.,
1114 Funes, G., Hamzehee, B., Khoshnevi, M., Perez-Harguindeguy, N., Perez-Rontome, M. C.,
1115 Shirvany, F. A., Vendramini, F., Yazdani, S., Abbas-Azimi, R., Bogaard, A., Boustani, S.,
1116 Charles, M., Dehghan, M., de Torres-Espuny, L., Falczuk, V., Guerrero-Campo, J., Hynd, A.,
1117 Jones, G., Kowsary, E., Kazemi-Saeed, F., Maestro-Martinez, M., Romo-Diez, A., Shaw, S.,
1118 Siavash, B., Villar-Salvador, P., and Zak, M. R.: The plant traits that drive ecosystems:
1119 Evidence from three continents. *J. Veg. Sci.*, 15, 295–304, <https://doi.org/10.1111/j.1654-1103.2004.tb02266.x>, 2004.

1121 Dong, N., Dechant, B., Wang, H., Wright, I. J., and Prentice, IC.: Global leaf-trait mapping based
1122 on optimality theory. *Global Ecol. Biogeogr.*, 32, 1152–1162,
1123 <https://doi.org/10.1111/geb.13680>, 2023.

1124 Du, L., Liu, H., Guan, W., Li, J., and Li, J.: Drought affects the coordination of belowground and
1125 aboveground resource-related traits in *Solidago canadensis* in China. *Ecol. Evol.*, 9, 9948–
1126 9960, <https://doi.org/10.1002/ece3.5536>, 2019.

1127 Elith, J., Leathwick, J. R., and Hastie, T.: A working guide to boosted regression trees. *J. Anim.
1128 Ecol.*, 77, 802–813, <https://doi.org/10.1111/j.1365-2656.2008.01390.x>, 2008.

1129 Elith, J., Kearney, M., and Phillips, S.: The art of modelling range-shifting species. *Methods Ecol.
1130 Evol.*, 1, 330–342, <https://doi.org/10.1111/j.2041-210X.2010.00036.x>, 2010.

1131 Elith, J., Graham, C. H., Anderson, R. P., Dudik, M., Ferrier, S., Guisan, A., Hijmans, R. J.,
1132 Huettmann, F., Leathwick, J. R., Lehmann, A., Li, J., Lohmann, L. G., Loiselle, B. A.,
1133 Manion, G., Moritz, C., Nakamura, M., Nakazawa, Y., Overton, J. M., Peterson, A. T.,
1134 Phillips, S. J., Richardson, K., Scachetti-Pereira, R., Schapire, R. E., Soberon, J., Williams, S.,
1135 Wisz, M. S., and Zimmermann, N. E.: Novel methods improve prediction of species'

1136 distributions from occurrence data. *Ecography*, 29, 129–151,
1137 <https://doi.org/10.1111/j.2006.0906-7590.04596.x>, 2006.

1138 Finzi, A. C., Austin, A. T., Cleland, E. E., Frey, S. D., Houlton, B. Z., and Wallenstein, M. D.:
1139 Responses and feedbacks of coupled biogeochemical cycles to climate change: examples
1140 from terrestrial ecosystems. *Front. Ecol. Environ.*, 9, 61–67, <https://doi.org/10.1890/100001>,
1141 2011.

1142 Foley, J. A., Prentice, I. C., Ramankutty, N., Levis, S., Pollard, D., Sitch, S., and Haxeltine, A.: An
1143 integrated biosphere model of land surface processes, terrestrial carbon balance, and
1144 vegetation dynamics. *Global Biogeochem. Cy.*, 10, 603–628,
1145 <https://doi.org/10.1029/96gb02692>, 1996.

1146 Freschet, G. T., Cornelissen, J. H. C., van Logtestijn, R. S. P., and Aerts, R.: Evidence of the ‘plant
1147 economics spectrum’ in a subarctic flora. *J. Ecol.*, 98, 362–373,
1148 <https://doi.org/10.1111/j.1365-2745.2009.01615.x>, 2010.

1149 Grime, J. P.: Benefits of plant diversity to ecosystems: immediate, filter and founder effects. *J.*
1150 *Ecol.*, 86, 902–910, <https://doi.org/10.1046/j.1365-2745.1998.00306.x>, 1998.

1151 He, N. P., Yan, P., Liu, C. C., Xu, L., Li, M. X., Van Meerbeek, K., Zhou, G. S., Zhou, G. Y., Liu,
1152 S. R., Zhou, X. H., Li, S. G., Niu, S. L., Han, X. G., Buckley, T. N., Sack, L., and Yu, G. R.:
1153 Predicting ecosystem productivity based on plant community traits. *Trends Plant Sci.*, 28, 43–
1154 53, <https://doi.org/10.1016/j.tplants.2022.08.015>, 2023.

1155 Hodgson, J. G., Montserrat-Marti, G., Charles, M., Jones, G., Wilson, P., Shipley, B., Sharafi, M.,
1156 Cerabolini, B. E. L., Cornelissen, J. H. C., Band, S. R., Bogard, A., Castro-Diez, P., Guerrero-
1157 Campo, J., Palmer, C., Perez-Rontome, M. C., Carter, G., Hynd, A., Romo-Diez, A., Espuny,
1158 L. D., and Pla, F. R.: Is leaf dry matter content a better predictor of soil fertility than specific
1159 leaf area? *Ann. Bot.*, 108, 1337–1345, <https://doi.org/10.1093/aob/mcr225>, 2011.

1160 Hoeber, S., Leuschner, C., Köhler, L., Arias-Aguilar, D., and Schuldt, B.: The importance of
1161 hydraulic conductivity and wood density to growth performance in eight tree species from a
1162 tropical semi-dry climate. *Forest Ecol. Manag.*, 330, 126–136,
1163 <https://doi.org/10.1016/j.foreco.2014.06.039>, 2014.

1164 Jónsdóttir, I. S., Halbritter, A. H., Christiansen, C. T., Althuisen, I. H. J., Haugum, S. V., Henn, J. J.,
1165 Björnsdóttir, K., Maitner, B. S., Malhi, Y., Michaletz, S. T., Roos, R. E., Klanderud, K., Lee,
1166 H., Enquist, B. J., and Vandvik, V.: Intraspecific trait variability is a key feature underlying
1167 high Arctic plant community resistance to climate warming. *Ecol. Monogr.*, 93, e1555,
1168 <https://doi.org/10.1002/ecm.1555>, 2022.

1169 Jung, V., Violle, C., Mondy, C., Hoffmann, L., and Muller, S.: Intraspecific variability and trait-
1170 based community assembly. *J. Ecol.*, 98, 1134–1140, <https://doi.org/10.1111/j.1365-2745.2010.01687.x>, 2010.

1172 Kattge, J., Diaz, S., Lavorel, S., Prentice, C., Leadley, P., Bonisch, G., Garnier, E., Westoby, M.,
1173 Reich, P. B., Wright, I. J., Cornelissen, J. H. C., Violle, C., Harrison, S. P., van Bodegom, P.

1174 M., Reichstein, M., Enquist, B. J., Soudzilovskaia, N. A., Ackerly, D. D., Anand, M., Atkin,
1175 O., et al.: TRY - A global database of plant traits. *Global Change Biol.*, 17, 2905–2935,
1176 <https://doi.org/10.1111/j.1365-2486.2011.02451.x>, 2011.

1177 Kattge, J., Bonisch, G., Diaz, S., Lavorel, S., Prentice, I. C., Leadley, P., Tautenhahn, S., Werner, G.
1178 D. A., Aakala, T., Abedi, M., Acosta, A. T. R., Adamidis, G. C., Adamson, K., Aiba, M.,
1179 Albert, C. H., Alcantara, J. M., Alcazar, C. C., Aleixo, I., Ali, H., Amiaud, B., et al.: TRY
1180 plant trait database - Enhanced coverage and open access. *Global Change Biol.*, 26, 119–188,
1181 <https://doi.org/10.1111/gcb.14904>, 2020.

1182 King, D. A., Davies, S. J., Tan, S., and Noor, N. S. M.: The role of wood density and stem support
1183 costs in the growth and mortality of tropical trees. *J. Ecol.*, 94, 670–680,
1184 <https://doi.org/10.1111/j.1365-2745.2006.01112.x>, 2006.

1185 Kirilenko, A. P., Belotelov, N. V., and Bogatyrev, B. G.: Global model of vegetation migration:
1186 incorporation of climatic variability. *Ecol. Model.*, 132, 125–133,
1187 [https://doi.org/10.1016/S0304-3800\(00\)00310-0](https://doi.org/10.1016/S0304-3800(00)00310-0), 2000.

1188 LeBauer, D. S., and Treseder, K. K.: Nitrogen limitation of net primary productivity in terrestrial
1189 ecosystems is globally distributed. *Ecology*, 89, 371–379, <https://doi.org/10.1890/06-2057.1>,
1190 2008.

1191 Li, C. X., Wulf, H., Schmid, B., He, J. S., and Schaepman, M. E.: Estimating plant traits of alpine
1192 grasslands on the Qinghai-Tibetan Plateau using remote sensing. *IEEE J. Sel. Top. Appl.*
1193 *Earth Obs. Remote Sens.*, 11, 2263–2275, <https://doi.org/10.1109/jstars.2018.2824901>, 2018.

1194 Li, D. J., Ives, A. R., and Waller, D. M.: Can functional traits account for phylogenetic signal in
1195 community composition? *New Phytol.*, 214, 607–618, <https://doi.org/10.1111/nph.14397>,
1196 2017.

1197 Li, Y. Q., Reich, P. B., Schmid, B., Shrestha, N., Feng, X., Lyu, T., Maitner, B. S., Xu, X., Li, Y. C.,
1198 Zou, D. T., Tan, Z. H., Su, X. Y., Tang, Z. Y., Guo, Q. H., Feng, X. J., Enquist, B. J., and
1199 Wang, Z. H.: Leaf size of woody dicots predicts ecosystem primary productivity. *Ecol. Lett.*,
1200 23, 1003–1013, <https://doi.org/10.1111/ele.13503>, 2020.

1201 Liang, X. Y., Ye, Q., Liu, H., and Brodribb, T. J.: Wood density predicts mortality threshold for
1202 diverse trees. *New Phytol.*, 229, 3053–3057, <https://doi.org/10.1111/nph.17117>, 2021.

1203 Liaw, A., and Wiener, M.: Classification and Regression by randomForest. *R News*, 2, 18–22,
1204 2002.

1205 Liu, H. Y., and Yin, Y.: Response of forest distribution to past climate change: an insight into
1206 future predictions. *Chinese Sci. Bull.*, 58, 4426–4436, <https://doi.org/10.1007/s11434-013-6032-7>,
1207 2013.

1208 Loozen, Y., Rebel, K. T., Karssenber, D., Wassen, M. J., Sardans, J., Peñuelas, J., and De Jong, S.
1209 M.: Remote sensing of canopy nitrogen at regional scale in Mediterranean forests using the
1210 spaceborne MERIS Terrestrial Chlorophyll Index. *Biogeosciences*, 15, 2723–2742,
1211 <https://doi.org/10.5194/bg-15-2723-2018>, 2018.

1212 Loozen, Y., Rebel, K. T., de Jong, S. M., Lu, M., Ollinger, S. V., Wassen, M. J., and Karssenber,
1213 D.: Mapping canopy nitrogen in European forests using remote sensing and environmental
1214 variables with the random forests method. *Remote Sens. Environ.*, 247, 111933,
1215 <https://doi.org/10.1016/j.rse.2020.111933>, 2020.

1216 Madani, N., Kimball, J. S., Ballantyne, A. P., Affleck, D. L. R., van Bodegom, P. M., Reich, P. B.,
1217 Kattge, J., Sala, A., Nazeri, M., Jones, M. O., Zhao, M., and Running, S. W.: Future global
1218 productivity will be affected by plant trait response to climate. *Sci. Rep.*, 8, 1–10,
1219 <https://doi.org/10.1038/s41598-018-21172-9>, 2018.

1220 Martínez-Vilalta, J., Mencuccini, M., Vayreda, J., and Retana, J.: Interspecific variation in
1221 functional traits, not climatic differences among species ranges, determines demographic
1222 rates across 44 temperate and Mediterranean tree species. *J. Ecol.*, 98, 1462–1475,
1223 <https://doi.org/10.1111/j.1365-2745.2010.01718.x>, 2010.

1224 Matheny, A. M., Mirfenderesgi, G., and Bohrer, G.: Trait-based representation of hydrological
1225 functional properties of plants in weather and ecosystem models. *Plant Divers.*, 39, 1–12,
1226 <https://doi.org/10.1016/j.pld.2016.10.001>, 2017.

1227 Moreno-Martínez, Á., Camps-Valls, G., Kattge, J., Robinson, N., Reichstein, M., van Bodegom, P.,
1228 Kramer, K., Cornelissen, J. H. C., Reich, P., Bahn, M., Niinemets, Ü., Peñuelas, J., Craine, J.
1229 M., Cerabolini, B. E. L., Minden, V., Laughlin, D. C., Sack, L., Allred, B., Baraloto, C., Byun,
1230 C., Soudzilovskaia, N. A., and Running, S. W.: A methodology to derive global maps of leaf
1231 traits using remote sensing and climate data. *Remote Sens. Environ.*, 218, 69–88,
1232 <https://doi.org/10.1016/j.rse.2018.09.006>, 2018.

1233 Myers-Smith, I. H., Thomas, H. J. D., and Björkman, A. D.: Plant traits inform predictions of
1234 tundra responses to global change. *New Phytol.*, 221, 1742–1748,
1235 <https://doi.org/10.1111/nph.15592>, 2019.

1236 NEODC, 2015. NEODC - NERC Earth Observation Data Centre. Natural Environment Research
1237 Council. <http://neodc.nerc.ac.uk/>.

1238 Peng, C. H.: From static biogeographical model to dynamic global vegetation model: a global
1239 perspective on modelling vegetation dynamics. *Ecol. Model.*, 135, 33–54,
1240 [https://doi.org/10.1016/S0304-3800\(00\)00348-3](https://doi.org/10.1016/S0304-3800(00)00348-3), 2000.

1241 Perez-Harguindeguy, N., Diaz, S., Garnier, E., Lavorel, S., Poorter, H., Jaureguiberry, P., Bret-
1242 Harte, M. S., Cornwell, W. K., Craine, J. M., Gurvich, D. E., Urcelay, C., Veneklaas, E. J.,
1243 Reich, P. B., Poorter, L., Wright, I. J., Ray, P., Enrico, L., Pausas, J. G., de Vos, A. C.,
1244 Buchmann, N., Funes, G., Quétier, F., Hodgson, J. G., Thompson, K., Morgan, H. D., ter
1245 Steege, H., van der Heijden, M. G. A., Sack, L., Blonder, B., Poschlod, P., Vaieretti, M. V.,
1246 Conti, G., Staver, A. C., Aquino, S., and Cornelissen, J. H. C.: New handbook for
1247 standardised measurement of plant functional traits worldwide. *Aust. Bot.*, 61, 167–234,
1248 <https://doi.org/10.1071/bt12225>, 2013.

1249 Piao, S. L., He, Y., Wang, X. H., and Chen, F. H.: Estimation of China's terrestrial ecosystem

1250 carbon sink: Methods, progress and prospects. *Sci. China Earth Sci.*, 65, 641–651,
1251 <https://doi.org/10.1007/s11430-021-9892-6>, 2022.

1252 Qiao, J. J., Zuo, X. A., Yue, P., Wang, S. K., Hu, Y., Guo, X. X., Li, X. Y., Lv, P., Guo, A. X., and
1253 Sun, S. S.: High nitrogen addition induces functional trait divergence of plant community in a
1254 temperate desert steppe. *Plant Soil*, 487, 133–156, [https://doi.org/10.1007/s11104-023-05910-](https://doi.org/10.1007/s11104-023-05910-1)
1255 1, 2023.

1256 Reich, P. B., and Oleksyn, J.: Global patterns of plant leaf N and P in relation to temperature and
1257 latitude. *P. Natl. Acad. Sci. USA*, 101, 11001–11006,
1258 <https://doi.org/10.1073/pnas.0403588101>, 2004.

1259 Reich, P. B., Uhl, C., Walters, M. B., and Ellsworth, D. S.: Leaf lifespan as a determinant of leaf
1260 structure and function among 23 Amazonian tree species. *Oecologia*, 86, 16–24,
1261 <https://doi.org/10.1007/BF00317383>, 1991.

1262 Ridgeway, G.: Gbm: generalized boosted regression models. R package version 1.5-6, Available at:
1263 <http://cran.r-project.org/web/packages/gbm/index.html>, accessed 11/02/2009, 2006.

1264 Roderick, M. L., and Berry, S. L.: Linking wood density with tree growth and environment: a
1265 theoretical analysis based on the motion of water. *New Phytol.*, 149, 473–485,
1266 <https://doi.org/10.1046/j.1469-8137.2001.00054.x>, 2002.

1267 Romero, A., Aguado, I., and Yebra, M.: Estimation of dry matter content in leaves using
1268 normalized indexes and PROSPECT model inversion. *Int. J. Remote Sens.*, 33, 396–414,
1269 <https://doi.org/10.1080/01431161.2010.532819>, 2012.

1270 Sakschewski, B., von Bloh, W., Boit, A., Rammig, A., Kattge, J., Poorter, L., Penuelas, J., and
1271 Thonicke, K.: Leaf and stem economics spectra drive diversity of functional plant traits in a
1272 dynamic global vegetation model. *Global Change Biol.*, 21, 2711–2725,
1273 <https://doi.org/10.1111/gcb.12870>, 2015.

1274 Scheiter, S., Langan, L., and Higgins, S. I.: Next-generation dynamic global vegetation models:
1275 learning from community ecology. *New Phytol.*, 198, 957–969,
1276 <https://doi.org/10.1111/nph.12210>, 2013.

1277 Schiller, C., Schmidlein, S., Boonman, C., Moreno-Martinez, A., and Kattenborn, T.: Deep
1278 learning and citizen science enable automated plant trait predictions from photographs. *Sci.*
1279 *Rep.*, 11, 16395, <https://doi.org/10.1038/s41598-021-95616-0>, 2021.

1280 Shangguan, W., Dai, Y. J., Liu, B. Y., Zhu, A. X., Duan, Q. Y., Wu, L. Z., Ji, D. Y., Ye, A. Z., Yuan,
1281 H., Zhang, Q., Chen, D. D., Chen, M., Chu, J. T., Dou, Y. J., Guo, J. X., Li, H. Q., Li, J. J.,
1282 Liang, L., Liang, X., Liu, H. P., Liu, S. Y., Miao, C. Y., and Zhang, Y. Z.: A China data set of
1283 soil properties for land surface modeling. *J. Adv. Model. Earth Syst.*, 5, 212–224,
1284 <https://doi.org/10.1002/jame.20026>, 2013.

1285 Siefert, A., Violle, C., Chalmandrier, L., Albert, C. H., Taudiere, A., Fajardo, A., Aarssen, L. W.,
1286 Baraloto, C., Carlucci, M. B., Cianciaruso, M. V., de, L. D. V., de Bello, F., Duarte, L. D.,
1287 Fonseca, C. R., Freschet, G. T., Gaucherand, S., Gross, N., Hikosaka, K., Jackson, B., Jung,

1288 V., Kamiyama, C., Katabuchi, M., Kembel, S. W., Kichenin, E., Kraft, N. J., Lagerstrom, A.,
1289 Bagousse-Pinguet, Y. L., Li, Y., Mason, N., Messier, J., Nakashizuka, T., Overton, J. M.,
1290 Peltzer, D. A., Perez-Ramos, I. M., Pillar, V. D., Prentice, H. C., Richardson, S., Sasaki, T.,
1291 Schamp, B. S., Schob, C., Shipley, B., Sundqvist, M., Sykes, M. T., Vandewalle, M., and
1292 Wardle, D. A.: A global meta-analysis of the relative extent of intraspecific trait variation in
1293 plant communities. *Ecol. Lett.*, 18, 1406–1419, <https://doi.org/10.1111/ele.12508>, 2015.

1294 Šímová, I., Sandel, B., Enquist, B. J., Michaletz, S. T., Kattge, J., Violle, C., McGill, B. J., Blonder,
1295 B., Engemann, K., Peet, R. K., Wisser, S. K., Morueta-Holme, N., Boyle, B., Kraft, N. J. B.,
1296 Svenning, J. C., and Hector, A.: The relationship of woody plant size and leaf nutrient content
1297 to large-scale productivity for forests across the Americas. *J. Ecol.*, 107, 2278–2290,
1298 <https://doi.org/10.1111/1365-2745.13163>, 2019.

1299 Sitch, S., Huntingford, C., Gedney, N., Levy, P. E., Lomas, M., Piao, S. L., Betts, R., Ciais, P., Cox,
1300 P., Friedlingstein, P., Jones, C. D., Prentice, I. C., and Woodward, F. I.: Evaluation of the
1301 terrestrial carbon cycle, future plant geography and climate-carbon cycle feedbacks using five
1302 Dynamic Global Vegetation Models (DGVMs). *Global Change Biol.*, 14, 2015–2039,
1303 <https://doi.org/10.1111/j.1365-2486.2008.01626.x>, 2008.

1304 Smart, S. M., Glanville, H. C., Blanes, M. d. C., Mercado, L. M., Emmett, B. A., Jones, D. L.,
1305 Cosby, B. J., Marrs, R. H., Butler, A., Marshall, M. R., Reinsch, S., Herrero-Járegui, C.,
1306 Hodgson, J. G., and Field, K.: Leaf dry matter content is better at predicting above-ground
1307 net primary production than specific leaf area. *Funct. Ecol.*, 31, 1336–1344,
1308 <https://doi.org/10.1111/1365-2435.12832>, 2017.

1309 Telenius, A.: Biodiversity information goes public: GBIF at your service. *Nord. J. Bot.*, 29, 378–
1310 381, <https://doi.org/10.1111/j.1756-1051.2011.01167.x>, 2011.

1311 Thomas, D. S., Montagu, K. D., and Conroy, J. P.: Changes in wood density of *Eucalyptus*
1312 *camaldulensis* due to temperature—the physiological link between water viscosity and wood
1313 anatomy. *Forest Ecol. Manag.*, 193, 157–165, <https://doi.org/10.1016/j.foreco.2004.01.028>,
1314 2004.

1315 Thomas, S. C.: Photosynthetic capacity peaks at intermediate size in temperate deciduous trees.
1316 *Tree Physiol.*, 30, 555–573, <https://doi.org/10.1093/treephys/tpq005>, 2010.

1317 Thuiller, W., Lafourcade, B., Engler, R., and Araújo, M. B.: BIOMOD – A platform for ensemble
1318 forecasting of species distributions. *Ecography*, 32, 369–373, <https://doi.org/10.1111/j.1600-0587.2008.05742.x>, 2009.

1320 Trabucco, A., and Zomer, R. J.: Global Aridity Index and Potential Evapo-Transpiration (ET0)
1321 Climate Database v2. CGIAR Consortium for Spatial Information (CGIAR-CSI),
1322 <https://cgiarcsi.community>, 2018.

1323 Vallicrosa, H., Sardans, J., Maspons, J., Zuccarini, P., Fernández-Martínez, M., Bauters, M., Goll,
1324 D. S., Ciais, P., Obersteiner, M., Janssens, I. A., and Peñuelas, J.: Global maps and factors
1325 driving forest foliar elemental composition: the importance of evolutionary history. *New*

1326 Phytol., 233, 169–181, <https://doi.org/10.1111/nph.17771>, 2022.

1327 van Bodegom, P. M., Douma, J. C., Witte, J. P. M., Ordoñez, J. C., Bartholomeus, R. P., and Aerts,
1328 R.: Going beyond limitations of plant functional types when predicting global ecosystem-
1329 atmosphere fluxes: exploring the merits of traits-based approaches. *Global Ecol. Biogeogr.*,
1330 21, 625–636, <https://doi.org/10.1111/j.1466-8238.2011.00717.x>, 2012.

1331 van Bodegom, P. M., Douma, J. C., and Verheijen, L. M. A fully traits-based approach to modeling
1332 global vegetation distribution. *P. Natl. Acad. Sci. USA*, 111, 13733–13738,
1333 <https://doi.org/10.1073/pnas.1304551110>, 2014.

1334 Verheijen, L. M., Aerts, R., Bonisch, G., Kattge, J., and van Bodegom, P. M.: Variation in trait
1335 trade-offs allows differentiation among predefined plant functional types: implications for
1336 predictive ecology. *New Phytol.*, 209, 563–575, <https://doi.org/10.1111/nph.13623>, 2016.

1337 Wang, H., Harrison, S. P., Prentice, I. C., Yang, Y. Z., Bai, F., Togashi, H. F., Wang, M., Zhou, S.
1338 X., and Ni, J.: The China Plant Trait Database: toward a comprehensive regional compilation
1339 of functional traits for land plants. *Ecology*, 99, 500, <https://doi.org/10.1002/ecy.2091>, 2018.

1340 Webb, C. T., Hoeting, J. A., Ames, G. M., Pyne, M. I., and LeRoy Poff, N.: A structured and
1341 dynamic framework to advance traits-based theory and prediction in ecology. *Ecol. Lett.*, 13,
1342 267–283, <https://doi.org/10.1111/j.1461-0248.2010.01444.x>, 2010.

1343 Wright, I. J., Dong, N., Maire, V., Prentice, I. C., Westoby, M., Diaz, S., Gallagher, R. V., Jacobs,
1344 B. F., Kooyman, R., Law, E. A., Leishman, M. R., Niinemets, U., Reich, P. B., Sack, L., Villar,
1345 R., Wang, H., and Wilf, P.: Global climatic drivers of leaf size. *Science*, 357, 917–921,
1346 <https://doi.org/10.1126/science.aal4760>, 2017.

1347 Wright, I. J., Reich, P. B., Westoby, M., Ackerly, D. D., Baruch, Z., Bongers, F., Cavender-Bares,
1348 J., Chapin, T., Cornelissen, J. H. C., Diemer, M., Flexas, J., Garnier, E., Groom, P. K., Gulias,
1349 J., Hikosaka, K., Lamont, B. B., Lee, T., Lee, W., Lusk, C., Midgley, J. J., Navas, M. L.,
1350 Niinemets, U., Oleksyn, J., Osada, N., Poorter, H., Poot, P., Prior, L., Pyankov, V. I., Roumet,
1351 C., Thomas, S. C., Tjoelker, M. G., Veneklaas, E. J., and Villar, R.: The worldwide leaf
1352 economics spectrum. *Nature*, 428, 821–827, <https://doi.org/10.1038/nature02403>, 2004.

1353 Wullschleger, S. D., Epstein, H. E., Box, E. O., Euskirchen, E. S., Goswami, S., Iversen, C. M.,
1354 Kattge, J., Norby, R. J., van Bodegom, P. M., and Xu, X.: Plant functional types in earth
1355 system models: past experiences and future directions for application of dynamic vegetation
1356 models in high-latitude ecosystems. *Ann. Bot.*, 114, 1–16,
1357 <https://doi.org/10.1093/aob/mcu077>, 2014.

1358 Yan, P., He, N. P., Yu, K. L., Xu, L., and Van Meerbeek, K.: Integrating multiple plant functional
1359 traits to predict ecosystem productivity. *Commun. Biol.*, 6, 239,
1360 <https://doi.org/10.1038/s42003-023-04626-3>, 2023.

1361 Yang, Y. Z., Zhu, Q. A., Peng, C. H., Wang, H., Xue, W., Lin, G. H., Wen, Z. M., Chang, J., Wang,
1362 M., Liu, G. B., and Li, S. Q.: A novel approach for modelling vegetation distributions and
1363 analysing vegetation sensitivity through trait-climate relationships in China. *Sci. Rep.*, 6,

1364 24110, <https://doi.org/10.1038/srep24110>, 2016.

1365 Yang, Y. Z., Wang, H., Harrison, S. P., Prentice, I. C., Wright, I. J., Peng, C. H., and Lin, G. H.:
1366 Quantifying leaf-trait covariation and its controls across climates and biomes. *New Phytol.*,
1367 221, 155–168, <https://doi.org/10.1111/nph.15422>, 2018.

1368 Yang, Y. Z., Zhao, J., Zhao, P. X., Wang, H., Wang, B. H., Su, S. F., Li, M. X., Wang, L. M., Zhu,
1369 Q. A., Pang, Z. Y., and Peng, C. H.: Trait-Based Climate Change Predictions of Vegetation
1370 Sensitivity and Distribution in China. *Front. Plant Sci.*, 10, 908,
1371 <https://doi.org/10.3389/fpls.2019.00908>, 2019.

1372 Yurova, A. Y., and Volodin, E. M.: Coupled simulation of climate and vegetation dynamics. *Izv.,*
1373 *Atmos. Ocean. Phy.*, 47, 531–539, <https://doi.org/10.1134/s0001433811050124>, 2011.

1374 Zaehle, S., and Friend, A. D.: Carbon and nitrogen cycle dynamics in the O-CN land surface
1375 model: 1. Model description, site-scale evaluation, and sensitivity to parameter estimates.
1376 *Global Biogeochem. Cy.*, 24, GB1005, <https://doi.org/10.1029/2009gb003521>, 2010.